Design of gutters and gutter outlets

Theory and experiment

R W P May MA, MSc, MICE

Report No. IT 205
April 1982

Hydraulics Research Station
Wallingford
England

Design of gutters and gutter outlets

Theory and experiment

R W P May MA, MSc, MICE

Report No. IT 205
April 1982

Hydraulics Research Station
Wallingford
Oxon OX10 8BA
Telephone 0491 35381

Summary

This report describes the theoretical and experimental background to the design methods for roof gutters and gutter outlets that are contained in a revised version of British Standard Code of Practice CP 308. The report is divided into two parts.

Part I describes theoretical solutions for smooth level gutters of rectangular, trapezoidal and half-round cross-sectional shape. The effects of resistance, bends and slope are then considered. The theoretical solutions are modified so as to provide a consistent factor of safety, and are presented in forms that are suitable for design.

Part II is concerned with the capacity of rectangular and circular outlets in gutters and box-receivers. The results of an experimental study of 77 different configurations are analysed, and used to produce suitable design formulae for the Code of Practice.

Symbols

A	= Cross-sectional area of flow
A_p	= Plan area of outlet
a	= (i) Acceleration of fluid (Part II) (ii) Strength of sink in potential flow (Appendix B)
B	= Surface width of flow
B_s	= Sole width of gutter
$\overline{B}$	= Depth-averaged width of flow in gutter (= A/y)
b	= (i) Effective side-slope of gutter, such that width increases b units per unit increase in depth (Parts I and II) (ii) Strength of vortex in potential flow (Appendix B)
C	= Discharge coefficient of drain pipe
C_d	= Discharge coefficient of outlet for orifice-flow
C_g	= Discharge coefficient of gutter
C_w	= Discharge coefficient of outlet for weir-flow
c	= Constant for cross-sectional shape of gutter; equation (65)
D	= Diameter of outlet
D_o	= Top diameter of outlet
D_i	= Bottom diameter of outlet
e	= Aspect ratio of rectangular gutter based on depth of flow at outlet (= B_s/y_o)
F_o	= Froude Number at outlet of gutter
f	= Quantity in analysis of sloping gutters; equation (131)
G	= $8S_o/\lambda$; non-dimensional quantity
g	= Acceleration due to gravity
H	= Total head above weir or orifice
h	= Static head above weir or orifice
I	= Exponent in approximate solution for effect of resistance in gutters; equations (92) and (95)
J	= Non-dimensional quantity for capacity of rectangular and trapezoidal gutters; equation (23)
K	= (i) Non-dimensional quantity for capacity of half-round gutters (Part I); equation (56) (ii) Constant describing effect of lateral inflow on resistance (Part I); equation (115)
k	= (i) Head loss coefficient at bend in gutter (Part I) (ii) Constant in equation for capacity of drain pipes (Part II and Appendix B); equation (208)
k_s	= Equivalent sand roughness
L	= (i) Length of gutter (Part I) (ii) Length of outlet measured along centre-line of gutter (Part II)
L_c	= Distance of critical section from upstream end of gutter
ℓ	= y_o/y_c

M = Flow force due to fluid pressure and momentum

m = Exponent for cross-sectional shape of gutter; equation (65)

N = Number of measurements

n = Manning's resistance coefficient

P = Wetted perimeter of flow

p = Ratio of depth of flow at upstream end of gutter to depth of flow at outlet ($= y_u/y_o$)

p_c = Value of p for a freely-discharging gutter

Q = Discharge

Q_{cg} = Theoretical discharge in gutter for a freely-discharging flow with a specified value of total head

Q_{cw} = Theoretical discharge at weir for a specified value of total head

q = Rate of inflow per unit length of gutter

R = (i) Hydraulic radius ($= A/P$) (Part I)
(ii) Radius of curvature of flow (Part II and Appendix B)

R_e = Reynolds Number ($= 4VR/\nu$)

r = Radius of half-round gutter

S_e = Standard error

S_f = Friction slope

S_o = Bed slope of channel

s = x/L

t = y_u/y_c

U = Non-dimensional quantity in analysis of resistance effects in level gutters; equation (100)

u = by_o/B_s

V = (i) Velocity of flow
(ii) Non-dimensional quantity in analysis of resistance effects in level gutters, equation (101)

v = B_s/B_u

W = (i) Top width of gutter (Part I)
(ii) Width of outlet measured normal to centre-line of gutter (Part II)

w = B_s/B_o

X = $1 + 1.5F_o^2$

x = Distance along gutter measured from upstream end

x_m = Distance of point of maximum depth from upstream end of gutter

Y_1, Y_2 = Depth-averaged widths of flow on either side of gutter outlet

y = Depth of flow measured normal to invert of gutter

y_f = Depth of freeboard

y_g = Overall depth of gutter

y_m = Maximum depth of flow in gutter

y_o = Depth of flow in gutter at outlet

y_u = Depth of flow at upstream end of gutter

y_w = Maximum depth up to which flow at outlet is of weir-type

$\bar{y}$ = Distance of centroid of area below fluid surface

Z, Z_o = Notional depths derived from discharge; equations (28) and (203)

z = Ratio of top width of gutter with restricted discharge to top width of gutter with same flow but discharging freely (= W/W_c)

α = (i) Non-dimensional resistance parameter (Part I); equation (89)
(ii) Coriolis energy coefficient (Part II)

α_o = Limiting value of α for a gutter wide in relation to the depth of flow

β = $1 - G/G_o$

γ = Discharge coefficient for partial width of gutter

γ_o = Discharge coefficient for unrestricted flow

δ = $1 - x_m/L$

ϵ = (i) $1 - S_f/S_o$
(ii) Measure of surface roughness; equation (115)

η = $1 - y_m/y_o$

θ = Half-angle subtended by water surface at centre of half-round gutter

λ = Darcy-Weisbach friction factor

ν = Kinematic viscosity

σ = Standard deviation

τ = $h/y_c - 1$

ϕ = Angle between streamline and normal to radius

ω = $y/y_c - 1$

Superscripts

T' = Value of quantity T including effect of friction

T'' = Value of quantity T including effect of bend

Subscripts

c = Critical depth

d = Design

e = Effective

m = Maximum

n = Normal depth

o = Outlet

r = Rectangular

t = Triangular

u = Upstream

* = Non-dimensional

Contents

Contents (Cont'd) Page

Contents (Cont'd)

Tables

Figures

Contents (Cont'd)

Plates

Contents (Cont'd)

1 Introduction to parts I and II

The capacity of a gutter depends upon the flow conditions at the outlet, and the way in which the flow profile varies along the length of the gutter. Lateral inflow from roofs or other surfaces is the principal distinguishing feature of flow in gutters, and it has been found that in level gutters it is the most important factor affecting the flow profile. The theoretical equations governing non-uniform flow with spatially-varying discharge are well established[11, 16], and can be solved directly for certain special cases. Beij[1] measured the capacities of level half-round and rectangular gutters, and found that they agreed quite well with the predicted capacities obtained by neglecting the effects of hydraulic resistance.

Guidance on the design of roof gutters was provided in a series of digests by the then Building Research Station (BRS)[7, 8, 9, 10]; the quoted capacities of eaves gutters were based on the results of experiments[12]. In 1974 a British Standard Code of Practice CP 308: 1974 "Drainage of Roofs and Paved Areas" was published, and incorporated some of the design methods proposed by BRS. Eaves gutters for small buildings were designed on the basis of the BRS experimental results[12], but valley gutters and gutters for larger buildings were designed according to the theoretical method developed by Beij[1] for rectangular gutters. Design methods recommended in other countries include those given by Martin[23] in Australia and Schwarz and Culligan[25] in South Africa.

In 1976 it was decided to revise CP 308 in order to improve its layout and to include new work on the meteorological and hydraulics aspects of the design methods. This report describes the hydraulics section of the work and is divided into two parts. Part I concerns the determination of the flow profile in gutters of different cross-sectional shapes, and is based on theoretical solutions of the gradually-varied flow equation. Part II concerns the determination of flow conditions at gutter outlets, and is based on an analysis of a large number of experiments which were carried out by the British Hydromechanics Research Association[13] under an extramural contract placed by the Hydraulics Research Station.

PART I FLOW IN GUTTERS

2 Governing equations

The general equation describing steady gradually-varied flow in a channel with lateral inflow is obtained by considering the balance between the forces acting on a small element of the fluid. The derivation of the equation is given in standard texts[11, 16], and may be written (see "Symbols" for the definitions of the symbols used)

$$\frac{dy}{dx} = \frac{S_o - S_f - 2qQ/(gA^2)}{1 - BQ^2/(gA^3)} \qquad (1)$$

In this form the equation contains the following assumptions:

(a) the lateral inflow q initially has no component of momentum in the direction of flow in the channel.

(b) pressures in the fluid are hydrostatic (ie the streamlines are not curved).

(c) the velocity over a cross-section is uniform (ie the energy and momentum coefficients are equal to unity).

Beij[1] determined theoretical flow profiles in certain types of level gutter ($S_o = 0$) by neglecting the effects of resistance (putting $S_f = 0$) and integrating equation (1) directly. The same results can be obtained more directly by considering the balance between the flow force exerted by the fluid at the upstream and downstream ends of the gutter. The flow force M acting at a channel cross-section is given by

$$M = \rho g A \bar{y} + \rho \frac{Q^2}{A} \qquad (2)$$

where $\bar{y}$ is the distance from the surface of the fluid to the centroid of its cross-sectional area; the first term is the force due to the hydrostatic pressure and the second term is the force due to the flux of momentum through the cross-section. Since the weight of the fluid has no component along a level gutter and since frictional effects are neglected, it follows that the flow force M_u at the upstream end of the gutter must equal the flow force M_o at the outlet. At the upstream end the velocity is zero so that from equation (2)

$$g A_u \bar{y}_u = g A_o \bar{y}_o + \frac{Q_o^2}{A_o} \qquad (3)$$

where Q_o is the discharge at the outlet. If flow conditions at the outlet are expressed in terms of the dimensionless Froude Number F_o defined by

$$F_o^2 = \frac{B_o Q_o^2}{g A_o^3} \qquad (4)$$

equation (3) may be written

$$A_u \bar{y}_u = A_o \bar{y}_o + F_o^2 \frac{A_o^2}{B_o} \qquad (5)$$

Equation (5) shows that the relationship between the depth of flow y_u at the upstream end and the corresponding depth y_o at the outlet depends only upon the cross-sectional shape of the gutter and the Froude Number F_o, for the case in which $S_o = 0$ and $S_f = 0$; it should be noted that the length of a gutter does not here affect its capacity.

3 Smooth level gutters

Trapezoidal gutters 3.1 The cross-sectional shape of a trapezoidal gutter may be described by two parameters: the width B_s of the sole of the gutter and its effective side-slope b. The effective side-slope b is defined such that the width of flow increases b units per unit increase in depth (see Fig 1a). The values of B, A and $\bar{y}$ for a trapezoidal gutter are therefore given by

$$B = B_s + b y \qquad (6a)$$

$$A = (B_s + \frac{1}{2} b y)y \qquad (6b)$$

$$\bar{y} = \frac{(B_s + by/3)y}{2 (B_s + by/2)y} \qquad (6c)$$

Substituting these relationships in equation (5) gives

$$\frac{1}{2} y_u^2 (B_s + \frac{1}{3} b y_u) = \frac{1}{2} y_o^2 (B_s + \frac{1}{3} b y_o) + F_o^2 \frac{(B_s + \frac{1}{2} b y_o)^2 y_o^2}{(B_s + b y_o)} \quad (7)$$

If ratio p and u are defined such that

$$p = \frac{y_u}{y_o} \quad (8)$$

$$u = \frac{b y_o}{B_s} \quad (9)$$

equation (7) can then be written in a simpler non-dimensional form as

$$p^2 + \frac{1}{3} p^3 u = 1 + \frac{1}{3} u + 2 \frac{(1 + \frac{1}{2} u)^2}{(1 + u)} F_o^2 \quad (10a)$$

For a given shape of gutter and for given conditions at the outlet (ie y_o and F_o), equation (10a) enables the value of the ratio $p (= y_u/y_o)$ to be determined. Unfortunately a direct solution is difficult because the equation is a cubic in p, but it can be re-arranged as a quadratic in u

$$u^2 (\frac{1}{3} p^3 - \frac{1}{3} - \frac{1}{2} F_o^2) + u(\frac{1}{3} p^3 + p^2 - \frac{4}{3} - 2F_o^2) + (p^2 - 1 - 2F_o^2) = 0 \quad (10b)$$

Values for a graphical plot can therefore be obtained by treating p and F_o as the independent variables and solving for u; results are shown in Figure 2.

Rectangular and triangular gutters may be treated as special types of trapezoidal gutter. For a rectangular gutter b = 0 and u = 0, so that equation (10a) becomes

$$p = (1 + 2F_o^2)^{1/2} \quad (11)$$

Thus for a level rectangular gutter discharging freely ($F_o = 1$), the depth at the upstream end is 1.732 times the depth at the outlet (neglecting the effects of resistance).

For a triangular gutter the sole width $B_s = 0$, but b is finite. Reverting to equation (7) it may be shown that

$$p = (1 + \frac{3}{2} F_o^2)^{1/3} \quad (12)$$

Thus for a level triangular gutter discharging freely, the depth at the upstream end is 1.357 times that at the outlet (neglecting the effects of resistance). Equations (11) and (12) are plotted in Figure 2, and it may be seen that the curves for trapezoidal gutters lie between those for rectangular and triangular gutters.

Half-round gutters 3.2 British Standard half-round gutters[4, 5, 6] may be of two types: true half-round and nominal half-round (see Figures 1b and 1c). Only a very small error is incurred if the cross-section of a nominal half-round gutter is assumed to be an arc of a circle (see Figure 1c). The cross-sectional shape of a half-round gutter may be defined by two parameters: the radius r and the angle θ (in radians) such that

$$\theta = \cos^{-1} (1 - \frac{y}{r}) \quad (13)$$

The values of B, A and $\bar{y}$ for such a gutter are given by

$$B = 2r \sin\theta \tag{14a}$$

$$A = \frac{1}{2} r^2 (2\theta - \sin 2\theta) \tag{14b}$$

$$\bar{y} = \frac{r(\frac{3}{2}\sin\theta - 2\theta\cos\theta + \frac{1}{6}\sin 3\theta)}{(2\theta - \sin 2\theta)} \tag{14c}$$

Substituting these results in equation (5) gives the following relationship between the values of θ at the upstream and downstream ends of the gutter

$$\frac{3}{2}\sin\theta_u - 2\theta_u\cos\theta_u + \frac{1}{6}\sin 3\theta_u = \frac{3}{2}\sin\theta_o - 2\theta_o\cos\theta_o + \frac{1}{6}\sin 3\theta_o + \frac{F_o^2}{4}\frac{(2\theta_o - \sin 2\theta_o)^2}{\sin\theta_o} \tag{15}$$

If this equation is solved by trial-and-error, the results can be converted by means of equation (13) to give values of the ratio $p\ (= y_u/y_o)$ for different values of the Froude Number F_o at the outlet. Figure 2 shows curves for true half-round and nominal half-round gutters when just flowing full at their upstream ends; it may be seen from these curves that half-round gutters are approximately equivalent to trapezoidal gutters having a value of u = 1 (see equation 9).

Flow profiles 3.3 The results obtained in 3.1 and 3.2 only deal with the conditions at the upstream and downstream ends of a gutter, and do not specify how the lateral inflow enters the gutter (except that initially it should have no momentum in the direction of flow). The relationship between the depths of flow at the upstream and downstream ends of a gutter is therefore the same whether or not the inflow is uniform along its length.

The flow profile in a smooth level gutter can be found by generalising equation (3) so that it applies to an arbitrary point along the gutter where the discharge is Q and the depth and cross-sectional area are respectively y and A:

$$gA\bar{y} + \frac{Q^2}{A} = gA_o\bar{y}_o + \frac{Q_o^2}{A_o} \tag{16}$$

Combining this with equation (4) and expressing the result in non-dimensional form gives

$$(\frac{A}{A_o})^2 (\frac{\bar{y}}{y_o}) + F_o^2 (\frac{A_o}{B_o y_o})(\frac{Q}{Q_o})^2 = \left\{\frac{\bar{y}_o}{y_o} + F_o^2 (\frac{A_o}{B_o y_o})\right\} (\frac{A}{A_o}) \tag{17}$$

As an example of its application, this result simplifies in the case of a rectangular gutter to

$$(\frac{y}{y_o})^3 + 2F_o^2 (\frac{Q}{Q_o})^2 = (1 + 2F_o^2)(\frac{y}{y_o}) \tag{18}$$

Thus the ratio y/y_o at any point depends only upon the Froude Number at the outlet and the ratio of the discharge at that point to the discharge at the outlet. If the lateral inflow is uniform, the ratio Q/Q_o may be replaced by the ratio x/L where L is the length of the gutter, and x is the distance from the upstream end of the gutter to the point in question. The equivalent result for a triangular gutter is

$$\left(\frac{y}{y_o}\right)^5 + \frac{3}{2} F_o^2 \left(\frac{Q}{Q_o}\right)^2 = \left(1 + \frac{3}{2} F_o^2\right) \left(\frac{y}{y_o}\right)^2 \quad (19)$$

Figure 3a shows the flow profiles in rectangular and triangular gutters when they discharge freely at their downstream ends ($F_o = 1.0$). When the discharge from the gutters is restricted, the profiles become flatter as shown in Fig 3b for the case of $F_o = 0.5$.

4 Design of gutters with free discharge

General 4.1 Beij[1] carried out experiments on level rectangular and half-round gutters discharging freely at their downstream ends. The depths measured at the upstream ends of the rectangular gutters were compared with the depths predicted by equations (11) and (4). As expected the measured depths were all greater than the theoretical depths obtained by neglecting the effects of resistance. The differences were however relatively small and varied between about 5% and 20% with an average of about 8%; the 152mm wide gutter that was used had a length of 9.6m, and the 76mm wide gutters had lengths varying between 2.1m and 6.7m.

CP 308: 1974[3] recommends that for a freely-discharging gutter the upstream depth of flow should be assumed to be twice the critical depth at the outlet, ie that a value of $p = 2$ should be used. For rectangular gutters this recommendation provides a safety factor (in terms of upstream depth) of 15% compared with the theoretical value of $p = 1.732$, and is on the safe side compared with almost all Beij's measurements. However, the same design figure of $p = 2$ is recommended in CP 308: 1974 for all types of gutter so that in the case of a triangular gutter there is an equivalent safety factor of 47%. The relative difference between rectangular and triangular gutters is even more marked in terms of discharge capacity, the theoretical safety factors being 24% and 164% respectively.

When the revision of CP 308 began, it was decided that the method of design should be altered so that the same theoretical safety factor would be applied to the discharge capacities of gutters of different cross-sectional shapes. A safety factor of 24% was chosen so that the design capacity of a rectangular gutter would be unchanged from that given in CP 308: 1974; the new method of design however leads to more economical design of trapezoidal and triangular gutters.

Capacity of trapezoidal gutters 4.2 It is recommended in CP 308 that outlets to gutters should be large enough to allow the flow to discharge freely at the downstream end (so that $F_o = 1$). A typical design problem therefore involves finding the capacity of a freely-discharging gutter with specified dimensions and cross-sectional shape. The design depth of flow y_u at the upstream end of a gutter is found by subtracting the freeboard y_f from the overall depth y_g. The freeboard is intended to allow for the effect of splashing and waves, and is in addition to the safety factor considered in 4.1; the figure recommended in CP 308 for y_f is 2/7 of y_g up to a maximum of 75mm.

Starting from equation (4), the discharge capacity Q_o of a freely-discharging gutter is given by

$$Q_o = \sqrt{g} \left(\frac{A_o^3}{B_o}\right)^{1/2} \quad (20)$$

The values of A_o and B_o are not initially known, and therefore need to be expressed in terms of y_u and the specified cross-sectional shape of the gutter. Let ratio p_c and v be defined such that

$$p_c = \frac{y_u}{y_o} \tag{21}$$

$$v = \frac{B_s}{B_u} \tag{22}$$

where the subscript c denotes the value for a freely-discharging gutter in which the depth y_o at the outlet is equal to the critical depth y_c. It can then be shown that

$$\frac{Q_o}{\sqrt{g}\ B_u\ y_u^{3/2}} = \left[\frac{(1 - v + 2p_c v)^3}{8p_c^5(1 - v + p_c v)}\right]^{1/2} = 0.4387\ J \tag{23}$$

where the factor J is equal to unity for a rectangular gutter. It is still necessary to determine the relationship between p_c and v, but this may be done by means of the results obtained in 3.1. Since

$$u = \frac{by_o}{B_s} = \left(\frac{B_u - B_s}{y_u}\right)\left(\frac{y_u}{B_s}\right)\left(\frac{y_o}{y_u}\right) = \frac{(1 - v)}{p_c v} \tag{24}$$

equation (10b) may be solved to give

$$v = \frac{\{2p_c^3 - 5\}}{-\{p_c^4 + p_c^3 - 10p_c + 5\} + p_c\sqrt{\{p_c^6 - 6p_c^5 + 9p_c^4 + 16p_c^3 - 30p_c^2 + 10\}}} \tag{25}$$

Equations (23) and (25) taken together enable the theoretical capacity of a freely-discharging, level, trapezoidal gutter to be determined directly from its dimensions. The upstream flow depth y_u is found by subtracting the freeboard allowance from the overall depth of the gutter. The value of the ratio v can then be calculated since the sole width B_s is known, and the width of flow B_u is determined by y_u and the cross-sectional shape of the gutter. The variation of the dimensionless quantity J in equation (23) with the shape factor v is shown in Figure 4.

As described in 4.1 it was decided that the new design method should provide a safety factor of 24% in terms of discharge so that it would give the same result for a rectangular gutter as the existing method in CP 308: 1974. The exact value of the ratio between the design capacity (given by $p_c = 2$, $v = 1$ for a rectangular gutter) and the theoretical capacity may be shown to be $3^{0.75}/2^{1.5} = 0.8059 = 1/1.241$. Applying this factor gives the design curves that are shown in Figure 5 and in which the relevant units are mm and l/s.

Although the above approach enables the capacity of a gutter to be estimated directly, it was found that it did not fit in well with some other parts of the code. Therefore in the final stages of the drafting it was decided to adopt an alternative approach that gave the same results, but in a way that was easier to follow. In this method the designer first has to determine the ratio of the depths of flow at the upstream and downstream ends of the gutter (ie the value of p_c), which depends upon the cross-sectional shape of the gutter. Having thereby found the depth y_o at the downstream end, he then calculates the discharge at the outlet from equation (20). This approach is similar to the one in CP 308: 1974, and should therefore be simpler to understand for designers who are familiar with the previous code.

The relationship between the theoretical value of p_c and the shape factor v of the gutter is found from equation (25) and is shown in Figure 5b. It is now necessary to modify the theoretical curve so that it will incorporate the required discharge factor. The design curve must give the same upstream depth of flow y_u as the theoretical curve but at a discharge which is 0.806 that predicted by equation (23). The value of v is the same in both cases so that equation (23) gives

$$\left[\frac{1 - v + 2p_{cd}v}{1 - v + 2p_c v}\right]^3 \left[\frac{p_c}{p_{cd}}\right]^5 \left[\frac{1 - v + p_c v}{1 - v + p_{cd}v}\right] = (\frac{3}{4})^{1.5} \qquad (26)$$

where p_{cd} is the design value of the ratio. The relation between p_c and v is fixed by equation (25), so that values of p_{cd} can be found by trial-and-error. The resulting design curve for p_{cd} is shown in Figure 5b, which also gives the theoretical and design curves for p_c and p_{cd} as functions of the ratio B_s/B_o (see 5.1).

Sizing of trapezoidal gutters 4.3

An alternative design problem to the one considered in 4.2 is that in which the discharge Q_o is specified and it is required to find the upstream depth of flow y_u. In order to solve the problem it is first necessary to choose suitable values for the sole width B_s and the effective side-slope b; in the case of a valley gutter these quantities are often determined by the cross-sectional shape of the roof.

Since the gutter is assumed to discharge freely, equation (4) may be written

$$\frac{Q_o^2}{g} = \frac{A_o^3}{B_o} \qquad (27)$$

It is now convenient to define a notional depth Z based on the specified discharge Q_o such that

$$Z = (\frac{Q_o^2}{g})^{1/5} \qquad (28)$$

Defining the ratios

$$p_c = \frac{y_u}{y_o} \qquad (21)$$

$$u = \frac{by_o}{B_s} \qquad (9)$$

where the subscript c denotes the value for a freely-discharging gutter, and using equations (6a), (6b) and (28) enables equation (27) to be written in the form

$$\frac{y_o}{Z} = \frac{(1 + u)^{1/3}}{(1 + \frac{1}{2}u)\,(\frac{B_s}{Z})^{2/3}} \qquad (29)$$

Substituting equation (9) in equation (29) and re-arranging gives

$$\frac{B_s}{Z} = \frac{(1 + u)^{1/5}}{(1 + \frac{1}{2}u)^{3/5}} (\frac{b}{u})^{3/5} \qquad (30)$$

The unknown upstream depth y_u can be related to B_s by combining equations (21) and (9) to give

$$\frac{y_u}{Z} = \frac{p_c u}{b} (\frac{B_s}{Z}) \qquad (31)$$

The relationship between p_c and u that is needed to complete the solution is found by putting $F_o = 1$ in equation (10b) so that

$$u = \frac{-\{p_c^3+3p_c^2-10\} + \sqrt{\{p_c^6-6p_c^5+9p_c^4+16p_c^3-30p_c^2+10\}}}{\{2p_c^3-5\}} \quad (32)$$

Equations (30), (31) and (32) together enable the upstream depth of flow y_u to be calculated for a freely-discharging gutter in which Q, B_s and b are specified. A general graphical solution can be constructed by choosing p_c as the independent variable. A value of p_c is first assumed (between the limits of 1.732 for a rectangular gutter and 1.357 for a triangular gutter), and the corresponding value of u found from equation (32). Together with the chosen value of b, this enables the corresponding values of B_s/Z and y_u/Z to be calculated from equations (30) and (31). The process may then be repeated for other values of b and then for other values of p_c. Rectangular and triangular gutters need to be treated as special cases since the above equations are not valid when u = 0 or b = 0. However it is simple to show that for a rectangular gutter

$$\frac{y_u}{Z} = \frac{\sqrt{3}}{(B_s/Z)^{2/3}} \quad (33)$$

and that for a triangular gutter

$$\frac{y_u}{Z} = (\frac{5}{2})^{1/3} \cdot \frac{8^{1/5}}{b^{2/5}} \quad (34)$$

Theoretical curves of y_u/Z versus B_s/Z for different values of b are shown in Figure 6a.

In order to use this method for design it is necessary to modify the theoretical curves so that gutters designed according to them have design capacities that are 80.6% of their theoretical capacities (see 4.2). This can be done by multiplying all the theoretical values of y_u/Z and B_s/Z by the ratio $0.806^{-0.4} = 1.090$, since from equation (28) Z is proportional to $Q^{0.4}$. The resulting design curves are shown in Figure 6b.

During the final stages of the drafting of the Code it was decided to shorten the text and reduce the number of design methods. The results obtained in this section have not therefore been included in the new Code.

Half-round gutters 4.4

The theoretical relationship between the depths of flow at the upstream and downstream ends of a freely-discharging half-round gutter is found by putting $F_o = 1$ in equation (15). Eaves gutters are normally designed to just flow full at the upstream end, so that for a true half-round gutter the upstream angle $\theta_u = \pi/2$ ($\equiv 90^o$) in equation (13). Solving equation (15) by trial-and-error gives at the downstream end the theoretical value $\theta_o = 1.217$ ($\equiv 69.8^o$). The corresponding values for a nominal half-round gutter (see Figure 1c) just flowing full at its upstream end are $\theta_u = 1.403$ ($\equiv 80.4^o$) and $\theta_o = 1.103$ ($\equiv 63.2^o$). The discharge Q_o corresponding to a value of θ_o is found by means of equations (4), (14a) and (14b) to be

$$Q_o = \frac{F_o}{4} \left\{\frac{(2\theta_o - \sin 2\theta_o)^3}{\sin\theta_o}\right\}^{\frac{1}{2}} \sqrt{(gr^5)} \quad (35)$$

Substituting the above values of θ_o in equation (35) gives for a true half-round gutter with free discharge ($F_o = 1$)

$$Q_o = 0.6159 \sqrt{(gr^5)} \quad (36)$$

while for a nominal half-round gutter the equivalent result is

$$Q_o = 0.4384 \sqrt{(gr^5)} \quad (37)$$

Capacities of half-round gutters have been measured by Beij[1], Crabb et al[12] and Marsh[22]. Beij[1] found that his measurements for true half-round gutters were approximated by

$$Q_o = 0.52 \sqrt{(gr^5)} \quad (38)$$

which is similar in form to equation (36) but with a coefficient that is 84% of the theoretical one. Table 1 shows a comparison between the measurements of Crabb et al[12] and Marsh[22] and the theoretical capacities predicted by equations (36) and (37). It can be seen that the ratios of the measured to the theoretical capacities are all fairly close to the figure of 80.6% that was adopted for the design of trapezoidal gutters in the revised version of CP 308 (see 4.2). It does appear however that nominal half-round gutters generally have higher relative capacities than true half-round gutters. Beij[1] and Crabb et al[12] both found that varying the length of a gutter had little effect on its capacity; this suggests that the effects of frictional resistance were relatively small. It is likely that the differences between the three sets of experimental results occurred because splashing and turbulence in the gutters made it difficult to determine the limits of overtopping precisely.

As mentioned above, no allowance for freeboard is normally made when designing eaves gutters. It was therefore decided that the factor of safety applied to the theoretical solutions should be somewhat higher for half-round eaves gutters than for trapezoidal valley gutters so as to give design capacities that were on the safe side compared with all the experimental measurements. A suitable factor was obtained by assuming the depth of flow at the downstream end of a freely-discharging gutter to be 5/9 the overall depth of the gutter; this gives design capacities that are respectively 72.9% and 71.8% of the theoretical capacities of true and nominal half-round gutters (compared with the figure of 80.6% used for trapezoidal gutters). Equations for the design capacities are found from equation (35) using a value of $\theta_o = 1.110$ ($\equiv 63.6^o$) for true half-round gutters and a value of $\theta_o = 1.004$ ($\equiv 57.5^o$) for nominal half-round gutters. Expressing the results in terms of the top width W of the gutter (see Figures 1b and 1c) and using the system of units (mm and l/s) adopted in CP 308 gives for true half-round gutters

$$Q_o = 7.861 \times 10^{-6} \ W^{5/2} \quad (39)$$

and for nominal half-round gutters

$$Q_o = 5.511 \times 10^{-6} \ W^{5/2} \quad (40)$$

If true half-round gutters are used as valley or parapet wall gutters, CP 308 recommends that an allowance of 2/7 the overall depth of the gutter should be made for freeboard. Thus the depth of flow at the upstream end of the gutter corresponds to an angle $\theta_u = 1.281$ ($\equiv 73.4^o$) in equation (13). Solving equation (15) for the case of a freely-discharging gutter gives at the downstream end a corresponding value of $\theta_o = 1.015$ ($\equiv 58.2^o$). Substituting this value in equation (35) gives for the theoretical capacity of a true half-round valley gutter

$$Q_o = 0.3276 \sqrt{(gr^5)} \quad (41)$$

Since CP 308 recommends the same amount of freeboard for all types of valley gutter, the same discharge factor of 80.6% has been used for half-round gutters as for trapezoidal gutters (see 4.2). Therefore in terms of the top width W, the design equation for freely-discharging true half-round gutters is

$$Q_o = 4.623 \times 10^{-6} \; W^{5/2} \qquad (42)$$

where the appropriate units are l/s and mm.

5 Design of gutters with restricted discharge

Trapezoidal gutters 5.1 Although CP 308 recommends that outlets should be sufficiently large to allow gutters to discharge freely, this may not be practicable or economic if the gutter has a considerably larger capacity than the design rate of flow; this can occur where the dimensions of a gutter are determined by the cross-sectional shape of the roof. In such cases it may be convenient to use a smaller size of outlet that prevents the gutter from discharging freely, and thereby causes some backing up of the flow.

In order to design a gutter with restricted discharge it is first necessary to assume a rate of flow and then to calculate the head needed to pass that flow through the outlet (using design equations such as those given in Part II). The relationship between the unknown depth of flow at the upstream end of the gutter and the known conditions at the outlet can be determined by means of the method described below. If the upstream depth exceeds the allowable depth in the gutter it is necessary to repeat the procedure with a lower rate of flow.

It will be assumed that the discharge Q_o has been specified and that the depth of flow y_o at the outlet has been calculated. The values of B_o and A_o that correspond to y_o are determined by the cross-sectional shape of the gutter which is also assumed to have been specified. The Froude Number F_o at the downstream end can then be determined from equation (4); if $F_o > 1$ the outlet does not in fact restrict the discharge of the gutter which may therefore be designed according to the methods given in 4.2 and 4.3. Ratios p, w and X are now defined such that

$$p = \frac{y_u}{y_o} \qquad (8)$$

$$w = \frac{B_s}{B_o} \qquad (43)$$

$$X = 1 + \frac{3}{2} F_o^2 \qquad (44)$$

where B_s is the sole width of the gutter. As described above the values of w and X are known and the problem is to find the corresponding value of p. From equation (9) it follows that

$$u = \frac{1 - w}{w} \qquad (45)$$

Equation (10b) can therefore be solved to give

$$w = \frac{2\{p^3 - X\}}{\{p^3 - 3p^2 + 2X\} + \sqrt{[p^3\{p^3 - 6p^2 + 9p - 4\} + 4X\{2p^3 - 3p^2 + 1\}]}} \quad (46)$$

The resulting variation of p with w and F_o is shown plotted in Figure 7a.

It is now necessary to modify the theoretical curves of p versus F_o and w in Figure 7a so that they are suitable for the design of gutters with restricted discharge. At the limit when $F_o = 1$, the design curves must be consistent with those for freely-discharging gutters (see Figure 5b), and must therefore give capacities that are 0.806 of the theoretical capacities. At the other limit when $F_o \to 0$, the water surface in the gutter will be horizontal in both the design and the theoretical cases. It therefore follows that there will be no reduction from the theoretical to the design capacity at the limit when $F_o \to 1$. The way in which the discharge factor is varied from 0.806 to 1 for values of F_o between 1 and 0 is a matter of choice, but is subject to one important condition. This condition requires that, for a given discharge, the depth of flow at the upstream end of a gutter must increase steadily as the depth of flow at the downstream end is increased. If this requirement is not satisfied a gutter with restricted discharge could be found to have a higher design capacity than one which discharges freely. Although this condition might seem easy to satisfy, it in fact proved crucial when defining the shape of the design curves of p versus F_o and w.

As explained above the limiting values of p versus w for freely-discharging gutters must be consistent with the design values in 4.2 which were obtained in terms of p versus $v = B_s/B_u$ (the use of v is unsuitable here because B_u is initially unknown). However it is simple to show from equation (6) that

$$w = \frac{vp}{1 + vp - v} \quad (47)$$

This enables the curves of p versus w for freely-discharging gutters to be obtained as shown in Figure 5b. Also it is known that when $F_o \to 0$ the value of p must $\to 1$ for all values of w. The problem is therefore to define the shape of the design curves of p versus F_o and w between these end points in a satisfactory way. The procedure described below is unfortunately rather complex, and is included here only for completeness. As there is no single "correct" set of design curves, it is perhaps sufficient to be aware that the procedure satisfies the condition described above.

The first step is to determine from the theoretical solution how the upstream depth of flow y_u varies when the discharge Q at the outlet is kept constant and the Froude Number F_o at the outlet is reduced. For this purpose it is useful to consider the ratio

$$t = \frac{y_u}{y_c} \quad (48)$$

where y_c is the value of critical depth corresponding to the discharge Q; if Q is kept constant, y_c also remains constant. The theoretical relationship between $p = y_u/y_o$, F_o and w has already been determined in equation (46); the required value of t can therefore be found if p is multiplied by the ratio

$$\ell = \frac{y_o}{y_c} \quad (49)$$

Now it can be shown from equations (4) and (6) that

$$\ell^5 \left\{ w\ell + (1 - w) \right\} \left\{ \frac{w + 1}{2w\ell + (1 - w)} \right\}^3 = \frac{1}{F_o^2} \qquad (50)$$

so that ℓ, like p, can be found as a function of F_o and w. Multiplying p from equation (46) by ℓ from equation (50) then gives the required ratio t as a function of F_o and w. The theoretical curves are shown in Figure 7b, and it can be seen that, although y_u/y_c increases as F_o decreases below 1, the curves are very flat between $F_o = 1$ and $F_o = 0.75$. Therefore the capacity of a gutter with restricted discharge will be only slightly lower than that of a freely-discharging gutter provided $F_o > 0.75$.

The curves in Figure 7b are not in their most suitable form because when F_o is decreased as the result of an increase in the downstream depth y_o (with Q_o kept constant), the value of $w = B_s/B_o$ also changes. A better method of presenting the results would therefore be to express them in terms of the ratio B_s/B_c rather than w, where B_c is the width of flow corresponding to y_c. For constant discharge the value of B_s/B_c would not then change when F_o is altered. Defining

$$w_c = \frac{B_s}{B_c} \qquad (51)$$

it is found from equation (6) that

$$\ell = \frac{w_c}{w} \frac{(1 - w)}{(1 - w_c)} \qquad (52)$$

Substituting in equation (50) gives

$$\frac{(1 - w_c^2)^3}{(1 - w^2)^3} \left(\frac{w}{w_c} \right)^5 = F_o^2 \qquad (53)$$

From this it can be shown that curves of y_u/y_c against F_o for constant values of B_s/B_c are slightly flatter than those for constant values of B_s/B_o. However the calculations involved in producing curves of constant B_s/B_c are difficult, and it was decided to use those in Figure 7b for constant B_s/B_o when obtaining the design curves.

The next step is to modify the theoretical curves in Figure 7b so as to give design curves which incorporate the required discharge factors at $F_o = 1$ and $F_o \to 0$. Although there is no one "correct" way of doing this, it is necessary to ensure that the design values of y_u/y_c increase steadily as F_o is decreased below 1. A suitable equation connecting the theoretical value of t to the design value t_d which satisfies this condition is

$$\frac{t_d}{t} = 1 + \left\{ \frac{t_{cd}}{t_c} - 1 \right\} \sin \left(\frac{\pi F_o}{2} \right) \qquad (54)$$

where the subscript c refers to the values for freely-discharging gutters, and the different t are all for the same values of $w = B_s/B_o$ and F_o. Other scaling equations can be used provided that they also satisfy the above condition. Having obtained the design value of t_d as a function of F_o and w, it is now possible to reverse the procedure that was used when obtaining the theoretical curves of t in Figure 7b. Thus the design value of p_d, which is the object of the exercise, is given by

$$p_d = \frac{t_d}{\ell} \qquad (55)$$

The ratio $\ell = y_o/y_c$ has already been determined as a function of F_o and w from equation (50), and, since this relationship is only concerned with conditions at the outlet, it applies to both the theoretical and the design cases. The resulting curves of p_d versus F_o and w are shown in Figure 7c, and are the ones included in the revised version of CP 308.

True half-round gutters 5.2 If a half-round gutter is prevented from discharging freely, the normal design problem involves finding a suitable value for the top width W of the gutter given the discharge Q and the corresponding depth of flow y_o at the outlet; the value of W needs to be such that the depth of freeboard at the upstream end is equal to 2/7 the overall depth of the gutter as recommended in CP 308. The problem can be solved by first considering the theoretical solution, and then applying suitable factors so that the results are consistent with the design method for freely-discharging half-round valley gutters given in 4.4.

The theoretical solution for the case of a true half-round gutter with restricted discharge is given by equations (13), (15) and (35). After allowing for the required amount of freeboard ($y_f = W/7$), the design depth of flow at the upstream end of the gutter corresponds to a value of $\theta_u = 1.281$ ($\equiv 73.4^o$) in equation (13). Equation (15) therefore defines the relationship between the Froude Number F_o and the corresponding angle θ_o at the downstream end of the gutter. Equation (35) may be re-arranged in the form

$$\frac{Q_o}{\sqrt{(gy_o^5)}} = K = \frac{F_o}{4}\left\{\frac{(2\theta_o - \sin 2\theta_o)^3}{\sin\theta_o}\right\}^{\frac{1}{2}} \left(\frac{r}{y_o}\right)^{5/2} \qquad (56)$$

In the design problem the value of the quantity K is known since Q and y_o are specified. From equation (13)

$$\frac{r}{y_o} = \frac{1}{(1 - \cos\theta_o)} = \frac{1}{2}\frac{W}{y_o} \qquad (57)$$

since for a true half-round gutter W = 2r. The theoretical solution may therefore be presented as a graphical plot of the non-dimensional quantity K against the ratio W/y_o; Points on the curve are obtained by first choosing a value of F_o and then solving equation (15) by trial-and-error to find the corresponding value of θ_o (since the value of θ_u is known). The ratios r/y_o and W/y_o are found from equation (57) and then substituted in equation (56) to give the value of K. The shape of the theoretical curve of W/y_o versus K is shown in Figure 8a; when the depth y_o is just low enough to allow the gutter to discharge freely $F_o = 1$, and K and W/y_o have values of 2.135 and 4.232 respectively (see point A on Figure 8a). The continuation of the curve to the right of the point A is found by re-arranging equation (41) in the form

$$\frac{Q_o}{\sqrt{(gy_o^5)}} = 0.3276\left(\frac{W}{2y_o}\right)^{5/2} \qquad (58)$$

The theoretical solution now needs to be modified so that it is consistent with the design method used in CP 308 for freely-discharging half-round valley gutters (see 4.4). In this latter case the gutter is assumed to reach its capacity at a rate of flow that is 80.6% of the theoretical maximum rate of flow; since the design capacity is less, the design value of the depth y_o will also be somewhat lower than the theoretical value of y_o. Thus if the equation for the design

capacity (equation (42)) is substituted in equation (35), it can be shown that the design value of θ_o is 0.956 ($\equiv 54.8^o$) compared with the theoretical value given in 4.4 of 1.015 ($\equiv 58.2^o$). It can thereby be shown that, in the design case, the co-ordinates of the point B in Figure 8a at which the gutter just discharges freely are K = 2.269 and $W/y_o = 4.728$. Thus in order to move from the theoretical point A to the design point B it is necessary to modify the theoretical values of both K and W/y_o in Figure 8a. The problem of determining the shape of the design curve to the left of point B is similar to that encountered in the case of trapezoidal gutters with restricted discharge (see 5.1), and as before there is no completely rigorous way of doing it. The procedure adopted is described below.

As in the case of the trapezoidal gutter it is necessary to ensure that the design curve does not give rise to an anomaly whereby the size of the gutter appears to decrease when the depth at the outlet is increased. Consider first the ratio W/W_c where W is the size of a gutter with restricted discharge and W_c is the size of a gutter carrying the same flow but just discharging freely. Now

$$\frac{W}{W_c} = \left(\frac{W}{y_o}\right)\left(\frac{y_c}{W_c}\right)\left(\frac{y_o}{y_c}\right) \tag{59}$$

Substituting from equation (56) then gives

$$\frac{W}{W_c} = \left(\frac{W}{y_o}\right)\left(\frac{y_c}{W_c}\right)\left(\frac{K_c}{K}\right)^{2/5} \tag{60}$$

where K is the value of the discharge parameter for the gutter with restricted discharge and K_c that of the gutter discharging freely. Values of W/y_o and K from the theoretical curve in Figure 8a enable W/W_c to be plotted in Figure 8b as a function of K/K_c. As expected W/W_c increases steadily as K/K_c is decreased, but it is interesting to note that the curve is extremely flat for values of $K/K_c > 0.6$.

It is now required to produce a design curve of W/W_c versus K/K_c from the theoretical curve in Figure 8b. Clearly the design curve must also pass through the point (1, 1) when the gutter discharges freely. When $K \to 0$, $W/y_o \to 2.8$ in both the theoretical and the design cases; the value equals 2.8 because of the provision of free-board equal to 2/7 the overall depth of the gutter. Writing

$$z = \frac{W}{W_c} \tag{61}$$

and using the subscript d to denote design values, it follows from equation (60) that

$$\frac{z_d}{z} = \left(\frac{W_c}{y_c}\right)\left(\frac{y_{cd}}{W_{cd}}\right)\left(\frac{K_{cd}}{K_c}\right)^{2/5} \text{ as } K \to 0 \tag{62}$$

Substituting the values obtained above gives

$$\frac{z_d}{z} = \left(\frac{4.232}{4.728}\right)\left(\frac{2.269}{2.135}\right)^{2/5} = 0.9172 \text{ as } K \to 0 \tag{63}$$

In order to scale from z to z_d for values of K/K_c between 0 and 1 the following equation was used

$$\frac{z_d}{z} = 0.9172 + 0.0828 \sin^{1/2}\left(\frac{\pi}{2}\frac{K}{K_c}\right) \tag{64}$$

where the square root power was chosen so as to ensure that values of z_d would increase uniformly as K/K_c was decreased below unity. Other types of scaling function could be used provided that they satisfy this requirement and give the correct values at the end points. Having obtained the value of z_d for a particular value of K/K_c, the corresponding design value of W/y_o was then found from equation (60).

The results of this procedure are shown plotted as the design curve in Figure 8a. At a late stage in the drafting of the revised CP 308 it was decided to omit this result because half-round gutters are seldom used as valley gutters and are therefore seldom designed for restricted discharge.

6 Gutters of non-standard cross-sectional shape

Exact theoretical results have been obtained in the previous sections for trapezoidal and half-round gutters, and corresponding results can in general be found for any gutter whose cross-sectional shape can be described by a single equation over the range of depths required. As an example, the surface width B of certain types of gutter may be related to the depth of flow y by a power-law equation such as

$$B = cy^m \tag{65a}$$

$$A = \frac{cy^{m+1}}{(m+1)} \tag{65b}$$

Particular cases of m = 0, 1, 2 correspond respectively to rectangular, triangular and parabolic cross-sectional shapes. Results will not however be given here since rectangular and triangular gutters are covered by the general case of trapezoidal gutters, and gutters with other values of m are seldom used.

If the cross-sectional shape of a gutter cannot be described by a single equation, approximate results may be obtained if it is represented by an equivalent trapezoidal gutter having equal values of B and A at a particular depth of flow y. It can easily be shown that the sole width B_s and the effective side-slope b of the equivalent gutter are given by

$$B_s = B\left(\frac{2A}{By} - 1\right) \tag{66}$$

$$b = \frac{2B}{y}\left(1 - \frac{A}{By}\right) \tag{67}$$

The equivalent gutter will normally only have the same values of A and B as the real gutter at one particular depth. If the sides of the real gutter become steeper with increasing depth, the value of b for the equivalent gutter will tend to decrease as y increases. In 3.1 it was shown that, for a given depth of flow at the downstream end, a rectangular gutter (b = 0) has a greater upstream depth of flow than a triangular gutter (b > 0). Therefore, if the sides of the real gutter become steeper with increasing depth, the values of A and B used in equations (66) and (67) should be those corresponding to the maximum depth of flow in the real gutter, which is the depth y_u at the upstream end. If, conversely, the sides become flatter as the depth increases, the values of A and B in equations (66) and (67) should correspond to the minimum depth of flow, which is the depth y_o at the downstream end. Approximate but conservative designs for non-standard gutters may then be obtained by using the previous results for trapezoidal gutters.

7 Effect of bends in gutters

If a length of gutter contains an angle or bend, some energy will normally be lost as the flow changes its direction. This energy loss will cause some backing-up of the flow at the upstream end of the gutter, and therefore will result in a reduction in the capacity of the gutter. The effect of energy loss at a bend in a smooth level gutter can be determined using the basic equations given in Section 2.

The case of a rectangular gutter of width B_s and length L having a bend at a distance x from the upstream end (see Figure 9) will be considered first; it will be assumed for convenience that the rate of lateral inflow is uniform along the length of the gutter. The depths of flow just upstream and downstream of the bend are y_2 and y_1 respectively, and it is assumed that the velocity distribution across the gutter is uniform at these points and at the outlet. Considering the balance between the flow forces at the outlet and at section 1 (just downstream of the bend) gives from equations (2) and (6)

$$\frac{1}{2}\rho g B_s y_o^2 + \frac{\rho Q_o^2}{B_s y_o} = \frac{1}{2}\rho g B_s y_1^2 + \frac{\rho Q_o^2}{B_s y_1}\left(\frac{x}{L}\right)^2 \qquad (68)$$

where Q_o is the discharge at the outlet. Introducing the Froude Number F_o defined by equation (4) and the ratios

$$p = \frac{y_u}{y_o} \qquad (8)$$

$$p_1 = \frac{y_1}{y_o} \qquad (8a)$$

$$p_2 = \frac{y_2}{y_o} \qquad (8b)$$

$$s = \frac{x}{L} \qquad (69)$$

enables equation (68) to be written as

$$p_1 (1 + 2F_o^2) = p_1^3 + 2F_o^2 s^2 \qquad (68a)$$

The energy loss at a bend is conventionally expressed as a proportion k of the velocity head of the flow entering the bend. Considering the total energy of the flow just upstream and downstream of the bend in the gutter therefore gives

$$E_2 - E_1 = \left(y_2 + \frac{v_2^2}{2g}\right) - \left(y_1 + \frac{v_1^2}{2g}\right) = k\frac{v_2^2}{2g} \qquad (70)$$

Using equations (4) and (8), this may be written as

$$p_2 + \frac{1}{2}(1 - k)\frac{F_o^2 s^2}{p_2^2} = p_1 + \frac{1}{2}\frac{F_o^2 s^2}{p_1^2} \qquad (71)$$

Finally, the balance between the flow forces at section 2 and the upstream end of the gutter gives

$$\frac{1}{2}p_2^2 + \frac{F_o^2 s^2}{p_2} = \frac{1}{2}p^2 \qquad (72)$$

If the values of k, F_o and s (the position of the bend) are fixed, there are three unknowns p, p_1 and p_2; the value of p can be found by eliminating p_1 and p_2 since there are three independent equations (68a),(71) and (72). A direct solution is possible for the case in which the gutter discharges freely ($F_o = 1$ and $p = p_c$, see 4.2) and the head loss coefficient k = 1 (an appropriate value for a sharp 90°

bend). It can then be shown that

$$s = \sqrt{\{p_1(3 - p_1^2)/2\}} \tag{73}$$

$$p_c = \sqrt{\left\{\frac{9(1 + p_1^2)^2}{16p_1^2} + \frac{4(3 - p_1^2)}{3(1 + p_1^2)}\right\}}, \tag{74}$$

The relationship between p_c and s can thus be found by choosing appropriate values of the ratio p_1. For a freely-discharging rectangular gutter it can be shown from equations (4), (6) and (21) that its capacity is given by

$$Q_o = B_s \sqrt{g} \left(\frac{y_u}{p_c}\right)^{3/2} \tag{75}$$

Since a straight rectangular gutter has a theoretical value of $p_c = \sqrt{3}$ (see 3.1), it follows that the capacity Q_o'' of the same gutter with a bend is given by

$$\frac{Q_o''}{Q_o} = \left(\frac{\sqrt{3}}{p_c}\right)^{3/2} \tag{76}$$

The variation of the ratio Q_o''/Q_o with the position of the bend is shown in Figure 10.

A similar method of solution can be used for the case of a smooth level triangular gutter. The balance between the flow forces at the outlet and at section 1 just downstream of the bend gives

$$(1 + \frac{3}{2} F_o^2)p_1^2 = p_1^5 + \frac{3}{2} F_o^2 s^2 \tag{77}$$

The loss of energy at the bend is given by equation (70) which may be written

$$p_2 + (1 - k) \frac{F_o^2 s^2}{4p_2^4} = p_1 + \frac{F_o^2 s^2}{4p_1^4} \tag{78}$$

while the balance of flow forces between section 2 and the upstream end gives

$$p_2^5 + \frac{3}{2} F_o^2 s^2 = p^3 p_2^2 \tag{79}$$

Taking as before the case in which $F_o = 1$, $k = 1$ and $p = p_c$, it is possible to express the ratios p_c and s in terms only of the ratio p_1 so that

$$s = p_1 \sqrt{\left(\frac{5 - 2p_1^3}{3}\right)} \tag{80}$$

$$p_c = \left[\left\{\frac{5(2p_1^3 + 1)}{12p_1^2}\right\}^3 + p_1^2 \frac{(5 - 2p_1^3)}{2} \left\{\frac{12p_1^2}{5(2p_1^3 + 1)}\right\}^2\right]^{1/3} \tag{81}$$

It can be shown from equations (4), (6) and (21) that the capacity Q_o of a freely-discharging triangular gutter is

$$Q_o = 2b \sqrt{g} \left(\frac{y_u}{2p_c}\right)^{5/2} \tag{82}$$

The theoretical value of p_c for a straight triangular gutter is $(5/2)^{1/3}$ (see 3.1), so that the capacity Q_o'' of the same gutter with a bend is given by

$$\frac{Q_o''}{Q_o} = \left(\frac{5}{2p_c}\right)^{5/6} \tag{83}$$

The variation of the ratio Q_o''/Q_o with the position of the bend is shown in Figure 10. Curves for trapezoidal and half-round gutters can be expected to lie between those for rectangular and triangular gutters because the results in previous sections have shown that the first two types of gutter are intermediate in character between the last two types. The closeness of the two curves in Figure 10 indicates that a single curve might be used for all normal types of gutter with little loss of accuracy.

Results from this Section are not included in the revised version of CP 308 because they are specific to the case of a freely-discharging gutter in which the head loss coefficient k = 1. In addition the assumption of a uniform velocity distribution across the gutter downstream of the bend is unlikely to be valid when the bend is close to the outlet. The method is however of interest and provides a means of determining effective values of the head loss coefficient k from experimental data.

8 Resistance effects in level gutters

Theory 8.1 The effect of hydraulic resistance on the capacity of level gutters is normally small, and can often be neglected since the design recommendations in CP 308 already apply a safety factor to the theoretical capacities obtained neglecting friction (see 4.1). It is shown below that frictional effects become more important as the length of a gutter is increased in relation to the depth of flow. Long lengths of gutter between outlets are sometimes used on large industrial buildings with clear internal spans (such as aircraft hangars), and it was therefore necessary to include in CP 308 a method for checking the effects of resistance in such cases.

The general equation describing steady gradually-varied flow in a gutter is given by equation (1). The friction slope S_f may be evaluated from the Darcy-Weisbach equation

$$S_f = \frac{\lambda V^2}{8gR} = \frac{\lambda Q^2 P}{8gA^3} \qquad (84)$$

where λ is a friction factor whose value varies with the Reynolds Number of the flow, the degree of turbulence in the flow and the relative roughness of the channel. Substituting equation (84) in equation (1) and putting $S_o = 0$ for a level gutter gives

$$\frac{dy}{dx} = \frac{(\lambda PQ^2/8 + 2AqQ)}{(BQ^2 - gA^3)} \qquad (85)$$

It will be assumed that the friction coefficient λ does not vary along the length of the gutter, and that the rate of lateral inflow q is uniform so that

$$q = \frac{Q_o}{L} \qquad (86)$$

where Q_o is the discharge at the outlet and L is the length of the gutter. Equation (85) can be written in a non-dimensional form by expressing the variable quantities A, B, P, Q x, y as ratios of the values which they have at the outlet. Using equation (4) therefore gives

$$\frac{d(y/y_o)}{d(x/L)} = \frac{(\frac{\lambda L}{8y_o}\frac{P_o}{B_o})(\frac{P}{P_o})(\frac{x}{L})^2 + 2(\frac{A_o}{B_o y_o})(\frac{A}{A_o})(\frac{x}{L})}{(\frac{B}{B_o})(\frac{x}{L})^2 - \frac{1}{F_o^2}(\frac{A}{A_o})^3} \quad (87)$$

For the case of a rectangular gutter this may be written in the form

$$\frac{dy_*}{ds} = \frac{\alpha\,(P/P_o)s^2 + 2y_* s}{s^2 - y_*^3/F_o^2} \quad (88)$$

where

$$\alpha = \frac{\lambda L}{8y_o} \cdot \frac{P_o}{B_o} \quad (89)$$

$$y_* = y/y_o \quad (90)$$

$$s = \frac{x}{L} \quad (69)$$

For convenience the asterisk for y_* will now be dropped, but it should be remembered that in the remainder of this section y is a non-dimensional quantity.

Equation (88) cannot be integrated directly, but Li[20] was able to obtain an approximate solution by assuming the quantity $(P/P_o)s^2$ to have a constant value. In fact the value of this quantity varies from 0 at the upstream end of the gutter to 1 at the outlet, so Li assumed it to have an average constant value of ½. Equation (88) can then be integrated and gives the following result for the value of $p' = y_u'/y_o$ at the upstream end of the gutter

$$p' = [1 + \frac{(8 + 3\alpha)}{4} F_o^2]^{I_r} \quad (91)$$

where

$$I_r = \frac{4 + \alpha}{8 + 3\alpha} \quad (92)$$

and y_u' is the non-dimensional depth of flow at the upstream end taking into account the effect of friction. This approximate solution has the advantage that when $\alpha = 0$ (ie $\lambda = 0$), it coincides with the theoretical value of p for a smooth gutter (equation (11)). The proportionate increase in p due to friction, $(p'-p)/p$, is shown plotted as a function of α and F_o in Figure 11a.

For the case of a triangular gutter, equation (87) gives

$$\frac{dy}{ds} = \frac{\alpha\,(P/P_o)s^2 + y^2 s}{ys^2 - y^6/F_o^2} \quad (93)$$

Li[20] was again able to solve this equation approximately by assuming the quantity $(P/P_o)s^2$ to have a constant value of ½, and obtained

$$p' = [1 + \frac{(6 + 5\alpha)}{4} F_o^2]^{I_t} \quad (94)$$

where

$$I_t = \frac{2 + \alpha}{6 + 5\alpha} \quad (95)$$

When $\alpha = 0$, p' coincides with the theoretical value of p for a smooth gutter (equation (12)). The proportionate increase in p due to friction, $(p'-p)/p$, is shown plotted as a function of α and F_o in Figure 11b. Comparison of Figures 11a and 11b shows that the curves for rectangular and triangular gutters are very similar.

The approximate solutions obtained by Li depend upon assuming the quantity $(P/P_o)s^2$ to have a constant value of ½ (similar types of solution could be obtained for other values of the constant). It can be shown that this assumption tends to underestimate the energy loss near the outlet, where it is greatest, but overestimate the energy loss further upstream. Therefore it was decided to obtain some numerical solutions of the exact equations for the flow profiles in order to provide a check of Li's approximate results. The calculations were carried out with an HP 67 programmable calculator, and involved use of a second-order difference scheme which gave the same level of accuracy as a first-order scheme in about one-third of the time.

The flow profile in a rectangular gutter is determined by equation (88) which may be written as

$$\frac{ds}{dy} = \frac{s^2 - y^3/F_o^2}{\alpha((e + 2y)/(e + 2))s^2 + 2ys} \tag{96}$$

where

$$e = \frac{B_s}{y_o} \tag{97}$$

The flow profile is therefore affected by the quantity e which is a measure of the aspect ratio of the channel; for the case of a wide rectangular gutter $e \to \infty$, so that in equation (96) the factor $(e + 2y)/(e + 2) \to 1$. It may be noted that the effect of the aspect ratio is not taken into account in Li's method. The numerical solution was carried out by specifying the values of F_o and e at the outlet, where $y = 1$ and $s = 1$, and then working in the upstream direction. Since the flow profiles rise steeply upstream of the outlet, a numerical scheme based on the use of equal increments Δs in the horizontal direction would not be very accurate; the method was therefore based on the inverse slope ds/dy and the use of equal increments Δy in the vertical direction. If the horizontal and vertical co-ordinates at two adjacent nodes are (s_n, y_n) and (s_{n+1}, y_{n+1}), with n increasing in the direction of flow, then Taylor's theorem gives to the second-order

$$s_n = s_{n+1} + (y_n - y_{n+1})\left(\frac{ds}{dy}\right)_{n+1} + \frac{1}{2}(y_n - y_{n+1})^2\left(\frac{d^2s}{dy^2}\right)_{n+1} \tag{98}$$

Since the calculations proceed in the upstream direction, the first and second derivatives are evaluated at the downstream node n+1; from equation (96) it can be shown that

$$\frac{d^2s}{dy^2} = \frac{1}{V^2}\left(V\frac{dU}{dy} - U\frac{dV}{dy}\right) \tag{99}$$

where

$$U = s^2 - \frac{y^3}{F_o^2} \tag{100a}$$

$$\frac{dU}{dy} = 2s\left(\frac{ds}{dy}\right) - \frac{3y^2}{F_o^2} \tag{100b}$$

$$V = \alpha\left(\frac{e + 2y}{e + 2}\right)s^2 + 2ys \tag{101a}$$

$$\frac{dV}{dy} = 2\left\{\alpha\left(\frac{e + 2y}{e + 2}\right)s + y\right\}\left(\frac{ds}{dy}\right) + 2s\left\{\frac{\alpha s}{(e+2)} + 1\right\} \tag{101b}$$

At the outlet of a freely-discharging gutter the slope ds/dy is zero, so in order to get the calculations started it was assumed that

$y = 1.000001$ when $s = 0$; the error introduced by this assumption was shown to be very small. Calculations proceeded in the upstream direction using equations (98) to (101) and a fixed increment $\Delta y = y_n - y_{n+1}$. The value of Δy was chosen so that there was a minimum of 100 increments between the outlet and the upstream end of the gutter; 100 increments correspond to a running-time on the HP 67 of about 20 minutes.

When the calculations approach the upstream boundary it is necessary to alter the numerical scheme so as to make the calculations terminate at the point $s = 0$. The values of y are increased steadily by the amount Δy until the calculated value of s just becomes negative; the calculations then return to the previous node whose co-ordinates are (s_1, y_1). The value of p' at the upstream end of the gutter is found by putting $n = 0$, $s_n = 0$ and $y_n = p'$ in equation (98) and solving as a quadratic to give

$$p' = y_1 + \frac{(ds/dy)_1}{(d^2s/dy^2)_1}\left[\left\{1 - \frac{2s_1(d^2s/dy^2)_1}{(ds/dy)_1^2}\right\}^{\frac{1}{2}} - 1\right] \qquad (102)$$

The program was checked by comparing the computed values of p for smooth gutters ($\alpha = 0$) with the theoretical values given by equation (11); the errors in the calculated values of the quantity $(p - 1)$ were all less than 0.35% when Δy was chosen to give at least 100 increments between the outlet and the upstream end of the gutter. As described above, the effect of the friction term α in equation (96) depends to a certain extent on the aspect ratio e of the gutter. Two cases were therefore considered, that of a wide rectangular gutter ($e \to \infty$) and that of a gutter having a value of $e = 3$; the latter corresponds to a gutter whose overall depth (including a suitable allowance for freeboard) is approximately equal to its width B_s. Results were obtained for various values of α and F_o, and are shown in Table 2a and Figure 11a, where they are compared with those obtained by Li[20].

A similar type of program was used to obtain numerical solutions for the effect of resistance in triangular gutters. The flow profile in a triangular gutter is given by equation (93) which may be written as

$$\frac{ds}{dy} = \frac{s^2 - y^5/F_o^2}{\alpha s^2 + ys} \qquad (103)$$

It should be noted that the aspect ratio of the gutter does not appear in this equation (cf equation (96) for rectangular gutters) since in triangular gutters the wetted perimeter P is always directly proportional to the depth of flow y. The numerical solution of equation (103) was obtained in a similar way to the solution described above for rectangular gutters, and used a second-order difference scheme based on equation (98). The second derivative d^2s/dy^2 in equation (98) is given by

$$\frac{d^2s}{dy^2} = \frac{1}{V'^2}\left(V'\frac{dU'}{dy} - U'\frac{dV'}{dy}\right) \qquad (104)$$

where

$$U' = s^2 - \frac{y^5}{F_o^2} \qquad (105a)$$

$$\frac{dU'}{dy} = 2s\left(\frac{ds}{dy}\right) - \frac{5y^4}{F_o^2} \qquad (105b)$$

$$V' = \alpha s^2 + ys \qquad (106a)$$

$$\frac{dV'}{dy} = (2\alpha s + y)\left(\frac{ds}{dy}\right) + s \qquad (106b)$$

Equation (102) was used, as before, to terminate the calculations at the upstream end of the gutter s = 0. The program was first checked against the theoretical values of p given by equation (12) for smooth triangular gutters (α = 0). Choosing the size of Δy so as to give a minimum of 100 increments between the outlet and the upstream end of the gutter produced results that, in terms of the quantity $(p - 1)$, were accurate to within 0.25% of the exact values. The calculations were then repeated for various values of α and F_o; results are shown in Table 2b and Figure 11b, where they are compared with those obtained by Li.

Since the values of p′ given by the numerical method are very close to the exact values, they provide a means of determining the accuracy of Li's approximate solutions, equations (91) and (94). Tables 2a and 2b and Figures 11a and 11b show that Li's method describes the theoretical results quite well, but tends to underestimate somewhat the effects of resistance. It is interesting to note from Table 2a that the aspect ratio e of a rectangular gutter can have a significant effect on the proportionate increase in p′; the effect is largest when the gutter is deep in relation to its width. Also the numerically-determined results show that the proportionate increase in the upstream depth, $(p'-p)/p$, is a maximum when the Froude Number is about 0.8, and not when F_o = 1.0 as indicated by Li's solutions. However, if one considers changes in the ratio $(p'-p)/(p-1)$, then one finds that the effect of resistance increases steadily as the Froude Number is decreased.

Friction factors for gutters 8.2 There is a large amount of experimental data concerning friction factors for channels with constant discharge, and summaries of the results are given in standard texts such as Henderson[16]. Briefly, it has been found that the non-dimensional friction factor λ defined in equation (84) depends upon the relative roughness of the channel and upon the Reynolds Number R_e where

$$R_e = \frac{4VR}{\nu} \qquad (107)$$

For $R_e < 2000$ approximately, the flow is laminar and

$$\lambda = \frac{64}{R_e} \qquad (108)$$

A transition between laminar and smooth-turbulent flow normally occurs when the Reynolds Number is in the range $2000 < R_e < 5000$. The roughness of the channel does not affect the value of the friction factor in smooth-turbulent flow and λ is given by

$$\lambda = \frac{0.316}{R_e^{1/4}} \quad \text{for } R_e < 10^5 \qquad (109)$$

$$\frac{1}{\sqrt{\lambda}} = 2.0 \log_{10}\left(\frac{R_e\sqrt{\lambda}}{2.51}\right) \quad \text{for } R_e > 10^5 \qquad (110)$$

Equation (109) is known as the Blasius equation. A further transition to rough-turbulent flow occurs at a Reynolds Number which depends upon the equivalent sand roughness k_s of the channel. In fully rough-turbulent flow the Reynolds Number does not influence the value of λ which is given by

$$\frac{1}{\sqrt{\lambda}} = 2 \log_{10} \left(\frac{12R}{k_s}\right) \qquad (111)$$

where k_s is the equivalent sand roughness of the surface. The transition between smooth- and rough-turbulent flow depends upon the type of roughness, but for many surfaces including those of commercial pipes it can be represented by the Colebrook-White equation[17]

$$\frac{1}{\sqrt{\lambda}} = -2 \log_{10} \left(\frac{k_s}{14.8R} + \frac{2.52}{R_e\sqrt{\lambda}}\right) \qquad (112)$$

There is a very limited amount of data concerning friction factors for channels with lateral inflow, and it is often assumed that appropriate values of λ can be calculated from the equations that apply to channels with constant discharge. Yen, Wenzel and Yoon[26] showed that this assumption is not generally valid, and that the friction factor required in the momentum equation is different from that required in the energy equation. In the case of the momentum equation (which is used in the present study, see Section 2) the friction factor should relate to the shear stress acting around the perimeter of the channel and not to the energy gradient of the flow. Yen, Wenzel and Yoon[26] analysed the results of experiments on overland flow produced by rainfall, and found that the friction factors calculated from the momentum equation were greater than those obtained from pipe test data. The results are not directly applicable to gutters because the depths of flow were small with Reynolds Numbers between 900 and 10^4 . Typical values of Reynolds Number at the downstream end of a roof gutter lie in the range $2 \times 10^4 < R_e < 5 \times 10^5$, although it should be noted that the Reynolds Number varies along the gutter and is zero at the upstream end.

Keulegan[19] analysed some unpublished data of Beij on flow profiles in sloping gutters in order to obtain estimates of the effective value of λ. The best fit to the data was given by

$$\lambda = \frac{1280}{R_e} \qquad (113)$$

which surprisingly has the form of the laminar flow equation, equation (108), but with a much larger numerator on the right-hand side. For a value of $R_e = 5 \times 10^4$, equation (113) gives $\lambda = 0.026$ which is somewhat higher than the corresponding figure of $\lambda = 0.021$ given by equation (109). The higher values of λ produced by equation (113) are presumably due to the additional turbulence caused by the lateral inflow. The inflow does not however appear to produce a transition to rough-turbulent flow since the form of equation (113) is very different from that of equation (111). Keulegan did not find any systematic variation of λ with the rate of inflow, but this may be because the extra dissipation due to the lateral inflow depends upon the ratio q/Q which remains constant irrespective of the absolute value of q. Equation (113) is assumed to be valid up to the point at which it crosses the Blasius equation, equation (109), which occurs at a value of $R_e = 6.5 \times 10^4$. At higher Reynolds Numbers it is assumed that the friction factor is the same as it would be if there were no lateral inflow. The data used by Keulegan exhibit quite a large scatter and the equation of the line which forms an upper bound to the values of λ is approximately

$$\lambda = \frac{400}{R_e^{0.85}} \qquad (114)$$

This gives a value of $\lambda = 0.041$ at $R_e = 5 \times 10^4$, and crosses the smooth-turbulent line at about $R_e = 1.4 \times 10^5$.

Fox and Goodwill[14] obtained numerical solutions of equation (1) and compared them with some experimental results. The authors proposed a modified version of Powell's equation in the form

$$\frac{1}{\sqrt{\lambda}} = -2.62 \log_{10} \left\{ \frac{4.01}{R_e\sqrt{\lambda}} + \frac{\epsilon}{R} + K \frac{u}{V} \right\} \qquad (115)$$

where ϵ is a measure of the surface roughness of the channel, and the third term in the bracket depends upon the lateral inflow; u is the mean velocity of the lateral inflow and V that of the flow along the channel. Details of the values of λ and the constant K were not however given. Gill[15] obtained approximate solutions of equation (1) for subcritical flows in sloping gutters using a series-type expansion in powers of the quantity F_o^2. Agreement between the theory and some experiments that were carried out was patchy, and it was found necessary to use a value of $\lambda = 0.08$ instead of the value of $\lambda = 0.026$ given by the Blasius equation, equation (109); the corresponding figures predicted by equations (113) and (114) would be $\lambda = 0.059$ and $\lambda = 0.082$ respectively. Lin et al[21] adopted a different approach by assuming that the friction factor was given correctly by the equations for flow with constant discharge, and that the apparent increase in λ was due to the non-uniform velocity distribution in the channel caused by the lateral inflow. This method was applied to the data used by Keulegan[19], and gave values of the momentum coefficient as high as 4.7, which seems improbable.

Equation (113) appears to be a reasonable fit to the limited amount of experimental data that are available, while equation (114) could be used for design when it is important not to underestimate the effects of friction. Data from the various experiments described above are generally consistent in showing that lateral inflow produces a larger increase in λ at low Reynolds Numbers than it does at high Reynolds Numbers.

Design curves 8.3 As described in 8.1, it was necessary to include in CP 308 a method for determining the effect of resistance in long gutters. The increase in the upstream depth of flow due to resistance can be calculated theoretically as described in 8.1, and Figures 11a and 11b show that the resulting curves for rectangular and triangular gutters are very similar. Since half-round and trapezoidal gutters are intermediate in character between rectangular and triangular gutters, it is possible to define a single set of curves that are sufficiently accurate for the design of nearly all types of gutter.

The major problem is, however, the choice of a suitable value of the friction factor λ when calculating the value of α from equation (89). In order to simplify the design method it was decided to use a fixed value of $\lambda = 0.04$. According to equation (113) this corresponds to a Reynolds Number of about 3×10^4, which might typically occur near the outlet of a rectangular gutter with a sole width of 0.15m and an aspect ratio of $e = 5$. Larger gutters would have smaller values of λ, but the use of a fixed value of $\lambda = 0.04$ should not lead to serious overdesign since the effects of resistance will be small in most practical cases. If one considers the case of a freely-discharging rectangular gutter with $e = 5$ (a typical value), it can be shown that $\lambda = 0.04$ is equivalent to a Manning's n of 0.011 when the sole width $B_s = 0.1$m and to $n = 0.015$ when $B_s = 0.5$m.

The value of α in Equation (89) depends also upon the ratio P_o/B_o. Gutters tend to be relatively wide in relation to their depth, and the worst case that might normally occur is that of a relatively deep rectangular gutter having an aspect ration e = 3 (see equation (97)). This gives a value of $P_o/B_o = 5/3$; most other types of gutter will have values of P_o/B_o that are closer to unity. If it is then assumed that $\lambda = 0.04$, it can be shown from equation (89) that $L/y_o = 120\alpha$. This simplifies the presentation of the results obtained in 8.1 since the increase in upstream depth can now be expressed in terms of L/y_o and F_o only. The resulting design curve for CP 308 is shown in Figure 12a, and provides a small margin of safety compared with the numerically-determined results given in Table 2.

When designing level gutters, it is reasonable to neglect the effects of resistance if they increase the upstream depth of flow by less than about 5%, since the standard design method in CP 308 already includes a factor of safety (see 4.1). From Figure 12a it can be seen that a 5% increase will not occur unless $L/y_o > 100$ approximately. In terms of the overall depth y_g of the gutter the limit is approximately equivalent to $L/y_g > 50$, and this has been adopted in CP 308 as the criterion for deciding whether the effect of resistance needs to be taken into account.

The application of Figure 12a to the case of half-round gutters is more difficult than to that of trapezoidal gutters, so a table of capacity reduction factors has been included in CP 308 for use when the length of an eaves gutter is more than 50 times its overall depth y_g. The figures in the table were obtained by the following procedure. First it was assumed that, with resistance taken into account, the gutter was just flowing full at its upstream end. A value for the proportionate increase in the upstream depth due to resistance was then chosen. This gave the upstream depth of flow that would occur in a smooth gutter if it were carrying a flow equal to the reduced capacity of the rough gutter. The corresponding depth at the downstream end was then found from the theoretical solution for smooth gutters (equation (15)with equation (13)). The reduced capacity Q_o' of the rough gutter was calculated from equation (35), and compared with the theoretical discharge Q_o for a similar smooth gutter just flowing full at its upstream end (equations (36) and (37)). Figure 12a was used next to find the value of L/y_o that corresponded to the chosen value of the proportionate increase in upstream depth. This ratio was then converted to an equivalent value of L/y_g and plotted against the value of the capacity reduction factor Q_o'/Q_o. Results for true half-round gutters are shown in Figure 12b, but nominal half-round gutters were found to give closely similar values. As described above, it was decided in CP 308 to neglect the effect of resistance if the length of the gutter was less than 50 times its overall depth. Figure 12b also shows the design curve that was adopted for CP 308, and from which the capacity reduction factors in the revised code were obtained.

9 Freely-discharging sloping gutters

General 9.1 Gutters around the periphery of a building are normally set either level or at a nominal fall (< 1/350) in order to prevent the ponding of water. However, unusual roof layouts may sometimes require the use of steeper gutters, and it is therefore of interest to know how the capacity of a gutter is affected by slope.

Flow profiles in sloping gutters can be determined by integrating the gradually-varied flow equation

$$\frac{dy}{dx} = \frac{S_o - S_f - 2qQ/(gA^2)}{1 - BQ^2/(gA^3)} \qquad (1)$$

The form of the equation prevents direct solutions, so integration normally has to be carried out numerically. The principal features of flow profiles in sloping gutters can however be found by considering the special case of a wide rectangular channel in which the wetted perimeter P approximately equals the width B_s of the gutter. Equation (1) can be written in a more suitable form by defining two notional depths of flow y_c and y_n: y_c is the depth that would occur if the flow were at critical depth, and y_n is the depth if the flow were at normal depth (ie $S_f = S_o$). From equations (4) and (84) it can be shown that for a wide rectangular channel

$$\frac{Q^2}{gB_s^2} = y_c^3 = \left(\frac{8S_o}{\lambda}\right) y_n^3 \qquad (116)$$

where Q is the discharge at a point distance x from the upstream end. Thus if the quantity $8S_o/\lambda > 1$, the normal-depth line along the gutter will lie below the critical-depth line, and vice versa. Substituting equations (116) and (84) in equation (1) and assuming the rate of lateral inflow to be uniform gives

$$\frac{dy}{dx} = S_o \left[\frac{1 - \left(\frac{y_n}{y}\right)^3 - 2\left(\frac{y_c}{S_o x}\right)\left(\frac{y_c}{y}\right)^2}{1 - \left(\frac{y_c}{y}\right)^3} \right] \qquad (117)$$

The third term of the numerator inside the bracket represents the effect of the lateral inflow, and has an important influence on the shape of the flow profiles, three examples of which are shown diagrammatically in Figure 13.

If the gutter has a mild slope ($8S_o/\lambda < 1$), the flow profile crosses the normal-depth line and reaches a maximum depth upstream of the outlet (Figure 13a); the position of the maximum depends upon the value of $8S_o/\lambda$, and moves to the upstream end of the gutter as the slope tends to zero. If the gutter has a steep slope ($8S_o/\lambda > 1$), the flow is supercritical at the outlet if the gutter is sufficiently long (Figure 13b). In this case the flow is subcritical near the upstream end, and passes smoothly through critical depth before becoming supercritical; the depth of flow does not reach a maximum but increases steadily towards the outlet. If the gutter is shorter, the flow does not have sufficient distance in which to become supercritical (Figure 13c); the depth increases to a maximum upstream of the outlet and then decreases again.

The three profiles considered in Figure 13 indicate that flow in a sloping gutter will remain subcritical provided that its length is less than a certain figure determined by the slope and roughness of the gutter. The general criterion dividing subcritical and supercritical flow can be found from equation (1). Since the denominator on the right-hand side of the equation is zero when the flow passes through critical depth, the numerator must also be zero otherwise there would be a discontinuity in the flow profile. If a critical section occurs at a distance L_c from the upstream end of the gutter, then it follows from equations (1) and (84) that

$$S_o - \frac{\lambda Q_c^2 P_c}{8gA_c^3} - 2\frac{Q_c^2}{gA_c^2 L_c} = 0 \qquad (118)$$

where it is assumed that the rate of lateral inflow is uniform. Since the flow is at critical depth

$$\frac{B_c Q_c^2}{g A_c^3} = 1 \qquad (119)$$

so that equation (118) may be written

$$L_c = \frac{(2\frac{A_c}{B_c})}{S_o - \frac{\lambda}{8}\frac{P_c}{B_c}} \qquad (120)$$

If the length of the gutter is less than L_c the flow will be sub-critical even though the slope might be sufficient to produce super-critical flow in a similar channel carrying a constant discharge; the difference in behaviour is due to the effect which the lateral inflow has on the flow in the gutter.

The exact equations for flow in sloping gutters are not amenable to further simplification, but useful results can be obtained by considering channels whose cross-sectional shape can be described by means of a power-law of the form

$$B = cy^m \qquad (65a)$$

$$A = \frac{c}{m+1} y^{m+1} \qquad (65b)$$

It will also be assumed that the channels are relatively wide compared with the depth of flow so that the wetted perimeter P can be taken to be equal to the width of flow B; if necessary, errors resulting from this assumption can be corrected by using an effective friction factor λ_e given by

$$\lambda_e = \lambda \frac{P}{B} \qquad (121)$$

Using equations (65) and (119) it is now possible to relate the critical length L_c in equation (120) directly to the rate of lateral inflow q (assumed uniform along the gutter). The general result is

$$L_c = \left[\frac{2}{S_o\,(1 - \frac{\lambda}{8S_o})}\right]^{\frac{2m+3}{2m+1}} \left[\frac{q}{(m+1)^m\, c\sqrt{g}}\right]^{\frac{2}{2m+1}} \qquad (122)$$

which for the case of a rectangular gutter ($m = 0$, $c = B_s$) gives

$$L_{cr} = \frac{8q^2}{g\, B_s^2 S_o^3\, (1 - \frac{\lambda}{8S_o})^3} \qquad (123)$$

and for a triangular gutter ($m = 1$, $c = b$) gives

$$L_{ct} = \left[\frac{8q^2}{g\, b^2 S_o^5\, (1 - \frac{\lambda}{8S_o})^5}\right]^{1/3} \qquad (124)$$

Trapezoidal gutters are intermediate in character between rectangular and triangular gutters, and therefore will have effective values of m that lie between 0 and 1. Equation (65) also enables equation (120) to be expressed in non-dimensional form as

$$\frac{\lambda L_c}{8y_c} = \frac{2}{(m+1)\,(\frac{8S_o}{\lambda} - 1)} \qquad (125)$$

The quantities $\lambda L_c/8y_c$ and $8S_o/\lambda$ will also be found to occur in the results obtained in the following sections.

Approximate solutions 9.2 Two approximate solutions of the gradually-varied flow equation, equation (1), can be obtained by assuming that the flow is either close to normal depth or close to critical depth. These solutions are useful in providing a general picture of the way in which the depth of flow in a gutter varies as the slope is altered.

If the flow is close to normal depth, the friction slope S_f differs from the bed-slope S_o of the gutter by only a small amount ϵ so that

$$S_f = S_o\,(1 - \epsilon) \tag{126}$$

where ϵ is small. From equation (1) ϵ is given by

$$\epsilon = \frac{1}{S_o}\left\{(1 - \frac{BQ^2}{gA^3})\,\frac{dy}{dx} + \frac{2Qq}{gA^2}\right\} \tag{127}$$

A first-order solution can be obtained by letting $\epsilon = 0$, which gives rise to a flow profile that coincides with the normal-depth line (see Figure 13). This first-order solution may then be used to calculate the corresponding value of ϵ from equation (127). Substituting in equation (84) gives to the second-order in ϵ

$$Q = (1 - \frac{\epsilon}{2})\,(\frac{8gA^3 S_o}{\lambda P})^{1/2} \tag{128}$$

Clearly the assumption that ϵ is small will not be valid at the upstream end, but it will be reasonable near the downstream end of a steep gutter in which the flow becomes supercritical (see Figure 13b). A second-order solution for the depth of flow y at a point x from the upstream end can be found from equation (128) when the gutter is wide and of the type described by equation (65); the result that is obtained after a certain amount of algebra is

$$y = (fx^2)^{\frac{1}{2m+3}}\left[1 + \frac{2}{(2m+3)S_o}\left\{\frac{(1-G)}{(2m+3)} + \frac{G}{(m+1)}\right\}(fx^{-(1+2m)})^{\frac{1}{2m+3}}\right] \tag{129}$$

where

$$G = \frac{8S_o}{\lambda} \tag{130}$$

$$f = \frac{(m+1)^3 q^2}{gc^2 G} \tag{131}$$

It is now convenient to express the value of y as a ratio of the depth y_c that would occur if the flow at the same point were at critical depth. Substituting equation (65) in equation (4) gives

$$y_c = \left[G\,fx^2\right]^{\frac{1}{2m+3}} \tag{132}$$

so that

$$\frac{y}{y_c} = G^{-\frac{1}{(2m+3)}}\left[1 + \frac{2}{(2m+3)}\,G^{-\frac{(2m+4)}{(2m+3)}}\left\{\frac{(1-G)}{(2m+3)} + \frac{G}{(m+1)}\right\}.(\frac{8y_c}{\lambda x})\right] \tag{133}$$

When a gutter is long enough for the flow to become supercritical the maximum depth y_m occurs at the outlet (x = L); this is the condition to which equation (133) approximates most nearly since the flow there is close to normal depth. Thus

$$\frac{y_m}{y_o} = G^{-\frac{1}{(2m+3)}}\left[1 + \frac{2}{(2m+3)}\,G^{-\frac{(2m+4)}{(2m+3)}}\left\{\frac{(1-G)}{(2m+3)} + \frac{G}{(m+1)}\right\}.\frac{1}{\alpha_o}\right] \tag{134}$$

where

$$\alpha_o = \frac{\lambda L}{8y_o} \tag{135}$$

and y_o is the depth at the outlet if the flow there were to be at critical depth; note that α_o is the limiting value of α (equation (89)) for a wide gutter.

A similar approach can be used for the case in which the slope of a gutter is not quite steep enough to produce supercritical flow at the outlet. The flow in the gutter is then subcritical and the maximum depth, which is located just upstream of the outlet, is only slightly greater than the critical depth at the outlet (see Figure 13c). At the point of maximum depth $x = x_m$, $y = y_m$ and $dy/dx = 0$. Therefore from equations (1) and (84)

$$S_o - \frac{\lambda Q_m^2 P_m}{8gA_m^3} - 2\frac{Q_m^2}{gA_m^2 x_m} = 0 \tag{136}$$

where the subscript m denotes the values of the quantities at the point $x = x_m$; it is assumed here that the rate of lateral inflow is uniform along the gutter. At the outlet the flow is at critical depth so that

$$\frac{B_o Q_o^2}{gA_o^3} = 1 \tag{4a}$$

Describing the cross-sectional shape of the gutter by equation (65), and assuming it to be wide in relation to the depth of flow (so that $P \approx B$), then gives

$$(\frac{x_m}{L})^2 + \frac{2}{(m+1)\alpha_o}(\frac{y_m}{y_o})(\frac{x_m}{L}) - G(\frac{y_m}{y_o})^{2m+3} = 0 \tag{137}$$

where y_o is the depth of flow at the outlet (equal to critical depth), and G and α_o are given by equations (130) and (135) respectively. For a given value of α_o (fixed by the properties of the gutter and by the discharge that it carries), there is a limiting value of G (ie slope S_o) for which the maximum depth is located at the outlet and just equals the critical depth. From equation (137) it may be seen that this limiting value G_o is given by

$$G_o = 1 + \frac{2}{(m+1)\alpha_o} \tag{138}$$

This agrees with equation (125) for the case where the critical section is located at the outlet so that $L_c = L$ and $y_c = y_o$. When G is slightly less than G_o, the flow in the gutter is subcritical and

$$\frac{G}{G_o} = 1 - \beta \tag{139a}$$

$$\frac{x_m}{L} = 1 - \delta \tag{139b}$$

$$\frac{y_m}{y_o} = 1 + \eta \tag{139c}$$

where the quantities β, δ and η are all small. Substituting in equation (137) and retaining terms up to the first-order in γ, δ and ϵ gives

$$(1 - 2\delta) + \frac{2}{(m+1)\alpha_o}(1 + \eta - \delta) - G_o(1 - \beta + (2m+3)\eta) = 0 \tag{140}$$

Equating terms of zero-order leads again to equation (138). Equating the first-order terms in γ, δ and ϵ and using equation (138) gives

$$G_o\beta - [1 + 2(m+1)G_o]\eta = (G_o + 1)\delta \tag{141}$$

Since the quantity $\delta \geqslant 0$ it follows that

$$\eta \leqslant \frac{G_o \beta}{[1 + 2(m+1)G_o]} \qquad (142)$$

which thus provides an upper limit for the value of η in relation to the value of β. Substituting for β and G_o from equations (139a) and (138) gives finally

$$\frac{y_m}{y_o} \leqslant 1 + \left[\frac{2 - (m+1)(G - 1)\alpha_o}{(m+1)[4 + (2m+3)\alpha_o]}\right] \qquad (143)$$

Although this approximate result is expressed as an inequality (the equality only applies when $y_m/y_o = 1$), it is useful since it indicates how the ratio y_m/y_o varies when α_o is fixed and G is reduced below the limiting value of G_o. It is interesting to note that the same quantities m, G and α_o also appear in equation (134), which applies when the flow is close to normal depth.

Approximate design method 9.3

The approximate results obtained in the previous section suggest that the variation of the maximum depth of flow y_m in a sloping gutter can be presented as a plot of the ratio y_m/y_o against the non-dimensional quantities G and α_o; y_o is the depth of flow at the outlet if the flow there were at critical depth, which is the case when G is less than the limiting value G_o. Although exact results have not been obtained they provide sufficient information to enable the shape of the curves to be estimated.

Figure 14a demonstrates the case of a wide rectangular gutter (m = 0) where curves of y_m/y_o versus G are plotted for constant values of α_o. For large values of G (ie for steep slopes), the flow at the outlet is supercritical and the maximum depth there is only slightly greater than the normal depth; this part of the curve is approximated by equation (134). The value of y_m/y_o increases as G (ie the slope) is decreased, but equation (134) tends to underestimate the amount of the increase when the flow is no longer close to normal depth. This can be seen from Figure 14a since each curve must pass through the point $y_m/y_o = 1$, $G = G_o$, where G_o is the limiting value given exactly by equation (138). The shape of the curves for $G < G_o$ is indicated by equation (143) which provides an upper limit for the value of y_m/y_o. Results have already been obtained in Section 8.1 for the case when G = 0, $\alpha_o > 0$ (ie a level, non-smooth gutter), and Figure 11a thus enables the upper ends of the curves to be located. Equation (143) no longer applies when G is significantly less than G_o, but it is apparent from Figure 14a that the curves must be concave upwards for $G < G_o$. Estimated shapes for the complete curves are shown dashed in Figure 14a. An equivalent set of curves for the case of a wide triangular gutter (m = 1) is shown in Figure 14b, and it can be seen that they exhibit the same features as those for the rectangular gutter.

The shapes of the curves in Figures 14a and 14b suggest a simple approximation that could be used for designing sloping gutters when the flow in them is subcritical (ie when $G \leqslant G_o$). As described above the curves of y_m/y_o versus G are concave upwards for $G < G_o$, so that a safe approximation to the maximum depth of flow can be obtained by assuming that each curve is in fact a straight line between the point where G = 0 and the point where $G = G_o$ and $y_m/y_o = 1$ (see Figure 14c). If the value of y_m/y_o at G = 0 is equal to p, then it follows that

$$\frac{y_m}{y_o} = 1 + (p - 1)\left(\frac{G_o - G}{G_o}\right) \qquad (144)$$

Substituting for G and G_o from equations (130) and (138) gives finally

$$\frac{y_m}{y_o} = p - (p - 1)\left\{\frac{8S_o}{\lambda + \frac{16}{(m+1)}\frac{y_o}{L}}\right\} \qquad (145)$$

It is recommended in CP 308 that a design figure of p = 2 be used for level rectangular gutters (G = 0), so that equation (145) then becomes

$$\frac{y_m}{y_o} = 2 - \left\{\frac{8S_o}{\lambda + 16\frac{y_o}{L}}\right\} \qquad (146)$$

The equivalent design figure for a level triangular gutter is approximately p = 1.5 (accurate value 1.480) so that equation (145) then gives

$$\frac{y_m}{y_o} = 1.5 - \left\{\frac{4S_o}{\lambda + 8\frac{y_o}{L}}\right\} \qquad (147)$$

Equations (146) and (147) provide a possible means of designing sloping gutters, and give safe estimates of the maximum depth of flow. They are only valid if the flow in the gutter is subcritical, and therefore should not be used if they give values of $y_m/y_o < 1$. The results were obtained for wide gutters in which $P \approx B$, but an effective value of λ (as given by equation (121)) can be used if this assumption is not reasonable; suitable values of P and B could be calculated for a depth intermediate between y_o and y_m. However the error caused by assuming the channel to be wide is unlikely to be significant compared with the error in choosing a suitable value for the friction factor λ (see 8.2).

The design method described above has not been included in the revised version of CP 308 because the method has not been checked experimentally. The Code states that a sloping gutter will have a higher capacity than a similar level gutter, but recommends that this increase should be viewed as an additional factor of safety.

PART II : GUTTER OUTLETS

10 Description of tests

It has been shown in Part I that the capacity of a gutter depends partly upon the capacity of the outlet to which it discharges. If the head required to pass flow through an outlet is less than the corresponding critical depth in the gutter, the flow is able to discharge freely from the gutter. However, if the outlet requires a head that is greater than critical depth, the flow will back up along the gutter and its capacity will be reduced. The purpose of the tests carried out for HRS by the British Hydromechanics Research Association (BHRA) was to determine the head-discharge relationship for various types of outlet in gutters and box-receivers. Full details of the tests and the experimental arrangement are given by Crow and Barnes [13], and will only be summarised briefly here.

Since the tests were concerned with flow conditions near the outlet, it was unnecessary to reproduce the effect of lateral inflow along the gutter. The experimental arrangement is shown in Figure 15 and 16, and consisted of two channels each approximately 2.5m long connected to a central section in which the outlets and the box-receivers were mounted. Independently variable flows were introduced at the upstream ends of the channels which were long enough to produce uniform flow conditions at the outlet. Two cross-sectional shapes of channel were used in the tests: one was rectangular with a width of 152.4mm, and the other was trapezoidal with a sole width of 152.4mm and equal side slopes of 2 units horizontal to 1 unit vertical (see Figures 17a, b). The tests were designed to study the effects of the following factors:

(a) The plan shape of the outlet (either rectangular or circular)

(b) The cross-sectional shape of the outlet (sharp-edged, round-edged or tapered)

(c) The size of the outlet relative to the size of the channel

(d) The position of the outlet in the channel or box-receiver

(e) Flows from one direction, and equal or unequal flows from opposite directions

(f) The cross-sectional shape of the channel (either rectangular or trapezoidal)

A total of 77 different conditions were tested, and these are summarised in Table 3.

The capacity of an outlet depends upon the length of downpipe to which it is connected. If the downpipe is short, a control section occurs at or near the level of the outlet in the gutter or box-receiver, and this determines the capacity of the outlet. If the downpipe is longer, the flow may entrain air in the downpipe and thereby cause it to run full. When this occurs the flow is no longer controlled at the outlet, but is subject to the full head between the gutter and the bottom of the downpipe. Although the capacity of the outlet increases considerably when this occurs, the "priming" of the downpipe tends to be intermittent and cannot be relied upon to occur. Outlets for roof gutters are therefore normally sized on the basis that the flow is controlled at the outlet itself.

In order to prevent priming occurring in the tests, only short downpipes were connected to the outlets; the length of the downpipes was made equal to the hydraulic diameter of the outlet (i.e. = 4 x plan area of outlet/wetted perimeter of outlet, see Fig. 16).

The rectangular outlets tested were all sharp-edged, but with the circular outlets comparisons were made between sharp-edged, round-edged and tapered outlets (see Figure 17). CP 308 : 1974 [3] states that it is possible to taper an outlet without reducing its capacity provided that the amount of taper does not exceed certain limits; the type of outlet that was tested (Figure 17e) corresponds to this limiting taper. The radius of curvature of the round-edged outlets (Figure 17d) was specified in terms of the diameter of the outlet, and chosen so that the ratio between the top and bottom diameters was equal to that of the tapered outlets.

Depths of flow along each length of channel were measured by means of six pressure tappings connected to gauge wells equipped with vernier point gauges (see Figure 15b). Water levels in the box-receivers were measured using two pressure tappings in the base of the box and three scales mounted around the sides (see Figure 15b).

11 Theoretical background

Previous studies 11.1 Kalinske [18] carried out experiments on the capacity of vertical drain and overflow pipes. Drain pipes are those which are installed flush with the base of a tank or channel, while overflow pipes are those which project above the base. The tests were carried out in a large cylindrical tank, and care was taken to ensure that the flow towards the outlet was radial. Kalinske tested pipes with internal diameters of 44mm, 94mm and 148mm, and in the case where the downpipes did not flow full obtained the following relation.

$$Q = CH^2\sqrt{gD} \qquad (148)$$

where Q is the discharge, H is the head above the outlet, D is the diameter and C is a dimensionless number. The values of C showed a fair amount of scatter, and varied between 4.3 and 3.3 for drain pipes and between 4.8 and 4.0 for overflow pipes. The head H is equal to the total head above the outlet since it was measured far away from the outlet where the velocity of the flow was effectively zero. The form of Eqn (148) is surprising because it does not correspond to the form that might be expected if the flow were of weir-type ($Q \propto DH^{1.5}$) or of orifice-type ($Q \propto D^2H^{0.5}$). A possible explanation is that critical-depth flow occurs upstream of the outlet so that the effective weir length is greater than the perimeter of the outlet; this possibility is considered in greater detail in Appendix A. Although Kalinske's results are of interest, they cannot be applied directly to the case of outlets in gutters because the approach conditions of the flow are very different.

Measurements of the capacity of a circular outlet connected to the sole of a gutter were made by Bonnington[2]. The gutter was 1.37m long, and the flow was introduced at its upstream end. The gutter was of trapezoidal cross-section (sole width of 114mm, and equal side-slopes of 2 units horizontal to 1 unit vertical), and the diameter of the sharp-edged outlet was 74mm. Two distinct types of flow were found to occur. At low heads (< D/4 approximately) the flow was of weir-type and given by

$$Q = 0.65 \sqrt{g}\ (\pi D)\ h^{3/2} \qquad (149)$$

This equation is, however, open to doubt because analysis of the measurements indicates that the flow in the gutter was super-critical with a Froude Number of about 1.3; this is not consistent with the existence of a critical-depth control around the perimeter of the outlet. At higher heads the flow was subcritical and of orifice-type. When swirl was prevented the capacity was given by

$$Q = 0.67\ A \sqrt{2gh} \qquad (150)$$

where A is the plan area of the outlet. When swirl occurred the capacity of the outlet was reduced to

$$Q = 0.52\ A \sqrt{2gh} \qquad (151)$$

In Eqns (149), (150) and (151) the head h was the static head measured by a pressure tapping located 152mm upstream of the outlet.

The equations given in CP 308: 1974[3] for the capacity of circular outlets are based on Bonnington's results described above, but the coefficients are somewhat reduced so as to give convenient values when the equations are expressed in metric units. The values of the coefficients used in CP 308: 1974 are 0.643 in Eqn (149), 0.606 in Eqn (150), and 0.454 in Eqn (151). In the code these equations apply both to an outlet in the sole of a gutter and to an outlet in a box-receiver, even though the approach conditions are different in the two cases. In the case of a box-receiver the flow moves only slowly around the sides so that the static head nearly equals the total head (as in the case of Kalinske's results, Eqn (148)). In a gutter, by contrast, the velocity of the flow approaching an outlet may account for a significant proportion of the total head. Since the equations in CP 308: 1974 use the actual depth of flow, it might have been expected that different values of the constants would have been needed in the two cases. This aspect is considered again in the light of the BHRA results.

Flow profile in channel 11.2 As described in Section 10 the measurements that were made in the BHRA tests included water level profiles along the channels, and it is interesting to compare these with the corresponding theoretical profiles. The flow in a channel may be described by the gradually-varied flow equation, Eqn (1), subject to the conditions listed in Section 2. Since the channel is level ($S_o = 0$) and the lateral inflow q is zero, Eqn (1) becomes

$$\frac{dy}{dx} = \frac{-S_f}{\left(1 - \frac{BQ^2}{gA^3}\right)} \qquad (152)$$

Substituting for S_f from Eqn (84) and re-arranging gives

$$\frac{dy}{dx} = \frac{-\frac{\lambda}{8}\frac{P}{B}}{\left(\frac{gA^3}{BQ^2} - 1\right)} \qquad (153)$$

If the Froude Number at the outlet is F_o then

$$F_o^{\,2} = \frac{B_o Q^2}{gA_o^{\,3}} \qquad (4)$$

where the subscript o denotes the values of A and B that correspond to the depth y_o at the outlet. Substituting in (153) then gives

$$\frac{dy}{dx} = \frac{-\frac{\lambda}{8}\frac{P}{B}}{\frac{1}{F_o^2}\left(\frac{A}{A_o}\right)^3\left(\frac{B_o}{B}\right) - 1} \tag{154}$$

For the case of a rectangular channel with a sole width of B_s, Eqn (154) becomes

$$\frac{dy}{dx} = \frac{-\frac{\lambda}{8}\left(1 + \frac{2y}{B_s}\right)}{\frac{1}{F_o^2}\left(\frac{y}{y_o}\right)^3 - 1} \tag{155}$$

If y is the depth of flow at a distance $x_1 = L - x$ upstream of the outlet, and if ratios y_* and e are defined such that

$$y_* = \frac{y}{y_o} \tag{90}$$

$$e = \frac{B_s}{y_o} \tag{97}$$

Eqn (155) may be written

$$\frac{1}{8y_o}\int_0^{x_1} \lambda \, dx = \int_1^{y_*} \left\{ \frac{\frac{y_*^3}{F_o^2} - 1}{1 + \frac{2y_*}{e}} \right\} dy_* \tag{156}$$

This can be integrated exactly provided that λ is assumed to be constant, and gives

$$\lambda = \frac{4y_o}{x_1}\,\frac{e}{F_o^2}\left[\frac{(y_*^3 - 1)}{3} - e\frac{(y_*^2 - 1)}{4} + e^2\frac{(y_* - 1)}{4} - \frac{(F_o^2 + e^3)}{8}\log_e\left(\frac{2y_* + e}{2 + e}\right)\right] \tag{157}$$

This equation therefore enables an average value of λ to be calculated from the measured flow profile along a channel. If the width of the rectangular channel is large compared with the depth of flow, $e \to \infty$ and Eqn (156) then gives

$$\lambda = \frac{8y_o}{x_1}\left[\frac{(y_*^4 - 1)}{4F_o^2} - (y_* - 1)\right] \tag{158}$$

A similar method can also be applied to the general case of a trapezoidal channel. If the channel has equal side-slopes of b/2 (see Eqn (6a), then it can be shown from (154) that

$$\lambda = \frac{8y_o}{x_1}\left[\left\{\frac{(1 + u)}{F_o^2\left(1 + \frac{u}{2}\right)^3}\right\} I_1 - I_2\right]_1^{y_*} \tag{159}$$

where

$$I_1 = \frac{u^2 y_*^6}{48a} + \frac{1}{5}\left(\frac{3}{4} - \frac{1}{8a}\right)\frac{uy_*^5}{a} + \frac{1}{4}\left(\frac{3}{2} - \frac{3}{4a} + \frac{1}{8a^2}\right)\frac{y_*^4}{a}$$

$$+ A\left\{\frac{y_*^3}{3au} - \frac{y_*^2}{2a^2u^2} + \frac{y_*}{a^3u^3} - \frac{1}{a^4u^4}\log_e(1 + auy_*)\right\} \qquad (160a)$$

$$I_2 = \frac{y_*}{a} + \frac{(a-1)}{a^2u}\log_e(1 + auy_*) \qquad (160b)$$

$$A = 1 - \frac{3}{2a} + \frac{3}{4a^2} - \frac{1}{8a^3} \qquad (160c)$$

$$y_* = \frac{y}{y_o} \qquad (90)$$

$$u = \frac{by_o}{B_s} \qquad (9)$$

$$a = \left(\frac{4 + b^2}{b^2}\right)^{\frac{1}{2}} \qquad (160d)$$

Eqn (157) was applied to some of the measurements obtained in the BHRA tests with the rectangular channel, and calculated values of λ are given in Table 4. Tests in which the flow discharged freely ($F_o = 1$) were chosen because they gave larger values of the ratio y_*, and therefore minimised the effect which standing waves in the channel had on the measurements of the depth of flow; the values of y_o at the downstream end were calculated from the discharge assuming that the flow was at critical depth. The calculated values of λ are compared in Table 4 with those predicted by the Blasius equation, Eqn 109, which is appropriate because the channel had a smooth finish and the Reynolds Number R_e was of the order of 2×10^4 to 1×10^5; the values of R_e were determined for the mean depth in the channel, i.e. $(y_o + y_1)/2$. The calculated values are somewhat higher than the predicted values, but the agreement is reasonable considering the sensitivity of Eqn (157) to any errors in the values of y_*.

Types of flow control 11.3

When plotted logarithmically the results of the BHRA tests generally have the form shown in Figure 18. At low heads the flow is of weir-type while at higher heads the flow is of orifice-type with $Q \propto h^{0.5}$. Weir-type flow occurs as a result of the existence of a control section at which the flow passes through critical depth. In the present tests the control section could either be located across the gutter a short distance upstream of the outlet or around the perimeter of the outlet itself. Crow & Barnes [13] plotted the critical-depth lines for the gutters together with the experimental values of discharge and head, and thereby showed that the control section occurred in the gutter for all but the smallest outlets. Figure 18a shows typical plots of discharge Q versus static head h (measured at tapping A in Figure 15b), while Figure 18b shows the corresponding plots of Q versus total head H. The values of H were calculated assuming the velocity distribution of the flow to be uniform across the channel so that

$$H = h + \frac{Q^2}{2gA^2} \qquad (161)$$

where A is the cross-sectional area of flow corresponding to the depth h. The equation of the critical depth line connecting the discharge Q to the critical depth y_c and the corresponding minimum total head (or specific energy) H_c is found by solving the equations

$$Q = \left(\frac{gA_c^3}{B_c}\right)^{\frac{1}{2}} \qquad (162)$$

$$H_c = y_c + \frac{A_c}{2B_c} \qquad (163)$$

where the subscript c denotes values at the critical depth. In the experiments the measurements of static head h in the weir-flow region sometimes lay a little above or below the theoretical critical depth line given by Eqns (162) and (163). Possible reasons for these discrepancies are considered below.

Measurements of the velocity distribution in the gutter were made at the start of the tests, and these indicated that the energy coefficient α had a value of about 1.10 which agrees with previously published data (see Chow [11] p. 28). If the value of α is greater than unity, Eqn (163) remains the same but Eqn (162) is altered to

$$Q = \left(\frac{gA_c^3}{\alpha B_c}\right)^{\frac{1}{2}} \qquad (162a)$$

Thus if the value of α in a rectangular channel is 1.10, it can be shown that the actual value of critical depth will be about 3% greater than that given by Eqn (162).

Discrepancies between measured and theoretical depths are also likely to occur if the control section is not located exactly at the pressure tapping where the head h is measured. Measurements by Rouse [24] of flow at a free overfall show that curvature of the flow causes the depth at the brink to be about 0.715 of the critical depth y_c. The critical section occurs at a distance of about 3-4 y_c upstream of the brink so that its position varies with discharge. A similar type of behaviour can be expected to occur just upstream of an outlet in a gutter. The pressure tapping in the gutter will therefore tend to underestimate or overestimate the critical depth, depending upon whether the critical section is located upstream or downstream of the tapping.

Errors in the depth of flow measured by a pressure tapping will also be caused by the curvature of the flow as it draws down towards the outlet. The effect of this curvature can be estimated as follows. The flow profile along a wide, rectangular gutter discharging freely ($F_o = 1$, $y_o = y_c$) is given by Eqn (158) which may be written in the form

$$\frac{\lambda x_1}{8y_c} = \frac{1}{4}\left(\frac{y}{y_c}\right)^4 - \left(\frac{y}{y_c}\right) + \frac{3}{4} \qquad (164)$$

If the depth is y at a distance x_1 upstream of the critical section, and if y is only slightly greater than the critical depth y_c so that

$$y = y_c\,(1 + \omega) \qquad (165)$$

then substituting in Eqn (164) gives to the second-order in ω

$$\omega = \left(\frac{\lambda x_1}{12 y_c}\right)^{\frac{1}{2}} \tag{166}$$

The radius of curvature R of the water surface is given by

$$R = \frac{\left\{1 + \left(\frac{dy}{dx}\right)^2\right\}^{3/2}}{\frac{d^2y}{dx^2}} \tag{167}$$

Substituting for dy/dx and d^2y/dx^2 from Eqn (155) and evaluating at the point x_1 upstream of the critical section gives to the first order in ω

$$R = \frac{8 y_c}{\lambda} \cdot \omega \tag{168}$$

The acceleration a of the fluid at the surface due to the curvature of the flow is

$$a = \frac{V^2}{R} \approx \frac{g\, y_c}{R} \tag{169}$$

since the flow is close to critical depth. Substituting for R from Eqn (168) and using Eqn (166) then gives to the first order

$$\frac{a}{g} = \left(\frac{3}{16}\ \lambda\ \frac{y_c}{x_1}\right)^{\frac{1}{2}} \tag{170}$$

The curvature of the flow as it draws down towards the outlet will cause the pressure at the tapping to be somewhat lower than hydrostatic. As an example consider the case of a wide rectangular channel in which $\lambda = 0.02$ and $y_c = 50$mm. At a point $x_1 = 25$mm upstream of the critical section the actual depth of flow y is found from Eqns (164) and (165) to be 51.4mm. However the curvature of the flow will, from Eqn (170), reduce the effective value of gravity to 0.913g. Thus the tapping would record a pressure equivalent to a hydrostatic depth of water of 47.0mm. This calculation tends to overestimate somewhat the effect of curvature because it is based on the curvature at the surface which is greater than the average curvature through the whole depth of the flow. However it does show how a tapping can indicate that the flow is supercritical when in fact it is still subcritical.

Although the experimental measurements of static head h do not always lie exactly on the critical depth line for the reasons described above, the discrepancies are very much smaller when the results are plotted in terms of the total head H. The reason for this can be found by considering the case of a rectangular gutter in which the static head h is slightly greater than the critical depth y_c so that

$$h = y_c(1 + \tau) \tag{171}$$

Substituting in Eqn (161) and using Eqns (162) and (163) gives to the second order in τ

$$\frac{H}{H_c} = 1 + \tau^2 \tag{172}$$

If, for example, the static head is 3% greater than the critical depth, the total head will be less than 0.1% greater than the minimum specific energy. Since the measurements of static head tend to show a certain amount of scatter, it was decided that the plots of discharge Q versus total head H provided the best means of determining whether or not the flow was controlled by a critical depth section in the gutter. For outlets in box-receivers there is no effective difference between static head and total head because the flow in the box is moving only slowly except in the immediate vicinity of the outlet.

Use of static head or total head 11.4 The experimental results show that the transition between weir-type flow and orifice-type flow is usually well defined (see Figure 18). Most of the outlets conformed surprisingly closely to an orifice-type equation, although some of the round-edged and tapered outlets behaved somewhat differently as described in 11.5. Before analysing the results, it is necessary to decide whether the orifice equation used should have the form $Q \propto h^{0.5}$ or $Q \propto H^{0.5}$. From a theoretical point-of-view one might expect the total head H to be the correct quantity because it takes into account the velocity of the flow approaching the outlet. If the static head h is used it implies that the initial velocity head of the flow is lost before it enters the outlet since it does not contribute to the velocity of the flow through the vena contracta which forms at the outlet. Visual observations during the tests suggested that when the flow was of orifice-type it entered the outlets smoothly with little sign of energy dissipation. However the choice between h and H must be made on the basis of the experimental results, and as described below these tend to support the use of the static head h.

At points well above the transition from weir-type flow to orifice-type flow, the difference between h and H becomes very small because the velocity of the flow is low. Therefore in order to differentiate between the two alternatives, it is necessary to consider the shapes of the experimental curves just above the point of transition. Assume first that the orifice equation has the form

$$Q = C_d \, A_p \, \sqrt{2gh} \qquad (173)$$

where A_p is the plan area of the outlet. If the transition from weir-flow to orifice-flow were well defined, a logarithmic plot of Q against h would show a sudden change of slope, as illustrated diagrammatically in Figure 19a. The corresponding total head H is found by substituting Eqn (173) in Eqn (161) to give

$$H = h \left\{ 1 + \left(\frac{C_d \, A_p}{A} \right)^2 \right\} \qquad (174)$$

where A is the cross-sectional area of the gutter corresponding to the depth h. When Q is plotted against H (see Figure 19b), this equation produces a transition curve that is convex upwards and which approaches the straight line in Figure 19a asymptotically as $H \to \infty$. If, however, the orifice equation is assumed to have the form

$$Q = C_{d1} \, A_p \, \sqrt{2gH} \qquad (175)$$

then a plot of Q versus H will show a sharp transition as shown in Figure 19d. The correspnding equation connecting Q and h is found from Eqns (161) and (175) to be

$$Q = C_{d1} A_p \sqrt{\left\{ \frac{2gh}{1 - \left(\frac{C_{d1} A_p}{A} \right)^2} \right\}} \qquad (176)$$

which when plotted logarithmically gives a transition curve that is convex downwards as shown in Figure 19c. Comparison of the experimental results with Figure 19 shows that the majority of the tests had curves which were closer to those in Figure 19a and b than those in Figures 19c and d. Therefore, despite an initial preference in favour of total head, it was decided that the results for orifice-flow should be analysed in terms of static head and Eqn(173).

The use of static head has the practical advantage of making the results easier to apply to the design of gutters. As seen in Part I, the capacity of a gutter depends upon finding the relationship between the depths of flow at the upstream and downstream ends of the gutter; Eqn (173) gives the downstream depth directly whereas an intermediate step would have been needed to determine h from H if Eqn (175) had been used. The differences between equations based on static head and total head do not arise when one considers outlets in box-receivers; here the depth of flow is measured at the side of the box where the flow is moving only slowly so the static head is effectively equal to the total head.

Round-edged and tapered outlets 11.5

As mentioned in 11.4 some of the round-edged and tapered outlets exhibited a different type of transition from the sharp-edged outlets. A typical example is shown in Figure 20, where it may be seen that the transition curve has a shape that is convex-downwards in the plots of both the static head and the total head. However as the head increases, the curve straightens out and tends towards a straight line that corresponds to "simple" orifice-type flow. Two possible explanations for this behaviour can be suggested.

Firstly, since the round-edged and tapered outlets provide smoother entry conditions than the sharp-edged outlets, less of the energy associated with the velocity of the flow in the gutter may be lost. This would suggest that an orifice equation involving total head (Eqn (175)) would be more suitable than one involving static head (Eqn (173)), and this would partly explain the shape of the transition curve in Figure 20a (cf Figure 19c). However the use of total head would not explain the curved transition in Figure 20b.

The second explanation concerns the position of the vena contracta which is produced by the outlet, and which causes it to act as an orifice. If the vena contracta is located a distance z below the plane of the outlet, then the correct form of the orifice equation is

$$Q = C_{d2} A_p \sqrt{2g(h+z)} \qquad (177)$$

Thus if Eqn (173) is used to analyse the results, the calculated values of C_d will be greater than the "correct" values of C_{d2} given by Eqn (177). In the case of a sharp-edged outlet, the distance z will be relatively small because the streamlines that form the vena contracta have to remain horizontal until they reach the lip of the outlet. This would explain why Eqn (173) appears to be a good fit to the experimental data for the sharp-edged outlets. In the case of a round-edged outlet, the streamlines are able to curve downwards before separating, and therefore form a vena contracta at a greater distance below the plane of the outlet. At low heads z will be of the same order as h, and will therefore give an effective value of C_d

that is significantly higher than C_{d2} in Eqn (177). At higher heads z may increase somewhat, but it is likely to become smaller in relation to h and therefore cause C_d to tend towards C_{d2}. Thus if the experimental data are analysed according to Eqn (173), the calculated values of C_d will appear to decrease as the head increases. This behaviour would therefore help to explain the shape of the curves in Figures 20a and b. Since the distance between the vena contracta and the plane of the outlet varies with the head and is difficult to predict, it was decided that the results for the round-edged and tapered outlets should be analysed in the same way, using Eqn (173), as the sharp-edged outlets.

12 Calculation of discharge coefficients

The experimental results, as discussed in Section 11.3, show that two distinct types of flow can occur in a gutter or box-receiver containing an outlet. At low heads the flow is of weir-type, but at higher heads it changes to orifice-type. The measurements in each test were therefore analysed at HRS to determine best-fit values of the discharge coefficients corresponding to the two types of flow.

The analysis of the data for the orifice-flow regime is simpler than that for the weir-flow regime, and will be considered first. The discharge equation used for the analysis was

$$Q = C_d A_p \sqrt{2gh} \qquad (173)$$

where Q is the rate of flow in the gutter, h is the corresponding static head measured at the tapping immediately upstream of the outlet (tappings A or B in Figure 15b), A_p is the inlet area of the outlet measured in plan, and C_d is the non-dimensional discharge coefficient for orifice flow. The values of A_p for the round-edged and tapered outlets were calculated in terms of their top diameters. In the case of the outlets in box-receivers, the value of h used was the depth of water measured by the pressure tappings and/or the scales on the sides of the box (see Section 10).

The best-fit value of C_d for a particular set of measurements depends to a certain extent on the variable that is chosen as the basis of the calculations. For example, it would be possible to treat the discharge Q as the independent variable and h as the dependent variable, and then minimize the standard deviation in h; this procedure would however tend to bias the results towards the values of C_d associated with the highest heads. The method adopted was to calculate from Eqn (173) the value of C_d corresponding to each pair of measurements of Q and h, and then to take the algebraic mean $\bar{C}_d$ of the values in each particular test. There are two main advantages of this approach. Firstly, the method is also suitable for calculating discharge coefficients for results in the weir-flow regime. Secondly, the standard deviation σ of the individual values of C_d provides a convenient measure of the accuracy of Eqn (173); the value of σ for a set of N measurements is given by

$$\sigma = \sqrt{\frac{\Sigma(C_d^2) - (\Sigma C_d)^2/N}{N-1}} \qquad (178)$$

Confidence limits for a particular mean value of $\bar{C}_d$ can be expressed in terms of the standard error S_e where

$$S_e = \frac{\sigma}{\sqrt{N}} \qquad (179)$$

For cases where the flow approached the outlet from two directions, separate values of $\bar{C}_d$ were calculated for the two flows using the corresponding measurements of h and Q. The overall value of $\bar{C}_d$ for the outlet was then obtained by adding the two individual values.

When the flow is of weir-type, the results indicate that a control section normally occurs in the gutter and not around the perimeter of the outlet. It is therefore possible to express the results in terms of a non-dimensional gutter coefficient C_g such that

$$Q = C_g \; Q_{cg} \qquad (180)$$

where Q is the measured flow and Q_{cg} is the theoretical flow that would occur if the outlet did not restrict the discharge of the gutter; Q_{cg} is therefore the maximum flow in the gutter corresponding to the measured value of total head H. It may be seen that C_g is similar but not equal to the Froude Number F_o in Eqn (4). In Section 11.4 it was decided that the analysis of the weir-flow results should be based on the total head H rather than on the static head h. From Eqn (163) the measured value of H has a corresponding value of critical depth y_c given by

$$H = y_c + \frac{A_c}{2B_c} \qquad (181)$$

It should be noted that since y_c is based on H, it is not the same as the value of critical depth that corresponds to the measured discharge Q. From Eqn (4) the theoretical discharge Q_{cg} is given by

$$Q_{cg} = \sqrt{\left(\frac{gA_c^3}{B_c} \right)} \qquad (182)$$

where A_c and B_c are the area and width of flow corresponding to y_c. Q_{cg} is therefore the theoretical discharge that would occur if a flow, with the same value of total head H that was measured in the experiments, were able to discharge freely.

For the case of a rectangular gutter of width B_s it is convenient to introduce non-dimensional forms of the measured discharge Q, the static head h, and the total head H, such that

$$Q_* = \frac{Q}{\sqrt{g}\, B_s^{\,5/2}} \qquad (183a)$$

$$h_* = \frac{h}{B_s} \qquad (183b)$$

$$H_* = \frac{H}{B_s} \qquad (183c)$$

It can then be shown from Eqns (161), (173), (181) and (182) that

$$H_* = h_* + \frac{1}{2} \left(\frac{Q_*}{h_*} \right)^2 \qquad (184)$$

$$C_g = Q_* \left(\frac{3}{2H_*}\right)^{3/2} \qquad (185)$$

Individual values of C_g were determined from Eqns (183) to (185) for each pair of measurements of Q and h, and the algebraic mean $\bar{C}_g$ of the values in each particular test then taken; the corresponding value of the standard deviation σ was calculated from Eqn (178) with C_g replacing C_d.

The case of weir-type flow in a trapezoidal gutter is a little more complicated. If the sole width of the gutter is B_s and the effective side-slope is b (Eqn (6)), then from Eqns (161) and (184)

$$H_* = h_* + \frac{Q_*^2}{h_*^2(2 + bh_*^2)} \qquad (186)$$

Next it is necessary to find from Eqn (181) the value of the critical depth y_c that corresponds to the measured total head H. Putting

$$y_{c*} = \frac{y_c}{B_s} \qquad (183d)$$

it can be shown that

$$y_{c*} = \frac{2bH_* - 3 + \sqrt{(9 + 8bH_* + 4b^2 H_*^2)}}{5b} \qquad (187)$$

Finally substituting y_{c*} in Eqns (180) and (182) gives

$$C_g = Q_* \left[\frac{(1 + by_{c*})}{y_{c*}^3 (1 + \frac{b}{2} y_{c*})^3}\right]^{1/2} \qquad (188)$$

The mean value $\bar{C}_g$ for each test, together with the corresponding value of the standard deviation σ, were calculated in the same way as described above for the rectangular gutter.

The results for the circular outlets in box-receivers suggest that, despite the confused flow conditions within the box, weir-type flow did occur at low heads. Since in this case the flow can be expected to be controlled at the outlet itself, the results were expressed in terms of a non-dimensional weir coefficient C_w such that

$$Q = C_w \, Q_{cw} \qquad (189)$$

where Q_{cw} is the theoretical capacity of a weir corresponding to the value of total head H measured in the experiments. Assuming that the flow passes through critical depth around the perimeter of the outlet, the theoretical discharge Q_{cw} is given by

$$Q_{cw} = \left(\frac{2}{3}\right)^{3/2} \pi D \, g^{1/2} \, H^{3/2} \qquad (190)$$

where D is the top diameter of the outlet. Since the depth of water in the box-receivers was measured at the sides where the flow was moving only slowly, the measured static head h was effectively equal to the total head H. The value of the weir coefficient for each pair of measurements of Q and h was therefore calculated from

$$C_w = \left(\frac{3}{2}\right)^{3/2} \frac{Q}{\pi D\, g^{1/2}\, h^{3/2}} \qquad (191)$$

The mean value $\bar{C}_w$ and the standard deviation σ for each test were calculated in the way described above for C_d and C_g.

The calculated values of $\bar{C}_d$ and $\bar{C}_g$ or $\bar{C}_w$ in each test are listed, together with their standard deviations, in Table 3. Values marked with an asterisk are those for which the experimental points did not conform very well to the orifice-flow or weir-flow equations. Values marked with a p are those where there was evidence that the outlet began to prime when it was deeply submerged.

13 Discussion of results

Orifice coefficients

13.1 The principal conclusions that can be drawn from the results in Table 3 are that the majority of the larger sharp-edged outlets conformed closely to the theoretical orifice-flow equation, Eqn (173), and that the values of C_d were mostly in the range 0.6 to 0.7. Overall mean values of C_d for each of the main types of outlet are given in the first parts of Tables 5a,b,c. It can be seen that the plan shape of the outlet (i.e rectangular, square or circular) had little effect on the overall values of C_d. More surprisingly perhaps, the circular outlets in the box-receivers had similar values of C_d to those of the circular outlets in the gutters, even though the approach conditions were very different. However it was necessary to list the 1″ x 1″ and 1″ϕ sharp-edged outlets separately in Tables 5a,b because they had significantly higher values of C_d than the other sizes of outlet. The discharge coefficients for the round-edged and tapered outlets were calculated in terms of their top diameters. Table 5b shows that the mean value of C_d for the round-edged outlets is about 14% less than that for the sharp-edged outlets, while the value for the tapered outlets is about 14% greater.

Some of the tests did not conform so closely to the theoretical orifice equation, and these are indicated in Table 3 by means of asterisks. This occurred mostly with the round-edged and tapered outlets which tended to exhibit a more gradual transition between weir-flow and orifice-flow; a possible explanation of this behaviour was discussed in 11.5. The values of C_d marked with a p in Table 3 indicate those tests where there was a sudden increase in discharge for only a small increase in head. This tended to occur with the smaller outlets when they were deeply submerged, and may have been due to the outlets priming and causing the short lengths of downpipe to run full.

The second parts of Tables 5a,b,c indicate how the values of C_d were influenced by the various factors listed in (a) to (f) of Section 10. The variations in C_d were calculated by comparing pairs of tests in which all but one of these conditions were the same. The "average variation in C_d" is the average percentage change for the group of tests used in that particular comparison; the significance of the average variation can be judged from the "range" which gives the maximum positive and negative changes within that group.

The effects of the various factors in Table 5 may be summarised as follows:

(a) *Plan shape of outlet.* Circular outlets generally have slightly higher discharge coefficients than rectangular outlets of the same size; the difference is more marked when the outlet is small.

(b) *Cross-sectional shape of outlet.* For circular outlets of the same top diameter, tapered outlets have higher capacities than sharp-edged outlets, which in turn have higher capacities than round-edged outlets. For outlets of the same bottom diameter, sharp-edged outlets have the lowest capacities.

(c) *Relative size of outlet.* This has the largest effect on the discharge coefficients of circular outlets; the smaller the outlet in relation to the gutter, the larger the value of C_d . However the relative size has little effect on rectangular outlets unless they are very small.

(d) *Position of the outlet.* Moving a circular outlet further from a stop-end decreases its capacity significantly. However the capacity of a circular outlet in a box-receiver may decrease slightly if it is moved from the centre of the box. Moving an outlet from the centre-line of the gutter to one side reduces the capacity if it is rectangular, but increases it if it is circular.

(e) *Flow from two directions.* The capacity of an outlet is generally higher when the flow approaches from two directions rather than one direction.

(f) *Cross-sectional shape of gutter.* Overall the capacity of an outlet varies little whether the gutter is rectangular or trapezoidal; however individual cases show quite large variations.

The above summary shows that it is difficult to draw definite conclusions about the effect of some of the factors. It is probable that all outlets in gutters are subject to a certain amount of swirl because the gutters prevent radial flow towards the outlets; Plates I & II indicate the existence of swirl in two typical tests. Although rectangular outlets are inherently less efficient than circular outlets because of their corners, they are likely to produce less swirl in the approaching flow and be less sensitive to changes in the local geometry. This is borne out by the results which show greater variability in the discharge coefficients of the circular outlets. The various effects noted above in (a) to (f) tend to suggest that the changes which increase the discharge coefficients are those which would be expected to reduce the amount of swirl. However the existence of swirl does not explain why the smaller outlets generally had higher values of C_d than the larger ones. All the outlets were tested over approximately the same range of flow depths, so that in terms of the ratio h/D the smaller outlets were more deeply submerged than the larger ones. Increasing the submergence of an outlet tends to straighten the flow lines and thereby increase the area of the vena contracta and lower the level at which it forms (see 11.5); both these effects would tend to produce an apparent increase in the discharge coefficient C_d. Finally it should be remembered that many of the variations in C_d considered above are relatively small and may not be very significant when determining design capacities.

Gutter coefficients 13.2 Observations and photographs of the tests show that the flow conditions around the gutter outlets were quite complex at low heads when the flow was of weir-type (see Plates III and IV). Plate III shows a case where the flow is from only one direction; the flow enters the outlet smoothly on the upstream side, but on the

downstream side a plunging jet is formed by the water which has backed up against the stop-end. Plate IV shows the case of flow from two directions: plunging jets form on either side of the outlet at the points where the two flows meet. Values of the weir coefficient C_w calculated from Eqns (189) and (190) were found to be considerably greater than unity, but in view of the observations described above it is not surprising that the results did not correspond to the normal type of weir equation based on the occurrence of critical depth around the perimeter of the outlet. As described in Section 12, it was found that the results could best be expressed in terms of a gutter coefficient C_g applied to the theoretical discharge Q_{cg} that would occur if a flow with the same total head H as the measured flow Q were able to discharge freely (Eqns (180) and (182)).

When flows approached an outlet from two directions it was found that the depths of water on either side of the outlet were approximately equal, and were determined by the larger of the two flows (and not by the combined flow as in the case of the orifice coefficients). Separate values of C_g for the two flows are given in Table 3 for tests C,F,H amd J. Where the flows were unequal, the value of C_g for the larger flow is written above that for the smaller flow; in these cases, however, the value for the smaller flow has little significance.

A study of Table 3 shows that the values of C_g are more variable than the orifice coefficients considered in 13.1. A general pattern in the values of C_g can be discerned by considering the amount of curvature which the geometry of the outlet (in plan) imposes on the flow: the greater the curvature, the lower the value of C_g. It can be shown (Appendix B) that the minimum energy required for a given discharge is greater if the flow is curved than if it is not. Conversely, for a given total energy, the discharge will be less if the flow is curved than if it is straight, even though both flows discharge freely. This argument suggests that a critical-flow section does occur in the gutter upstream of the outlet, but that the velocity of flow through the section is non-uniform because of the curvature produced by the outlet. As a result the discharge is somewhat less than predicted by the normal critical-flow equation for uniform flow.

It can be seen from Table 3 that the values of C_g for the largest outlets were very close to unity, being in the range 0.98 to 0.99. This indicates that the outlets did not significantly affect or restrict the flow in the gutter upstream of the outlet. In the case of the smaller rectangular outlets it is reasonable to assume that the portion of the flow which discharges directly into the outlet along its upstream-facing edge is little affected by the geometry of the outlet. However the remainder of the flow has to converge inwards towards the sides of the outlet, and this can be expected to reduce the value of C_g. It is therefore suggested that the overall value of C_g for a rectangular outlet can be expressed in the form

$$C_g = \frac{\gamma_o W + \gamma_1 Y_1 + \gamma_2 Y_2}{\bar{B}} \qquad (192)$$

where $\bar{B}$ is the depth-averaged width of flow (= A/y), W is the width of the outlet measured normal to the centre-line of the gutter, and Y_1 and Y_2 are the depth-averaged widths of flow on either side of the outlet (see Figure 21). The quantity γ_o is the unrestricted value of the discharge coefficient C_g, which for convenience can be taken as constant and equal to 0.985; γ_1 and

γ_2 are the coefficients corresponding to the widths Y_1 and Y_2 respectively.

In the case of the tests in the rectangular gutter $\bar{B}$ was constant and equal to the sole width of the gutter. The outlets were positioned either on the centre-line of the gutter so that $Y_1 = Y_2$ or offset so that $Y_2 = 0$. For these two positions Eqn (192) can therefore be written

$$C_g = \gamma_o \frac{W}{\bar{B}} + \gamma_1 \left(1 - \frac{W}{\bar{B}}\right) \qquad (193)$$

Putting $\gamma_o = 0.985$, it was therefore possible to calculate a value of γ_1 for each test.

In the case of the trapezoidal gutter $\bar{B}$ varied with the depth of flow so it was necessary to use an average figure when calculating γ_1. A suitable value of the depth-averaged width of flow in each test was calculated from the formula

$$\bar{B} = B_s + \frac{1}{4} b\, y_w \qquad (194)$$

where B_s is the sole width of the gutter, b is the effective side slope (see 3.1), and y_w is the maximum depth up to which weir-flow persisted in the test. In most of the tests the outlet was positioned on the centre-line of the gutter so that γ_1 could be calculated from Eqn (193). However, in Tests E.1 and E.2 the outlets were offset so that the width Y_2 in Figure 21 was small but not zero. Since the curvature of the flow in the width Y_2 is small, it is reasonable to assume that the corresponding value of γ_2 is equal to the unrestricted value γ_o. Eqn (192) can then be written

$$C_g = \gamma_o \left(1 - \frac{Y_1}{\bar{B}}\right) + \gamma_1 \frac{Y_1}{\bar{B}} \qquad (195)$$

This equation, with $\gamma_o = 0.985$, was therefore used to calculate the values of γ_1 in Tests E.1 and E.2.

As described above the value of γ_1 is believed to depend upon the amount of curvature of the flow near the outlet, and a suitable measure of this is the ratio Y_1/L_e where L_e is the effective length of the outlet measured parallel to the centre-line of the gutter (see Figure 21). If the flow is from one direction L_e is equal to the actual length L of the outlet; if there are flows from two directions, the length L has been divided between the flows in proportion to their magnitudes (see Plate IV). Calculated values of the quantities γ_1 and Y_1/L_e for the rectangular outlets are given in Table 6 and plotted in Figure 22. The latter shows that γ_1 tends to decrease steadily as the value of Y_1/L_e is increased. When $Y_1/L_e < 0.5$, it appears that the sides of the outlet are long enough to accept the flow without causing any significant backing-up in the gutter. When $Y_1/L_e > 0.5$ the flow is forced to turn more sharply into the outlet, and this has the effect of reducing γ_1. Although there is a greater amount of scatter at the higher values of Y_1/L_e, there do not seem to be any consistent differences between the various sets of data.

Tables 3c,d,e show that the values of C_g for the circular outlets are affected by the following factors:

(a) *Relative size of the outlet*. Decreasing the size of the outlet decreases C_g.

(b) *Position of the outlet*. The value of C_g increases when the outlet is moved away from a stop-end, and decreases when it is offset from the centre-line of the gutter.

(c) *Flow from two directions*. The value of C_g for the gutter carrying the larger flow is decreased as the flow from the other direction is increased.

Thus changes which increase the curvature of the flow at the outlet reduce the value of C_g. It is interesting to note that the effects on C_g of the above factors are the opposite of their effects on the orifice coefficient C_d (see 13.1).

Unlike the case of the rectangular outlets, it is difficult to devise a simple theory for predicting the overall value of C_g for a circular outlet. The values of C_g have therefore been plotted in Figure 23 as a function of the quantity $D_o/\bar{B}$, where D_o is the top diameter of the outlet and $\bar{B}$ is the depth-averaged width of flow defined by Eqn (194); the values of C_g and $D_o/\bar{B}$ are listed in Table 7. The data for the outlets positioned on the centre-line of the gutter have been divided into three groups: flow from one direction ($Q_B = 0$); unequal flows from two directions ($Q_A = 2Q_B$); equal flows from two directions ($Q_A = Q_B$). It can be seen in Figure 23 that the three sets of results show a similar trend with C_g decreasing as $D_o/\bar{B}$ is decreased; three curves defining the lower limits of the data for the central outlets (but ignoring one doubtful point) have therefore been drawn. The values of C_g for the offset outlets are generally somewhat lower than the corresponding values for the central outlets.

Weir coefficients 13.3

Observations of the tests with the circular outlets in the box-receivers showed that the flow conditions were very complex at low heads (see Plate V). Sub-atmospheric pressure between the falling jet and the side of the box caused the water-level behind the nappe to be about 20–30mm higher than it was in the centre of the box. The water-level in the centre of the box also depended upon whether the jet landed on top of the outlet or in front of it. When flow was from two directions, oscillations in the positions of the nappes sometimes caused the water in the centre of the box to "slosh" backwards and forwards.

For these reasons the results obtained at low heads can only be approximate. However some of the tests do indicate the occurrence of weir-type flow and values of the weir coefficient C_w are given in Table 3f. These values were mainly calculated using the measurements of water level around the sides of the box where the flow was not affected by the sub-atmospheric pressures behind the nappes; the readings from the pressure tapping in the base of the box were used if they did not seem to be affected by the impact of the jets (see Crow & Barnes [13]).

The calculated values of C_w show a great deal of scatter so it is difficult to draw firm conclusions. However the discharge coefficient does seem to increase significantly when the outlet is moved away from the centre of the box.

14 Design recommendations

Orifice coefficients 14.1

As described in 11.1 CP 308: 1974 recommends the use of two values of the orifice coefficient C_d. If swirl is "prevented" by

placing the centre of the outlet not more than one diameter away from the vertical side of the gutter or box-receiver, then C_d = 0.606; if swirl does take place then C_d = 0.454. The results for the rectangular and circular sharp-edged outlets in Table 3 show that values of $C_d < 0.606$ occurred in 6 out of the 52 tests; of these six, two values were only marginally less than 0.606, two were within one standard error (Eqn (179)), and two were within about two standard errors; the lowest value was C_d = 0.522. Table 5 shows that the overall mean values of C_d for the sharp-edged rectangular and circular outlets were 0.647 and 0.657 respectively; these figures do not include the 1″ x 1″ and 1″ ϕ outlets which had significantly higher values of C_d.

Although the value of C_d tended to increase when the circular outlets were moved closer to the sides of the gutter, there was a small reduction in the case of the rectangular outlets and the circular outlets in the box-receivers. It was concluded in 13.1 that all the outlets were subject to swirl but that the strength of the swirl depended in a complicated way upon the shape of the outlet and upon its position in the gutter. Since the overall variations in C_d were generally small, it was decided in the revised version of CP 308 to use a single value of C_d = 0.606 for all sharp-edged circular outlets; when Q is in l/s and h is in mm the resulting discharge equation is

$$Q = \frac{D^2 \, h^{0.5}}{15\,000} \qquad (196)$$

This maintains continuity with the previous version of the code, and gives a safety factor of about 7% compared to the average discharge coefficient of 0.647; in the case of the smallest outlets the safety factor is considerably higher. For rectangular outlets a slightly lower value of C_d = 0.595 was adopted in order to give the following design equation for CP 308

$$Q = \frac{A \, h^{0.5}}{12\,000} \qquad (197)$$

Eqn (196) can be used for all types of circular outlet if D is defined as the effective diameter; in the case of sharp-edged outlets D is equal to the diameter of the outlet. Table 5 shows that the average value of C_d for the round-edged outlets was about 86% that for the sharp-edged outlets when the coefficient was calculated using the top diameter D_o. The revised version of CP 308 therefore recommends that $D = 0.9 \, D_o$ be used for the design of round-edged outlets of this type (Figure 17d). For the tapered outlets (Figure 17c) it was decided to let $D = D_o$ even though this gave a somewhat higher factor of safety.

Gutter coefficients **14.2** CP 308: 1974 recommends the use of a single weir equation for outlets in gutters and box-receivers; this equation is based on the perimeter of the outlet and is similar to Eqn (149) but with a slightly reduced discharge coefficient of 0.643.

As described in 13.2 the present experiments have demonstrated that weir-type flow in a gutter is normally controlled by the cross-sectional shape of the gutter and not by the outlet. The gutter coefficient C_g defined by Eqns (180) and (182) ought therefore to be used when determining the depth of flow upstream of an outlet. Suitable design curves for rectangular and circular outlets have been derived from the experimental results that were presented in 13.2. Figure 24 gives the values of γ_1 and γ_2 for a rectangular outlet in terms of the ratios Y_1/L_e and Y_2/L_e (see Figure 21). Comparison with the experimental data in Figure 22

shows that only two measurements lie significantly below the design curve. The value of C_g for the outlet is then calculated from

$$C_g = \frac{W + \gamma_1 Y_1 + \gamma_2 Y_2}{\bar{B}} \qquad (192a)$$

Note that the value of γ_o in Eqn (192) has for convenience been assumed to be equal to unity. Figure 25 for circular outlets is based on the curves of C_g versus $D_o/\bar{B}$ drawn in Figure 23, but gives four design curves for outlets that are central and offset and for flows from one or two directions.

When the value of C_g for the outlet has been determined from Figures 24 or 25, it can be used to determine the depth of flow y_o in the gutter upstream of the outlet. Unfortunately this calculation is not straightforward because C_g is a discharge coefficient and is therefore only indirectly related to the depth of flow. The first step is to convert C_g into an equivalent value of the Froude Number F_o defined by

$$F_o^2 = \frac{B_o Q^2}{g A_o^3} \qquad (4)$$

where Q is the discharge in the gutter, and A_o and B_o are the area and width of flow corresponding to the depth y_o. The discharge Q and the corresponding total head H may therefore be written

$$Q = F_o \sqrt{g} \left(\frac{A_o^3}{B_o}\right)^{1/2} \qquad (4b)$$

$$H = y_o + F_o^2 \frac{A_o}{2B_o} \qquad (198)$$

The coefficient C_g is defined as the ratio between the actual discharge Q and the theoretical discharge Q_{cg} for a freely-discharging flow having the same total head H (see Eqn (180)). Therefore

$$Q_{cg} = \sqrt{g} \left(\frac{A_c^3}{B_c}\right)^{1/2} \qquad (182)$$

where A_c and B_c correspond to the critical depth y_c; the relationship between H and y_c is

$$H = y_c + \frac{A_c}{2B_c} \qquad (181)$$

It follows therefore that

$$C_g = F_o \left(\frac{A_o}{A_c}\right)^{3/2} \left(\frac{B_c}{B_o}\right)^{1/2} \qquad (199)$$

It can be shown from the above equations that for the special case of a rectangular gutter

$$C_g = F_o \left(\frac{3}{2 + F_o^2}\right)^{3/2} \qquad (200)$$

The corresponding result for a triangular gutter is

$$C_g = F_o \left(\frac{5}{4 + F_o^2} \right)^{5/2} \qquad (201)$$

Figure 26 shows a plot of Eqns (200) and (201), and it can be seen that the curves for rectangular and triangular gutters are very similar; it can also be shown that results for trapezoidal gutters lie between these two limiting curves. For purpose of design a single curve based on that for rectangular gutters may be used because it provides a small margin of safety for other types of gutter.

Knowing F_o it is now possible to calculate from Eqn (4) the depth of flow y_o upstream of the outlet. Although this can be done directly for rectangular and triangular gutters, a trial-and-error procedure is necessary for trapezoidal gutters. However this difficulty can be avoided by means of the following graphical type of solution. For a trapezoidal gutter (see 3.1), Eqn (4) can be written in the form

$$\frac{Q^2}{gF_o^2} = \frac{(B_s + \frac{1}{2} by_o)^3 y_o^3}{(B_s + by_o)} \qquad (202)$$

It is now convenient to define the notional depth Z_o given by

$$Z_o = \left(\frac{Q^2}{gF_o^2} \right)^{1/5} \qquad (203)$$

Eqn (202) then becomes

$$\left(\frac{B_s}{Z_o} + \frac{1}{2} \frac{by_o}{Z_o} \right)^3 \left(\frac{y_o}{Z_o} \right)^3 = \frac{B_s}{Z_o} + b \frac{y_o}{Z_o} \qquad (204)$$

This suggests that a general graphical solution can be constructed by plotting y_o/Z_o against B_s/Z_o for different values of the effective side-slope b. Values of y_o/Z_o and B_s/Z_o can be found by expressing them in terms of the parameter u defined by

$$u = \frac{by_o}{B_s} \qquad (9)$$

From Eqn (204) it can then be shown that

$$\frac{y_o}{Z_o} = \frac{(1 + u)^{1/5}}{(1 + \frac{u}{2})^{3/5}} \left(\frac{u}{b} \right)^{2/5} \qquad (205)$$

$$\frac{B_s}{Z_o} = \frac{(1 + u)^{1/5}}{(1 + \frac{u}{2})^{3/5}} \left(\frac{b}{u} \right)^{3/5} \qquad (206)$$

Choosing values of u and b enables the curves in Figure 27 to be obtained. In the design problem Q, F_o and B_s are known, so it is possible to calculate Z_o and B_s/Z_o; the curve for the relevant value of b then gives the ratio y_o/Z_o and hence the required depth of flow y_o. It may be noted that Figure 27 can also be used to find the value of critical depth y_c in a freely-discharging gutter by putting $F_o = 1$ in Eqn (203).

The process described above can be shortened slightly so as to avoid the need to convert from C_g to F_o. A slightly different notional depth Z has already been used for the design of freely-discharging gutters (see Eqn (28)); the relationship between Z_o and Z is simply

$$\frac{Z_o}{Z} = \frac{1}{F_o}^{2/5} \qquad (207)$$

Using the design curve in Figure 26 connecting F_o and C_g it is therefore possible to plot Z_o/Z as a function of C_g as shown in Figure 28. Thus the value of Z_o required in Figure 27 can be found from Eqn (28) and from the value of C_g for the outlet.

When designing an outlet in a gutter it is necessary to determine whether the flow is of weir-type or orifice-type. The depth of flow y_o calculated as described above should therefore be compared with the head h given by the relevant orifice equation Eqn (196) or (197). If $y_o > h$, the flow is of weir-type, and is controlled by the gutter; if $h > y_o$ the flow is of orifice-type and is controlled by the outlet.

The above procedure for calculating the depth of flow upstream of an outlet is necessary because of the form in which the experimental results have been analysed and presented. Unfortunately the procedure is most probably too complicated for use by engineers and architects who cannot be expected to have a specialist knowledge of hydraulics. It therefore proved necessary in the revised CP 308 to adopt a simpler method of design for weir-type flow in gutters. This method, which is described in 14.3, reverts to the use of a weir-flow equation based on the perimeter of the outlet, as in CP 308: 1974. From a theoretical point-of-view this is less satisfactory than the procedure described above, because it is not well supported by the experimental data. However the simplified method should give results that err consistently on the safe side.

Weir coefficients 14.3

When weir-type flow occurs in a box-receiver or on a flat roof, the flow is controlled by the outlet. The depth of water h in a box or on a flat roof is effectively equal to the total head H since the velocity of flow is small except near the outlet itself. The design equation for such an outlet should therefore be based on Eqn (191) where C_w is the weir coefficient.

As described in 13.3 the values of C_w obtained in the present experiments are only approximate, and show a large amount of scatter between a minimum of about 0.35 and a maximum of about 1.0 (Table 3f). Kalinske's [18] results for drain pipes (see 11.1) do not fit Eqn (191) exactly, but the explanation proposed in Appendix A suggests that the effective value of the weir coefficient is given by

$$C_w = 1 + \frac{4}{3} k \frac{H}{D} \qquad (208)$$

where typically k has a value of about 0.75. This indicates that the value of C_w is approximately unity at low heads and increases as the head increases.

Based on these considerations a discharge coefficient for circular outlets of $C_w = 0.787$ was adopted in the revised version of CP 308; when Q is in l/s and D and h are in mm this gives

$$Q = \frac{D\ h^{1.5}}{7\ 500} \qquad (209)$$

For general use D is taken to be the effective diameter described in 14.1. The corresponding equation in terms of the length L of the weir is

$$Q = \frac{L\ h^{1.5}}{24\ 000} \qquad (210)$$

which is equivalent to a value of $C_w = 0.773$.

It may be noted that Eqn (209) gives only 2/3 of the capacity predicted by the weir-flow equation in CP 308: 1974. This latter equation was based on Bonnington's[2] experiments with gutter outlets (see 11.1), and was not checked for outlets in box-receivers. Also the experimental results may themselves have been misinterpreted because it is likely that the depth of flow in the gutter would have been controlled by its cross-sectional shape rather than by the size of the outlet.

When designing an outlet in a box-receiver or on a flat roof, it is necessary to determine whether the flow is of weir-type or orifice type. Comparing the equations recommended in the revised version of CP 308 (Eqns (196) and (209)), it can be seen that the transition for a circular outlet occurs when h = D/2; for a rectangular outlet the corresponding limit (see Eqns (197) and (210)) is h = 2A/L, where A is the plan area of the inlet and L is its wetted perimeter.

As described in 14.2 the preferred method of design for weir-type flow in gutters proved too complicated for use in the revised version of CP 308. It was therefore decided to use an equation based upon the weir coefficient C_w and the wetted perimeter of the outlet rather than the gutter coefficient C_g and the cross-sectional shape of the gutter. Since it was desirable to have, if possible, only one type of weir-flow equation in the Code, the design equations for box-receivers, Eqns (209) and (210), were checked to see whether they could also be applied to gutters. As explained above the static head h in a box-receiver is equivalent to the total head H because the flow is moving only slowly around the sides of the box. Therefore if Eqn (209) or (210) is used to find the depth of flow in a gutter, the velocity head ought to be subtracted from the value of head given by the equation. However this adds an extra complication to the design procedure so it was decided to neglect the velocity head term and treat it as an additional safety factor on the predicted depth of flow.

The adequacy of Eqns (209) and (210) for describing weir-flow in a gutter was checked by calculating values of the ratio h/y_o, where h is the static head predicted by Eqns (209) or (210) and y_o is the corresponding depth of flow obtained from the experimental values of C_g in Table 3. The values of C_g were converted to equivalent values of F_o by means of the curves in Figure 26; the relationship between discharge Q and the depth of flow y_o is given by Eqn (4b) which for a rectangular gutter becomes

$$Q = F_o \sqrt{g}\ B_s\ y_o^{3/2} \qquad (4c)$$

The values of h/y_o were found to be less than unity in only 5 out of the 39 tests carried out in the rectangular gutter; the maximum value was 2.02 (Test C.5), the minimum was 0.66 (Test H.11, a doubtful result), and the average was 1.31. Also in 2 out of these 5 tests it was found that the predicted value of h was less

than the corresponding critical depth y_c, so that the flow in the gutter would not in fact have been controlled by the outlet.

Therefore in the revised version of CP 308 it was decided to use Eqns (209) and (210) for weir-type flow in both box-receivers and gutters. Although this usage is not very satisfactory from a theoretical point-of-view, it simplifies the method of design and should give conservative results in nearly all practical cases.

15 Conclusions to Parts I and II

British Standard Code of Practice CP 308: Drainage of Roofs and Paved Areas has recently been revised, and this report explains the basis of its recommendations on the hydraulics aspects of roof drainage design. The two quantities that normally need to be determined in a design are the capacity of the roof gutter and the capacity of the outlet that drains it.

In order to calculate the capacity of a gutter it is necessary to determine the relationship between the depths of flow at the upstream and downstream ends of the gutter. A theoretical solution for level gutters can be obtained by means of the momentum principle if the effects of resistance are neglected. Experimental studies have shown that observed capacities of gutters agree quite well with those predicted by the theoretical solution. CP 308: 1974 used a simplified version of this solution for valley and parapet-wall gutters, but relied upon experimental results for half-round eaves gutters. The design method in the revised version of the code is based on the full theoretical solution (neglecting friction), and takes proper account of the cross-sectional shape of the gutter. The method is therefore more consistent and accurate than the old one, and leads to more economical design of non-rectangular valley gutters. The results are presented in graphical form so that most problems involving gutters with free or restricted discharge can be solved directly. A new method of determining the effect of resistance in long gutters is included, and is based on numerical solutions of the non-uniform flow equations. Two other topics were also studied although they were not included in the new code. The first was a theoretical solution for the effect of bends in level gutters; the second was an approximate method for calculating the capacity of sloping gutters. Both results require experimental verification.

The depth of flow at the downstream end of a gutter depends upon the capacity of the outlet; if the depth is too great, the gutter will be prevented from discharging freely. The capacities of outlets in gutters and box-receivers depend upon many factors and are best determined by means of experiment. HRS therefore commissioned the British Hydromechanics Research Association to test various types of rectangular and circular outlets in rectangular and trapezoidal gutters; a total of 77 different conditions were studied. The results of these tests form the basis of the relevant recommendations in the revised version of CP 308. The main findings were that:

a) Flow at outlets is of weir-type at low heads and of orifice-type at higher heads.

b) Weir-type flow in a gutter is controlled by the cross-sectional shape of the gutter and not directly by the size of the outlet. Curvature of the flow towards the outlet can cause a backing-up of the flow in the gutter.

c) If unequal flows approach a gutter outlet from two directions and the flow is of weir-type, then the depths of flow on either side of the outlet are approximately equal and determined by the larger of the two flows.

d) Weir-type flow in box-receivers is controlled by the size of the outlet. Flow conditions inside the box are very complex at low heads.

e) Rectangular and circular outlets have very similar values of orifice coefficient.

f) The depth of flow at a gutter outlet is determined by the total discharge into the outlet if the flow is of orifice-type.

g) Swirl occurs at most outlets but does not cause the value of the orifice coefficient to vary greatly.

16 Acknowledgements

The work described in this report was supervised by Mr J A Perkins and was carried out in the Rivers and Drainage Division headed by Mr A J M Harrison. The project formed part of the research programme of the Hydraulics Research Station, and this report is published with the permission of the Director.

The author would like to acknowledge the encouragement given by Mr J H Walton, a fellow member of the drafting committee for British Standard Code of Practice 308.

17 References

1 BEIJ K H. Flow in roof gutters. J.Res., US Nat. Bur. Stand., Vol 12, Res. Paper 644, 1934.

2 BONNINGTON S T. Measurements of the capacity of outlets from small open channels. British Hydromech. Res. Assn., RR 562, 1957.

3 BRITISH STANDARDS INSTITUTION. Code of Practice 308, Drainage of roofs and paved areas, 1974.

4 BRITISH STANDARDS INSTITUTION. British Standard 460, Cast iron rainwater goods, 1964.

5 BRITISH STANDARDS INSTITUTION. British Standard 1091, Pressed steel gutters – rainwater pipes – fittings and accessories, 1963.

6 BRITISH STANDARDS INSTITUTION. British Standard 2997, Aluminium rainwater goods, 1958.

7 BUILDING RESEARCH ESTABLISHMENT. Roof drainage: Part I, Digest 188, Apr 1976; Part 2, Digest 189, May 1976.

8 BUILDING RESEARCH STATION. Roof drainage. Digest 116 (first series), Nov 1958.

9 BUILDING RESEARCH STATION. Design of gutters and rainwater pipes. Digest 34 (second series), May 1963.

10 BUILDING RESEARCH STATION. Roof drainage, Digest 107 (second series), July 1969.

11 CHOW V T. Open-channel hydraulics. McGraw-Hill, New York, 1959.

12 CRABB F J, SAN F R and TURNER P F. An investigation into roof drainage by eaves gutter. Building Research Station, Note No. E 811, 1958.

13 CROW D and BARNES S D L. Capacity of gutter outlets. British Hydromech. Res. Assn., RR 1622, 1980.

14 FOX J A and GOODWILL I M. Spatially varied flow in open channels. Proc. Inst. Civ. Eng., Vol 46, July 1970.

15 GILL M A. Perturbation solution of spatially varied flow in open channels. J. Hydr. Res., Vol 15, 1977, No.4.

16 HENDERSON F M. Open channel flow. Macmillan, New York, 1966.

17 HYDRAULICS RESEARCH STATION. Tables for the hydraulic design of channels and pipes. 4th ed, HMSO, 1978.

18 KALINSKE A A. Hydraulics of vertical drain and overflow pipes. Iowa Inst. Hyd. Res., Studies in Eng., Bull 26, 1939–40.

19 KEULEGAN G H. Determination of critical depth in spatially variable flow. Proc 2nd Midwestern Conf. on Fluid Mech., Ohio State Univ., Bull 149, Sept 1952.

20 LI W-H. Open channels with non-uniform discharge. Tr. Amer. Soc. Civ. Eng., Vol 120, Paper No 2739, 1955.

21 LIN J D, SCOTTRON V E and SOONG H K. Friction effects on spatially varied open channel flows with increasing discharge. Rivers '76, 3rd Symp, WW Div ASCE, Vol II, Aug 1976.

22 MARSH G J W. The practical sizing of pvc eaves gutters. Marley Plumbing Tech. Publ. No.1, 1976.

23 MARTIN K G. Roof drainage. Commonw. Sci & Ind. Res. Org. (Australia), Building Res. Tech. Paper (2nd series) No.1, 1973.

24 ROUSE H. Discharge characteristics of the free overfall. Civil Engng, Vol 6, April 1936, p 257.

25 SCHWARTZ H I and CULLIGAN P T. Roof drainage of large buildings in South Africa. The Civ. Eng. in S. Africa, Aug 1976.

26 YEN B C, WENZEL H G and YOON Y N. Resistance coefficients for steady spatially varied flow. Proc. Amer. Soc. Civ. Eng., Vol 98, HY8, Aug 1972.

Appendices

Appendix A

Theory for capacity of drain pipes

The results of Kalinske's [18] tests on overflow and drain pipes were found to fit a discharge equation of the form

$$Q = C\, g^{1/2}\, D^{1/2}\, H^2 \qquad (A.1)$$

where H is the head above the outlet. The pipes were tested in a large cylindrical tank so that the flow towards the outlets was radial. The head H was measured at the side of the tank and therefore corresponds to the total head. Values of the dimensionless constant C showed a certain amount of scatter, but were found to depend upon the ratio H/D (see Table 8).

The form of Eqn (A.1) is unusual because it does not correspond to the normal types of equation for weir-flow or orifice-flow. In the case of the drain pipes a possible explanation may be provided by the behaviour of flow at a free overfall (see Henderson [16], p.191). If the flow upstream of an overfall is subcritical, it is found that the flow does not pass through the critical depth y_c at the brink itself, but at a point $3y_c - 4y_c$ upstream of the brink. This upstream displacement of the critical section is caused by the vertical curvature of the flow which induces non-hydrostatic pressures in the fluid. It appears possible that flow at a drain pipe could behave in a similar type of way to that at a free overfall, especially if the outlet is large in relation to the depth of flow. It will now therefore be assumed that the critical section occurs at a distance ky_c upstream from the lip of the outlet.

The standard theoretical equation for flow over a level weir is

$$Q = L g^{1/2}\, y_c^{\,3/2} \qquad (A.2)$$

where L is the length of the weir. In the present case the effective diameter of the outlet is $D + 2ky_c$, so that

$$Q = \pi\, (D + 2ky_c)\, g^{1/2}\, y_c^{\,3/2} \qquad (A.3)$$

Since the total head H relative to the weir crest is $3y_c/2$, Eqn (A.3) becomes

$$Q = \pi \left(\frac{2}{3}\right)^{3/2} \left(1 + \frac{4}{3}\, k\, \frac{H}{D}\right) g^{1/2}\, D\, H^{3/2} \qquad (A.4)$$

Comparing this with Kalinske's Eqn (A.1) shows that

$$C = \pi \left(\frac{2}{3}\right)^{3/2} \left(1 + \frac{4}{3}\, k\, \frac{H}{D}\right) \left(\frac{D}{H}\right)^{1/2} \qquad (A.5)$$

so that C is a function of H/D and the factor k. If k is assumed to remain constant, it can be shown that C has a minimum value of

$$C = \frac{8\pi}{9}\, \sqrt{2k} \qquad (A.6)$$

when

$$\frac{H}{D} = \frac{3}{4k} \qquad (A.7)$$

Estimated mean values of C from Kalinske's results for drain pipes are given in Table 8. These show that C reaches a minimum of about 3.5 when H/D = 0.6, and then starts to rise again; according to Eqn (A.6) this minimum corresponds to a value of about k = 0.79. Table 8 also gives the individual values of k calculated directly from Eqn (A.5). These show that k varies gradually from a value of about 0.68 when H/D = 0.25 to 0.82 when H/D = 1.2. The variation in k is however relatively small, and suggests that the proposed explanation of Kalinske's results is a plausible one.

Appendix B

Curvature of flow at gutter outlet

The effect of curvature on flow in a gutter will be illustrated by the example of a spiral vortex. The flow is assumed to be irrotational and to consist of a sink and a superimposed free vortex located at the origin of a cylindrical co-ordinate system, in which r and θ are in the horizontal plane and y is in the vertical direction (see Figure 29). At a general point (r, θ) the sink produces a radial velocity

$$\frac{dr}{dt} = -\frac{a}{r} \tag{B.1}$$

and the vortex produces a tangential velocity

$$r\frac{d\theta}{dt} = -\frac{b}{r} \tag{B.2}$$

where a and b are constants which depend upon the strengths of the sink and the vortex respectively.

A property of the spiral vortex is that all the streamlines crossing a radius from the origin are parallel; the angle ϕ between a streamline and the normal to the radius (see Figure 29) is given by

$$\phi = \tan^{-1}\left(\frac{b}{a}\right) \tag{B.3}$$

The velocity V of the flow is found from Eqns (B.1) and (B.2) to be

$$V = \frac{(a^2 + b^2)^{\frac{1}{2}}}{r} \tag{B.4}$$

The equation of a streamline in the spiral vortex can be determined by integrating Eqns (B.1) and (B.2). If the streamline passes through the point (r_o, 0), then it can be shown that

$$\frac{r_o}{r} = e^{-\theta}\tan\phi \tag{B.5}$$

Since the flow is irrotational the total head H is constant and equal along each streamline. The depth of flow y is therefore given by

$$y = H - \frac{(a^2 + b^2)}{2gr^2} \tag{B.6}$$

The discharge Q crossing a radius between $r = R_1$ and $r = R_2$ is

$$Q = \int_{R_1}^{R_2} Vy\cos\phi\, dr \tag{B.7}$$

Substituting from Eqns (B.3), (B.4) and (B.6) gives

$$Q = b\left[H\log_e\frac{R_2}{R_1} - \frac{b^2}{4g\cos^2\phi}\left\{\frac{R_2^2 - R_1^2}{R_1^2 R_2^2}\right\}\right] \tag{B.8}$$

It will now be assumed that the curvature of the streamlines is fixed so that the angle ϕ in Eqn (B.3) is a constant. The value of b may then be varied so as to find the maximum discharge Q_m that can occur for a given value of total head H. Differentiating Eqn (B.8) shows that the critical value of b is given by

$$b^2 = \frac{4}{3} gH \cos^2\phi \left\{ \frac{R_1^2 R_2^2}{R_2^2 - R_1^2} \right\} \log_e \frac{R_2}{R_1} \qquad \text{(B.9)}$$

Substituting into Eqn (B.8) gives the corresponding maximum discharge

$$Q_m = \frac{4}{3\sqrt{3}} \sqrt{gH^3} \frac{R_1 R_2 \cos\phi}{(R_2^2 - R_1^2)^{1/2}} \left[\log_e \frac{R_2}{R_1} \right]^{3/2} \qquad \text{(B.10)}$$

If R is defined as the mean radius of curvature so that

$$R = \frac{R_1 + R_2}{2} \qquad \text{(B.11)}$$

and if the normal distance between the two outer streamlines is B (see Figure 29) so that

$$B = (R_2 - R_1) \cos\phi \qquad \text{(B.12)}$$

then Eqn (B.10) can be expressed in the form

$$Q_m = \frac{\sqrt{gH^3}}{3\sqrt{3}} \frac{(4R^2\cos^2\phi - B^2)}{\sqrt{2RB\cos\phi}} \left[\log_e \left\{ \frac{2R\cos\phi + B}{2R\cos\phi - B} \right\} \right]^{3/2} \qquad \text{(B.13)}$$

This equation gives the discharge Q_m that will occur if a curved flow having a total head H is allowed to discharge freely. This can be compared with the discharge Q_{mo} that would occur if a uniform flow having no curvature is allowed to discharge freely; it is simple to show that

$$Q_{mo} = \left(\frac{2}{3}\right)^{3/2} B \sqrt{gH^3} \qquad \text{(B.14)}$$

Defining the coefficient C_g as the ratio of Q_m and Q_{mo} it follows that

$$C_g = \frac{1}{2\sqrt{2}} \frac{(4R^2\cos^2\phi - B^2)}{B\sqrt{2RB\cos\phi}} \left[\log_e \left\{ \frac{2R\cos\phi + B}{2R\cos\phi - B} \right\} \right]^{3/2} \qquad \text{(B.15)}$$

When $R\cos\phi >> B$ it can be shown that

$$C_g = 1 - \frac{B^2}{8R^2\cos^2\phi} - \frac{19}{1920} \frac{B^4}{R^4\cos^4\phi} - \ldots\ldots \qquad \text{(B.16)}$$

The above example shows that the discharge coefficient C_g for flow in a spiral vortex decreases as the curvature of the flow is increased. Although flow at a gutter outlet tends to be rather complicated, it does show certain similarities to that in a spiral vortex. It is therefore reasonable to expect that the discharge coefficient of a gutter will depend upon the amount of curvature which the outlet imposes upon the flow.

Tables

Table 1 Comparison of measured and theoretical capacities of half-round gutters

Type	Size W mm	Material	Measured capacity l/s	Theoretical capacity l/s	Measured / theoretical
True half-round	102	Asbestos cement*	0.84–0.88	1.13	74%–78%
	114		1.12–1.16	1.50	75%–78%
	127		1.50–1.59	1.96	77%–81%
	152	PVC+	2.38	3.07	77%
Nominal half-round	102	Cast-iron+	0.64–0.66	0.81	79%–82%
	76	PVC+	0.33	0.39	85%
	102		0.77	0.81	95%
	114		1.01	1.07	95%
	127		1.14	1.40	82%

* Crabb et al[12]

\+ Marsh[22]

Table 2a Effect of resistance in level rectangular gutters

Resistance parameter α	Aspect ratio e	F_o	Δy	Numerical solution p′	Numerical solution (p′−p)/p %	Approx soln: eqn (91) p′	Approx soln: eqn (91) (p′−p)/p %
0 (Smooth)	∞ (Wide)	1.0	0.005	1.7339	–	1.7320	–
		0.9	0.005	1.6027		1.6186	
		0.8	0.005	1.5114		1.5100	
		0.6	0.0025	1.3125		1.3115	
		0.4	0.0015	1.1494		1.1489	
		0.2	0.0003	1.03932		1.03923	
1	∞ (Wide)	1.0	0.005	1.8200	4.97	1.8236	5.28
		0.8	0.005	1.5916	5.30	1.5864	5.06
		0.6	0.0025	1.3763	4.86	1.3672	4.25
		0.4	0.0015	1.1882	3.37	1.1803	2.73
		0.2	0.0003	1.05156	1.18	1.04858	0.90
1	3	1.0	0.005	1.8350	5.83	1.8236	5.28
		0.9	0.005	1.7163	5.92	1.7033	5.23
		0.8	0.005	1.6006	5.90	1.5864	5.06
		0.6	0.0025	1.3805	5.18	1.3672	4.25
		0.4	0.0015	1.1894	3.48	1.1803	2.73
		0.2	0.0003	1.05164	1.18	1.04858	0.90
3	∞ (Wide)	1.0	0.005	1.9532	12.65	1.9794	14.28
		0.8	0.005	1.7154	13.49	1.7176	13.75
		0.6	0.0025	1.4785	12.65	1.4655	11.74
		0.4	0.0015	1.2550	9.19	1.2382	7.77
		0.2	0.0003	1.07471	3.40	1.06678	2.65
3	3	1.0	0.005	1.9945	15.03	1.9794	14.28
		0.8	0.005	1.7417	15.24	1.7176	13.75
		0.6	0.0025	1.4925	13.71	1.4655	11.74
		0.4	0.0015	1.2596	9.59	1.2382	7.77
		0.2	0.0003	1.07518	3.45	1.06678	2.65
5	∞ (Wide)	1.0	0.005	2.0581	18.69	2.1111	21.88
		0.8	0.005	1.8121	19.89	1.8292	21.14
		0.6	0.0025	1.5602	18.87	1.5510	18.26
		0.4	0.0015	1.3118	14.13	1.2908	12.35
		0.2	0.0003	1.09643	5.49	1.08438	4.34
5	3	1.0	0.005	2.1217	22.36	2.1111	21.88
		0.8	0.005	1.8550	22.73	1.8292	21.14
		0.6	0.0025	1.5837	20.66	1.5510	18.26
		0.4	0.0015	1.3203	14.86	1.2908	12.35
		0.2	0.0003	1.09743	5.59	1.08438	4.34
8	3	0.9	0.005	2.1381	31.96	2.1267	31.39
		0.6	0.0025	1.6977	29.34	1.6627	26.78
		0.4	0.0015	1.3990	21.71	1.3622	18.56
		0.2	0.0003	1.1287	8.60	1.1097	6.78

Table 2b Effect of resistance in level triangular gutters

Resistance parameter α	F_o	Δy	Numerical solution		Approx soln: eqn (94)	
			p′	(p′−p)/p %	p′	(p′−p)/p %
0 (Smooth)	1.0	0.0025	1.3579	–	1.3572	–
	0.9	0.0020	1.3042		1.3035	
	0.8	0.0015	1.2520		1.2515	
	0.6	0.0010	1.1551		1.1548	
	0.4	0.0005	1.07451		1.07434	
	0.2	0.00015	1.01966		1.01961	
1	1.0	0.0025	1.4402	6.06	1.4340	5.66
	0.9	0.0020	1.3848	6.18	1.3765	5.60
	0.8	0.0015	1.3288	6.13	1.3190	5.40
	0.6	0.0010	1.2171	5.37	1.2064	4.47
	0.4	0.0005	1.1126	3.55	1.1046	2.81
	0.2	0.00015	1.03181	1.19	1.02887	0.91
3	1.0	0.0025	1.5482	14.01	1.5470	13.98
	0.8	0.0015	1.4305	14.26	1.4199	13.46
	0.6	0.0010	1.3040	12.89	1.2875	11.49
	0.4	0.0005	1.1726	9.13	1.1562	7.62
	0.2	0.00015	1.05412	3.38	1.04643	2.63
5	1.0	0.0025	1.6247	19.64	1.6320	20.24
	0.8	0.0015	1.5019	19.96	1.4964	19.57
	0.6	0.0010	1.3670	18.34	1.3510	16.99
	0.4	0.0005	1.2196	13.50	1.1997	11.67
	0.2	0.00015	1.07424	5.35	1.0629	4.24

Table 3a Discharge coefficients of rectangular outlets in rectangular gutter

Test No.	Size of outlet L x W	Position of outlet	Ratio of flows $Q_1 : Q_2$	Weir flow			Orifice flow		
				$\bar{C}_g$	σ	N	$\bar{C}_d$	σ	N
A1	6 x 6	Central	1 : 0	0.9803	0.0115	9	–	–	–
A2	3 x 3			0.9719	0.0265	7	0.6413	0.0026	4
A3	6 x 3			0.9869	0.0115	17	0.6521	0.0073	4
A4	2 x 2			0.8678	0.0175	4	0.6426	0.0042	6
A5	4 x 2			0.9781	0.0166	7	0.6771	0.0119	5
A6	1 x 1			0.4255	0.0789	3	0.6849	0.0094	8
B1	3 x 3	Offset	1 : 0	0.9160	0.0429	7	0.6364	0.0067	3
B2	6 x 3			0.9928	0.0683	9	–	–	–
B3	2 x 2			0.8661	0.0734	6	0.6424	0.0055	5
B4	4 x 2			0.9064	0.0181	6	0.6348	0.0067	4
C1	3 x 3	Central	1 : 1	0.9284 0.9047	0.0448 0.0368	6 6	0.6602	0.0063	5 5
C2	3 x 3		2 : 1	0.9615 0.6143	0.0236 0.0549	4 4	0.6415	0.0106	5 5
C3	6 x 3		1 : 1	0.9743 0.9876	0.0184 0.0122	12 12	0.6541	0.0254	13 13
C4	6 x 3		2 : 1	0.9916 0.9178	0.0067 0.0998	13 13	0.6549	0.0161	11 11
C5	1 x 1		1 : 1	0.6084* 0.7320	0.1082 0.0967	3 3	0.8709	0.1252	8 8
C6	1 x 1		2 : 1	0.7730 0.4718	0.0335 0.0220	3 3	0.7979	0.1421	9 9

Dimensions are in multiples of 25.4mm (1 inch) – see Figures 16 and 17

* Data does not fit theoretical equation very well

Table 3b Discharge coefficients of rectangular outlets in trapezoidal gutter

Test No.	Size of outlet L x W	Position of outlet	Ratio of flows $Q_1 : Q_2$	Weir flow			Orifice flow		
				$\bar{C}_g$	σ	N	$\bar{C}_d$	σ	N
D1	6 x 6	Central	1 : 0	0.9898	0.0068	23	–	–	–
D2	3 x 3			0.9656	0.0336	6	0.6436	0.0334	5
D3	6 x 3			0.9721	0.0373	14	0.6191	0.0203	9
D4	2 x 2			0.7820	0.0305	4	0.6248	0.0358	5
D5	1 x 1			0.5012	0.0356	2	0.7396[p]	0.0547	7
E1	3 x 3	Offset	1 : 0	0.8926	0.0194	6	0.6630	0.0159	4
E2	6 x 3			0.9843	0.0252	7	0.6419	0.0388	3
F1	6 x 6	Central	1 : 1	0.9893 0.9860	0.0148 0.0207	16 16	0.6596	0.0125	4 4
F2	3 x 3		1 : 1	0.8860 0.8188	0.0671 0.0464	4 4	0.6514	0.0085	4 4
F3	3 x 3		2 : 1	0.9448 0.5599	0.0380 0.0406	5 5	0.6513	0.0079	6 6
F4	6 x 3		1 : 1	0.9664 0.9174	0.0258 0.0616	12 12	0.6402	0.0049	10 10
F5	6 x 3		2 : 1	0.9937 0.7385	0.0082 0.0688	14 14	0.6339	0.0124	10 10
F6	1 x 1		1 : 1	0.4173 0.4534	0.0112 0.0100	2 2	0.7966[p]	0.0643	7 7
F7	1 x 1		2 : 1	0.4850 0.2134	0.0339 0.0185	4 4	0.7686	0.0321	7 7

Dimensions are in multiples of 25.4mm (1 inch) – see Figures 16 and 17

[p] Outlet may have primed

Table 3c Discharge coefficients of circular outlets in rectangular gutter

Test No.	Type of circular outlet	Top/bottom diameters of outlet D_0 / D_1	Position of outlet		Ratio of flows $Q_1 : Q_2$	Weir flow			Orifice flow		
			C	E		$\bar{C}_g$	σ	N	$\bar{C}_d$	σ	N
G1	S	3	3	3		0.9441	0.0411	4	0.6052	0.0277	4
G2	R	4.5/3	3	3		0.9664	0.0060	5	0.5405*	0.0536	3
G3	S	3	3	6		0.9697	0.0156	4	0.6029	0.0309	4
G4	S	2	3	2		0.7795	0.0438	5	0.7096	0.0096	5
G5	R	3/2	3	2		0.9042	0.0341	4	0.4699	0.0140	4
G6	S	2	3	4	1 : 0	0.8205	0.0607	3	0.6325[p]	0.0555	7
G7	S	2	2	2		0.6982	0.0557	5	0.6880	0.0107	5
G8	S	2	2	4		0.6501	0.0721	5	0.6690	0.0270	6
G9	T	4.5/3	3	3		0.9777	0.0041	10	0.7925	0.0868	2
G10	T	3/2	3	2		0.9879	0.0080	8	0.7306*	0.0916	5
G11	S	1	3	1		0.8155	0.0056	2	0.9501[p]	0.0491	9

Types of outlet: S = sharp-edged R = round-edged T = tapered

Dimensions are in multiples of 25.4mm (1 inch) – see Figures 16 and 17

* Data does not fit theoretical equation very well

[p] Outlet may have primed

Table 3d Discharge coefficients of circular outlets in rectangular gutter

Test No.	Type of circular outlet	Top/bottom diameters of outlet D_0 / D_1	Position of outlet		Ratio of flows $Q_1 : Q_2$	Weir flow			Orifice flow		
			C	E		$\overline{C}_g$	σ	N	$\overline{C}_d$	σ	N
H1	S	2	3		1 : 1	0.5949 0.6056	0.0412 0.0310	4 4	0.6831	0.0153	6 6
H2	R	3/2	3		1 : 1	0.7856 0.8722	0.0536 0.0229	7 7	0.6592*	0.0941	4 4
H3	S	2	3		2 : 1	0.6709 0.3796	0.0466 0.0427	3 3	0.6693	0.0412	5 5
H4	R	3/2	3		2 : 1	0.9176 0.4242	0.0279 0.0731	5 5	0.6340	0.0770	3 3
H5	S	2	2		1 : 1	0.5521 0.6253	0.0416 0.0361	4 4	0.6999	0.0151	6 6
H6	S	2	2	–	2 : 1	0.6916 0.5607	0.0405 0.3830	3 3	0.7255	0.0180	5 5
H7	R	4.5/3	3		1 : 1	0.9959 0.9932	0.0043 0.0072	6 6	0.5848*	0.0848	6 6
H8	R	4.5/3	3		2 : 1	0.9954 0.8371	0.0024 0.0769	5 5	0.5085	0.0233	8 8
H9	T	3/2	3		1 : 1	0.9604 0.9707	0.0118 0.0173	8 8	0.7982*	0.1826	5 5
H10	T	3/2	3		2 : 1	0.9961 0.7352	0.0044 0.1455	10 10	0.6780*	0.0664	6 6
H11	S	1	3		1 : 1	0.1236* 0.0965*	0.0691 0.0541	4 4	0.8854	0.0466	6 6
H12	S	1	3		2 : 1	0.8399* 0.7658	0.2108 0.2270	4 4	1.0623	0.0660	6 6

Types of outlet: S = sharp-edged R = round-edged T = tapered

Dimensions are in multiples of 25.4mm (1 inch) – see Figures 16 and 17

* Data does not fit theoretical equation very well

Table 3e Discharge coefficients of circular outlets in trapezoidal gutter

Test No.	Type of circular outlet	Top/bottom diameters of outlet D_0 / D_1	Position of outlet		Ratio of flows $Q_1 : Q_2$	Weir flow			Orifice flow		
			C	E		$\bar{C}_g$	σ	N	$\bar{C}_d$	σ	N
I1	S	3	3	3	1 : 0	0.9128	0.0601	3	0.5979	0.0472	5
I2	S	3	3	6		0.9912	0.0054	2	0.5216*	0.0962	6
I3	S	2	3	2		0.8330	0.1078	4	0.6913	0.0193	7
I4	S	1	3	1		0.5851	0.0577	3	0.9073	0.0125	6
J1	S	3	3		1 : 1	0.7187 0.7584	0.0493 0.0390	4 4	0.6334	0.0152	6 6
J2	S	3	3		2 : 1	0.9815 0.7118	0.0186 0.1009	3 3	0.6632	0.0177	5 5
J3	S	2	3		1 : 1	0.7237 0.6364	0.0379 0.0091	3 3	0.7145	0.0162	6 6
J4	S	2	3	—	2 : 1	0.7279 0.3999	0.0509 0.0436	6 6	0.7367	0.0226	5 5
J5	S	1	3		1 : 1	0.3945 0.3230	0.0201 0.0372	2 2	0.9219	0.0322	4 4
J6	S	1	3		2 : 1	0.5513* 0.2882	0.1198 0.1106	4 4	0.9295	0.0634	6 6

Type of outlet: S = sharp-edged

Dimensions are in multiples of 25.4mm (1 inch) -- see Figures 16 and 17

* Data does not fit theoretical equation very well

Table 3f Discharge coefficients of circular outlets in box-receivers

Test No.	Type of circular outlet	Top/bottom diameters of outlet D_0 / D_1	Type of gutter	Size of box-receiver L x W	Depth of box-receiver H	Position of outlet in box-receiver E	Ratio of flows $Q_1 : Q_2$	Weir flow			Orifice flow		
								$\bar{C}_w$	σ	N	$\bar{C}_d$	σ	N
K1	S	3		12 x 6	7.5	6		0.3843	0.0030	3	0.6200*	0.0919	12
K2	R	4.5/3		12 x 6	7.5	6		0.3486	0.0389	11	–	–	–
K3	S	3	Rect	12 x 6	7.5	3	1 : 0	0.5016	0.0926	5	0.5922[p]	0.0706	6
K4	S	2		12 x 6	5	2		0.6378	0.1497	6	0.6527	0.0375	4
K5	S	1.5		6 x 3	3.75	1.5		–	–	–	0.6560	0.0496	7
L1	S	3		12 x 6	7.5	6	1 : 1	–	–	–	0.5807	0.0533	9
L2	R	4.5/3		12 x 6	7.5	6	1 : 1	0.5259*	0.1330	5	0.4690	0.0353	7
L3	S	3	Rect	12 x 6	7.5	6	2 : 1	0.8218	0.1703	2	0.6780	0.0911	6
L4	S	3		12 x 6	7.5	3	2 : 1	0.9999	0.0795	3	0.6282	0.0755	4
L5	S	1.5		6 x 3	3.75	3	1 : 1	–	–	–	0.6327	0.0264	6
L6	S	1.5		6 x 3	3.75	1.5	2 : 1	–	–	–	0.7090	0.0700	5
M1	S	1.5		6 x 3	3.75	3	1 : 1	–	–	–	0.7066	0.0767	5
M2	S	1.5	Trap	6 x 3	3.75	3	2 : 1	–	–	–	0.6710	0.0731	7
M3	S	1.5		6 x 3	3.75	1.5	2 : 1	–	–	–	0.6891	0.0567	7

Types of outlet: S = sharp-edged R = round-edged

Dimensions are in multiples of 25.4mm (1 inch) – see Figures 16 and 17

* Data does not fit theoretical equation very well

[p] Outlet may have primed

Table 5b Circular outlets in gutter: Variations in orifice coefficient C_d

	Mean value of C_d	Variation in C_d	
		Average	Range
All sharp-edged outlets except 1ϕ	0.661	–	+11% to –21%
1ϕ sharp-edged outlets	0.943	–	+13% to –6%
All round-edged outlets	0.566	–	+16% to –17%
All tapered outlets	0.750	–	+6% to –10%
Effect of off-setting outlet to one side of gutter		+ 3%	+8% to –3%
Effect of moving outlet away from stop-end of gutter		– 8%	0% to –13%
Effect of flow from two directions relative to flow from one direction			
$Q_1 = Q_2$		+ 4%	+13% to –7%
$Q_1 = 2Q_2$		+ 6%	+12% to –7%
Effect of decreasing size of geometrically-similar outlets			
sharp-edged $3\phi \rightarrow 2\phi$		+ 14%	+17% to +11%
sharp-edged $2\phi \rightarrow 1\phi$		+ 37%	+59% to +29%
Effect of varying gutter shape rectangular → trapezoidal			
flow from one direction		–5%	–1% to –13%
flow from two directions		+ 5%	+7% to +4%

Dimensions are in multiples of 25.4mm (1 inch)

Table 5c Circular outlets in box-receivers: Variations in orifice coefficient C_d

	Mean value of C_d	Variation in C_d	
		Average	Range
All sharp-edged outlets	0.651	–	+9% to −11%
Round-edged outlet (one only)	0.469	–	–
Effect of moving outlet from centre of box-receiver		− 3%	+3% to −7%
Effect of flow approaching box from two directions instead of one			
$Q_1 = Q_2$		+ 2%	–
$Q_1 = 2Q_2$		+ 8%	+9% to +7%
Effect of decreasing size of geometrically-similar outlets			
sharp-edged $3\phi \rightarrow 1.5\phi$		+ 12%	+22% to +9%

Dimensions are in multiples of 25.4mm (1 inch)

Table 6 Analysis of gutter coefficients for rectangular outlets

Test No.	Outlet size L x W inches	C_g	L_e inch	$\bar{B}$ inch	$\frac{Y_1}{L_e}$	γ_1
A1	6 x 6	0.9803	6		0	–
A2	3 x 3	0.9719	3		0.5	0.9588
A3	6 x 3	0.9869	6	6	0.25	0.9888
A4	2 x 2	0.8678	2		1.0	0.8092
A5	4 x 2	0.9781	4		0.5	0.9746
A6	1 x 1	0.4255	1		2.5	0.3136
B1	3 x 3	0.9160	3		1.0	0.8470
B2	6 x 3	0.9928	6	6	0.5	1.0006
B3	2 x 2	0.8661	2		2.0	0.8067
B4	4 x 2	0.9064	4		1.0	0.8671
C1	3 x 3	0.9165	1.5		1.0	0.8480
C2	3 x 3	0.9615	2		0.75	0.9380
C3	6 x 3	0.9809	3	6	0.5	0.9768
C4	6 x 3	0.9916	4		0.375	0.9982
C5	1 x 1	0.6702	0.5		5.0	0.6072
C6	1 x 1	0.7730	0.67		3.75	0.7306
D1	6 x 6	0.9898	6	8.76	0.230	1.0002
D2	3 x 3	0.9656	3	7.46	0.743	0.9526
D3	6 x 3	0.9721	6	8.13	0.427	0.9646
D4	2 x 2	0.7820	2	7.02	1.255	0.7011
D5	1 x 1	0.5012	1	6.51	2.756	0.4134
E1	3 x 3	0.8926	3	7.69	1.282	0.8002
E2	6 x 3	0.9843	6	8.48	0.707	0.9836
F1	6 x 6	0.9876	3	8.24	0.373	0.9946
F2	3 x 3	0.8524	1.5	7.26	1.420	0.7590
F3	3 x 3	0.9448	2	7.18	1.045	0.9160
F4	6 x 3	0.9419	3	7.65	0.775	0.9141
F5	6 x 3	0.9937	4	7.54	0.567	0.9994
F6	1 x 1	0.4353	0.5	6.35	5.350	0.3325
F7	1 x 1	0.4850	0.67	6.75	4.312	0.3981

Table 3 gives details of test conditions

Table 7 Analysis of gutter coefficients for circular outlets

Test No.	Outlet size D_o inch	Outlet type	C_g	$\overline{B}$ inch	$\frac{D_o}{\overline{B}}$
G1	3	S	0.9441	6	0.5
G2	4.5	R	0.9964		0.75
G3	3	S	0.9697		0.5
G4	2	S	0.7795		0.333
G5	3	R	0.9042		0.5
G6	2	S	0.8205		0.333
G7	2	S	0.6982		0.333
G8	2	S	0.6501		0.333
G9	4.5	T	0.9777		0.75
G10	3	T	0.9879		0.5
G11	1	S	0.8155		0.167
H1	2	S	0.6002	6	0.333
H2	3	R	0.8289		0.5
H3	2	S	0.6709		0.333
H4	3	R	0.9176		0.5
H5	2	S	0.5887		0.333
H6	2	S	0.6916		0.333
H7	4.5	R	0.9945		0.75
H8	4.5	R	0.9954		0.75
H9	3	T	0.9655		0.5
H10	3	T	0.9961		0.5
H11	1	S	0.1100		0.167
H12	1	S	0.8399		0.167
I1	3	S	0.9128	7.34	0.409
I2	3	S	0.9912	7.10	0.423
I3	2	S	0.8330	6.75	0.296
I4	1	S	0.5851	6.43	0.155
J1	3	S	0.7385	6.98	0.430
J2	3	S	0.9815	6.94	0.432
J3	2	S	0.6800	6.59	0.303
J4	2	S	0.7279	6.87	0.291
J5	1	S	0.3587	6.55	0.153
J6	1	S	0.5513	6.47	0.155

S = sharp-edged R = round-edged T = tapered

Table 3 gives details of test conditions

Table 8 Analysis of Kalinske's data for drain pipes (see Ref (18))

H/D	C	(Eqn A5) k	Comment
0.25	4.20	0.684	Values of C from Kalinske's mean curve
0.4	3.65	0.656	
0.5	3.52	0.683	
0.6	3.50	0.732	
0.8	3.54	0.798	
1.0	3.61	0.833	
1.2	3.70	0.856	
0.8	3.53	0.793	Values of C giving closer fit to experimental data
1.0	3.56	0.811	
1.2	3.61	0.820	

Figures

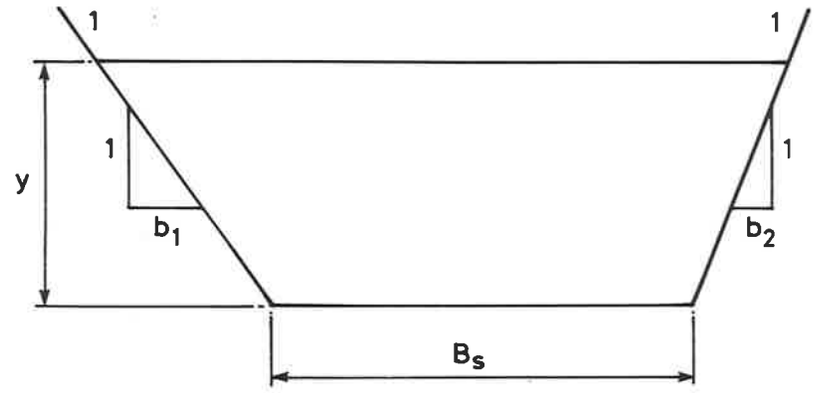

$b = b_1 + b_2$

(a) Trapezoidal gutter

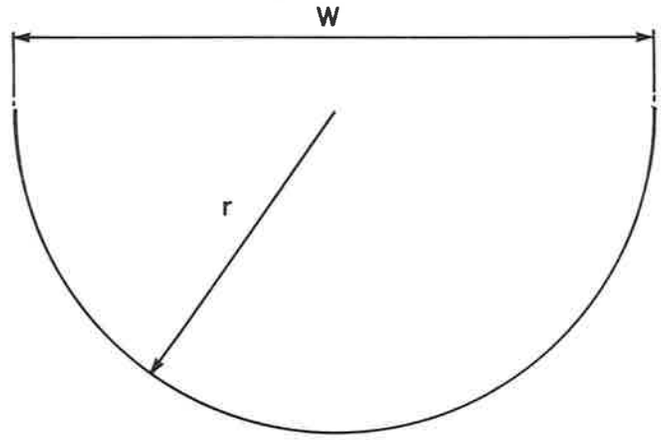

$r = \frac{W}{2}$

(b) True half-round gutter

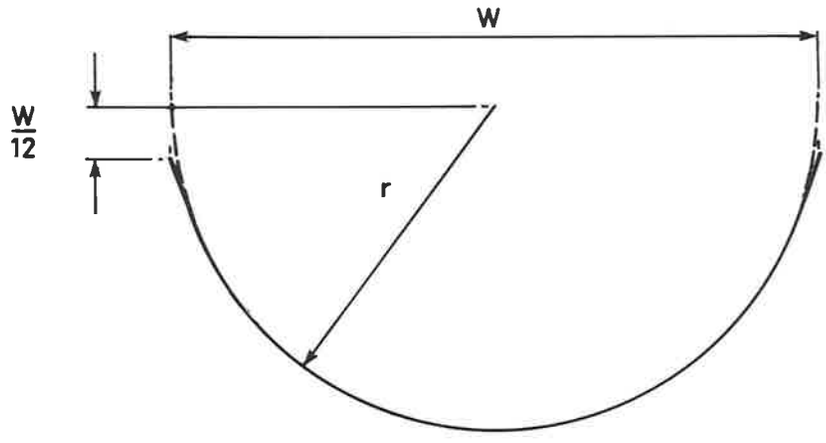

$r = \frac{W}{2}$

(c) Nominal half-round gutter

Fig 1 Cross-sectional shapes of gutters

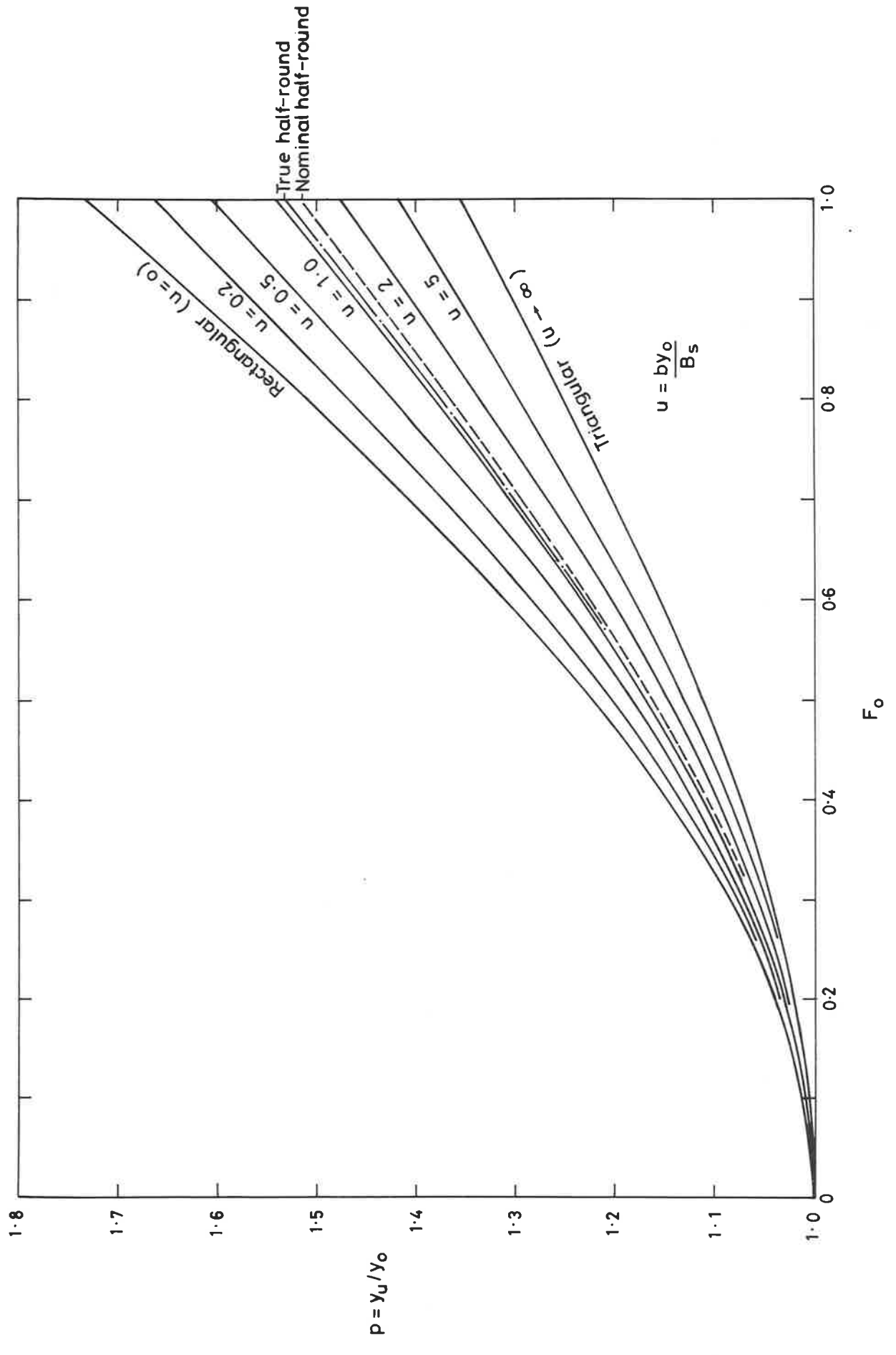

Fig 2 Variation of p with F_o and u for trapezoidal gutters

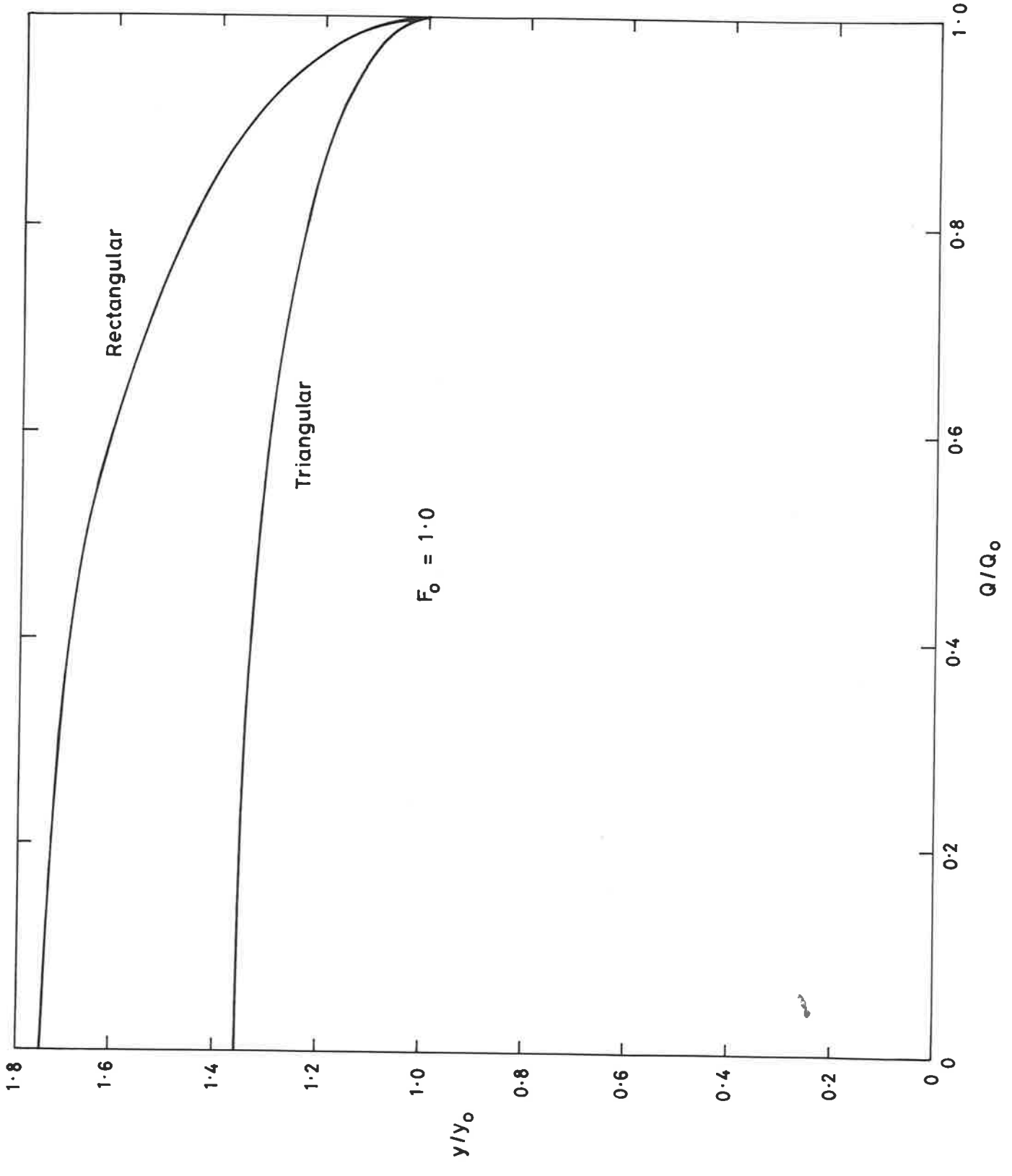

Fig 3a Profiles along freely-discharging rectangular and triangular gutters

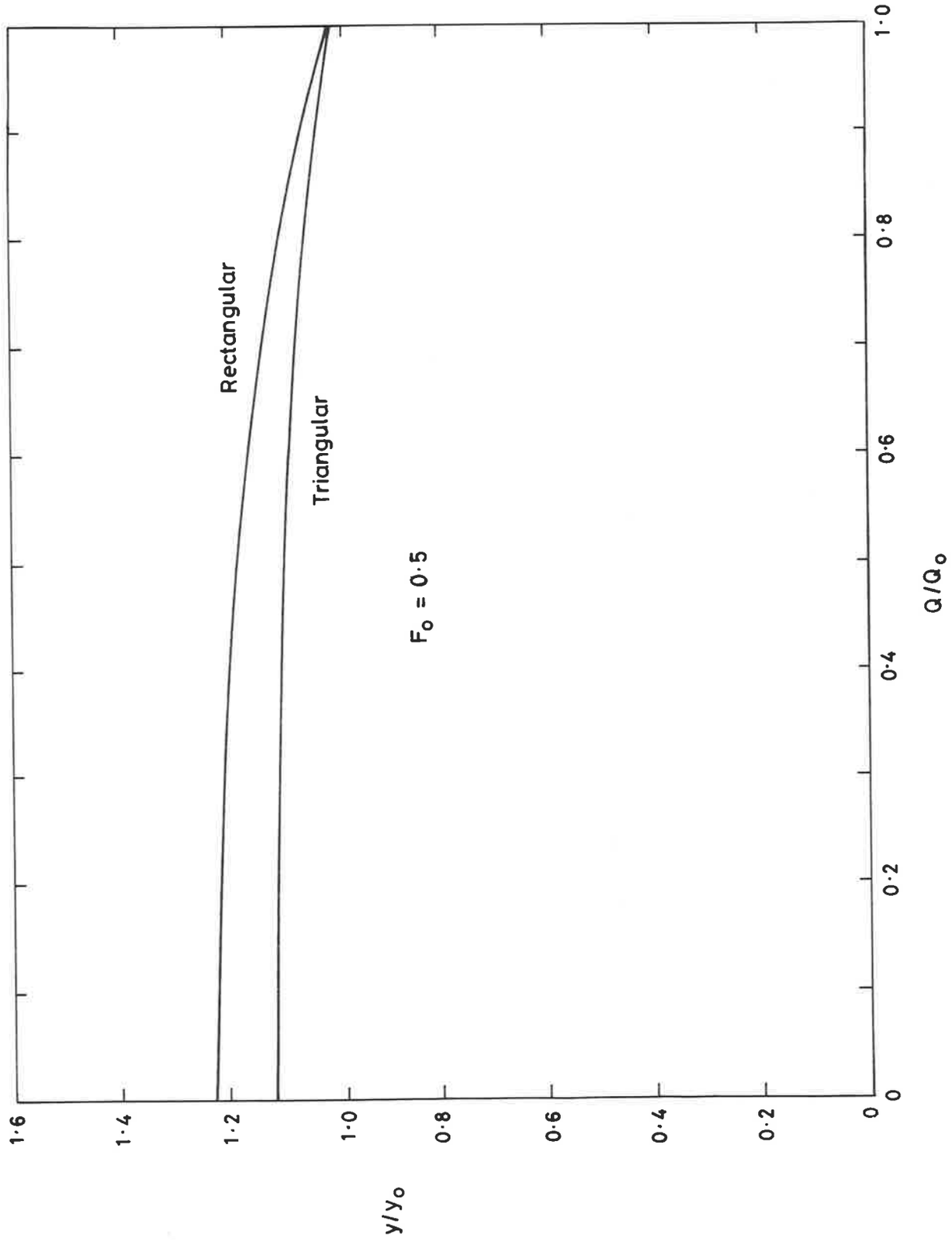

Fig 3b Flow profiles along rectangular and triangular gutters with restricted discharge

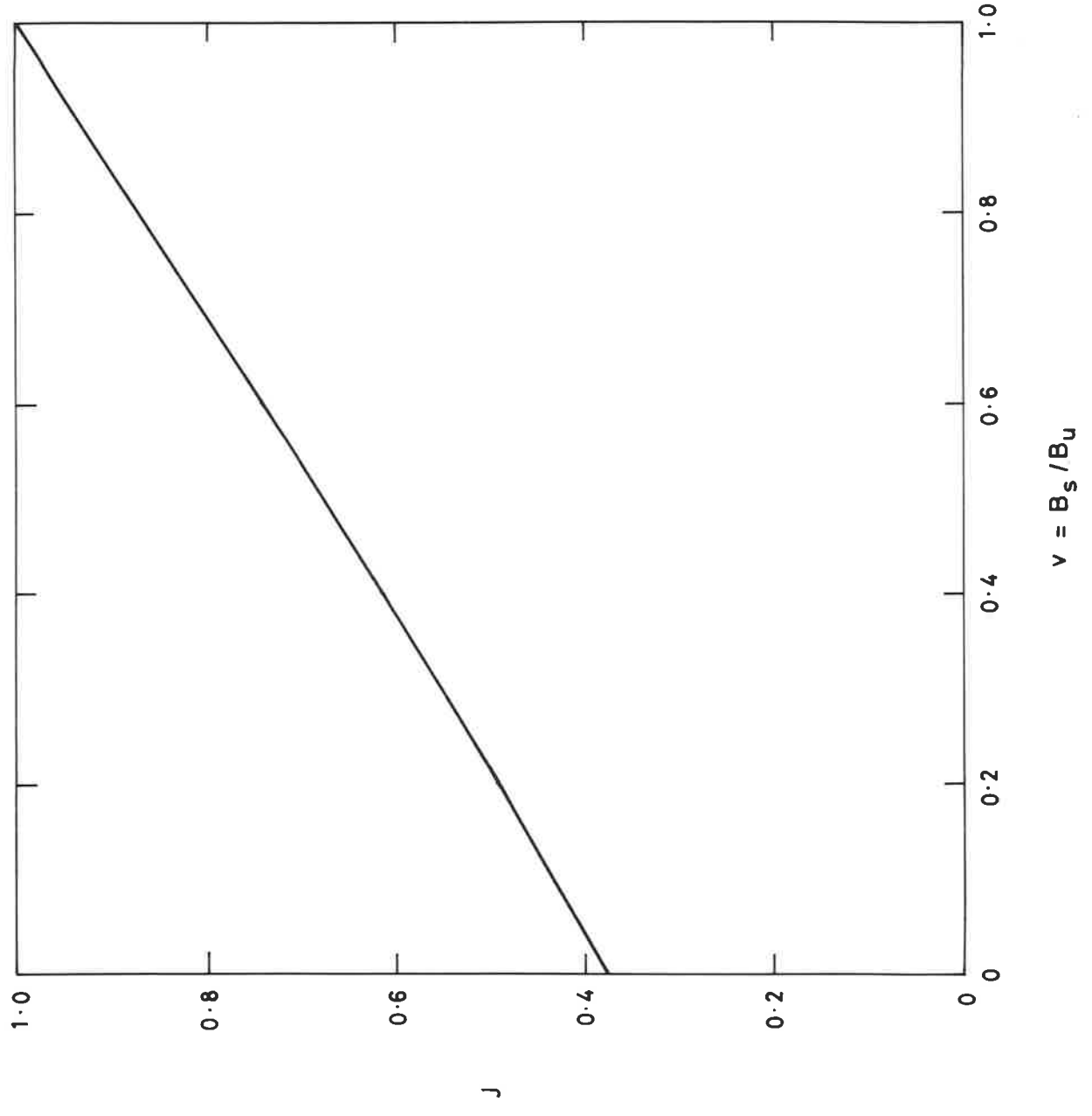

Fig 4 Variation of J with shape factor v for freely-discharging trapezoidal gutters

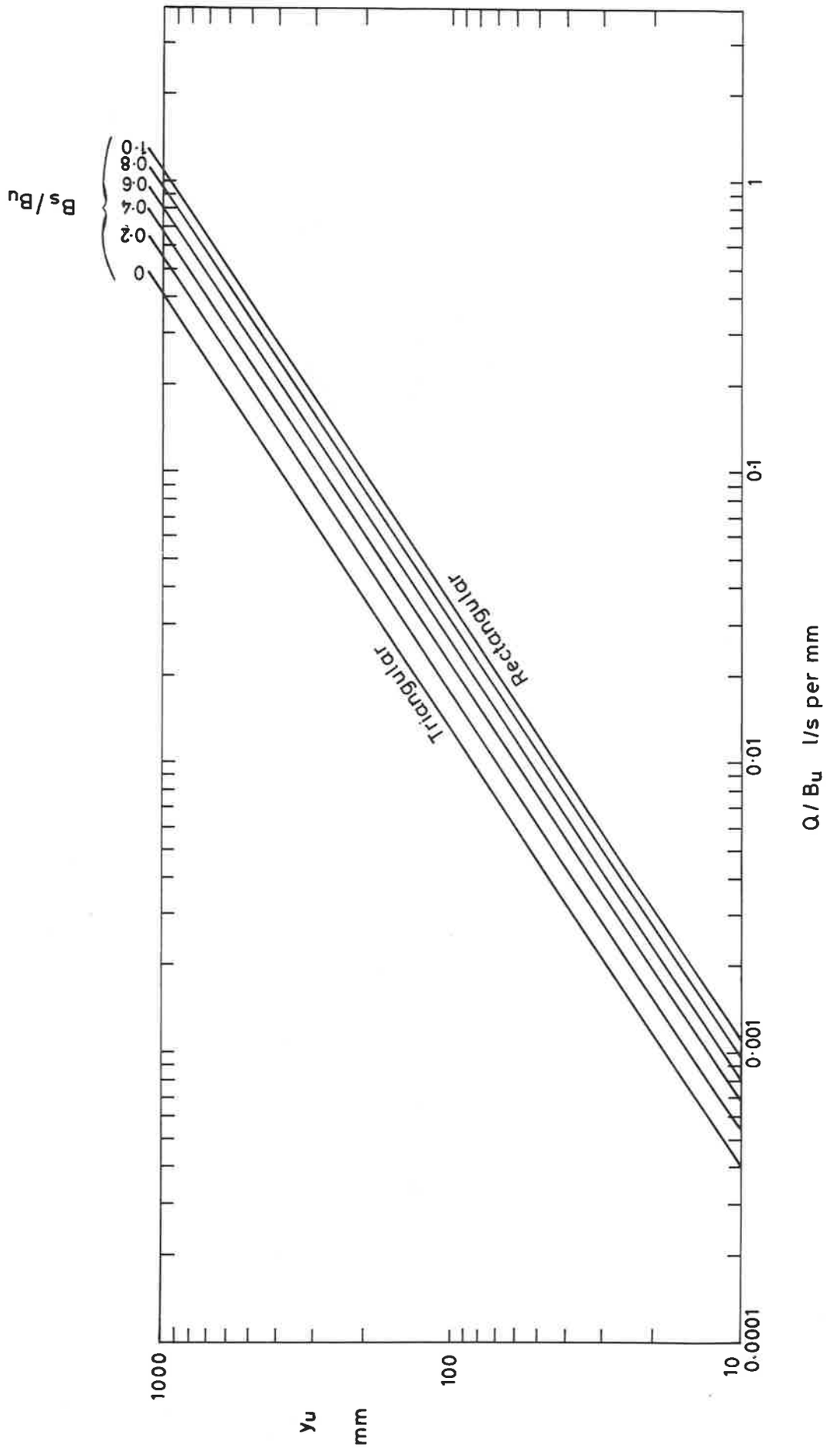

Fig 5a Design chart for capacity of freely-discharging trapezoidal gutters

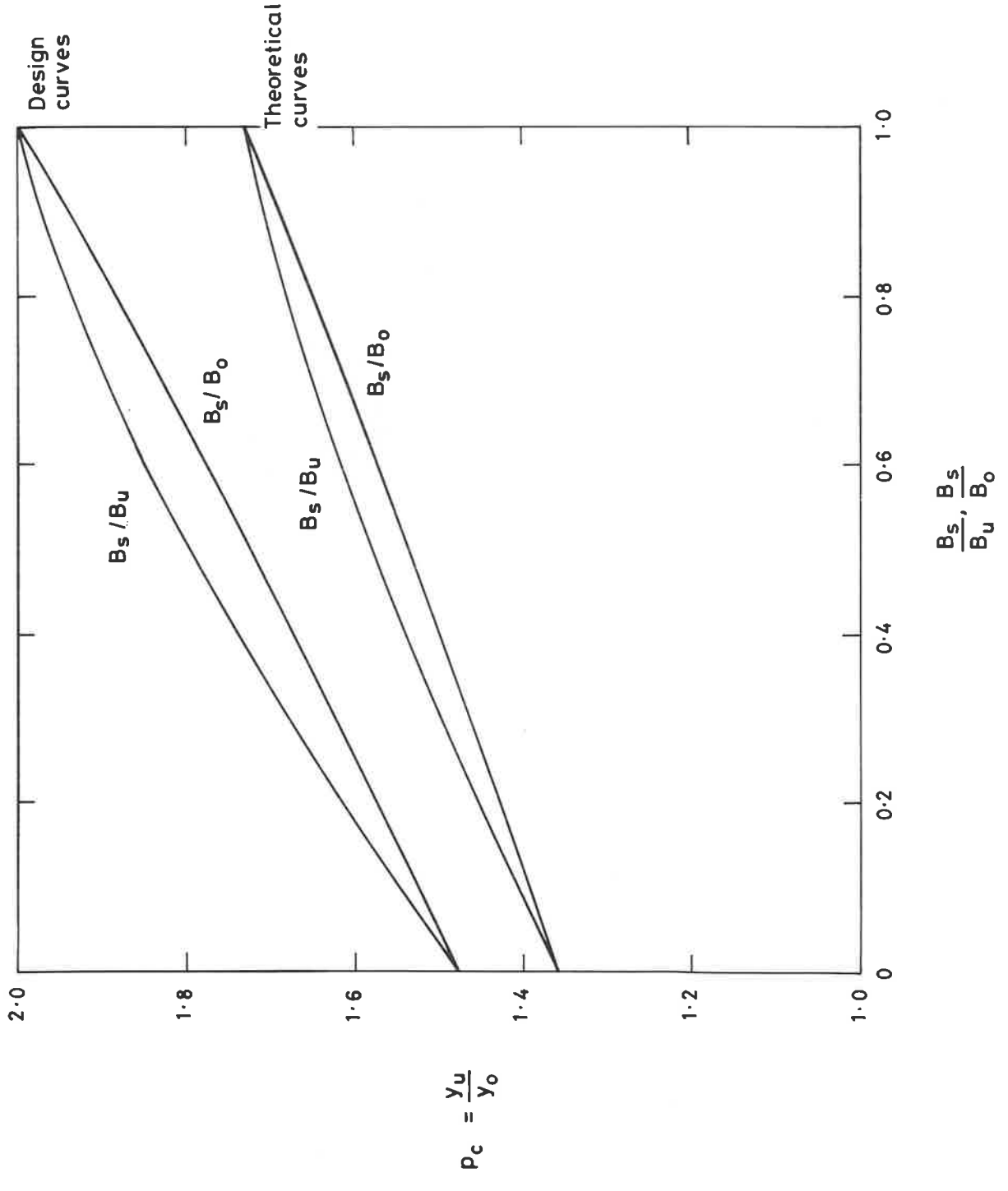

Fig 5b Variation of p_c with shape of freely-discharging trapezoidal gutters

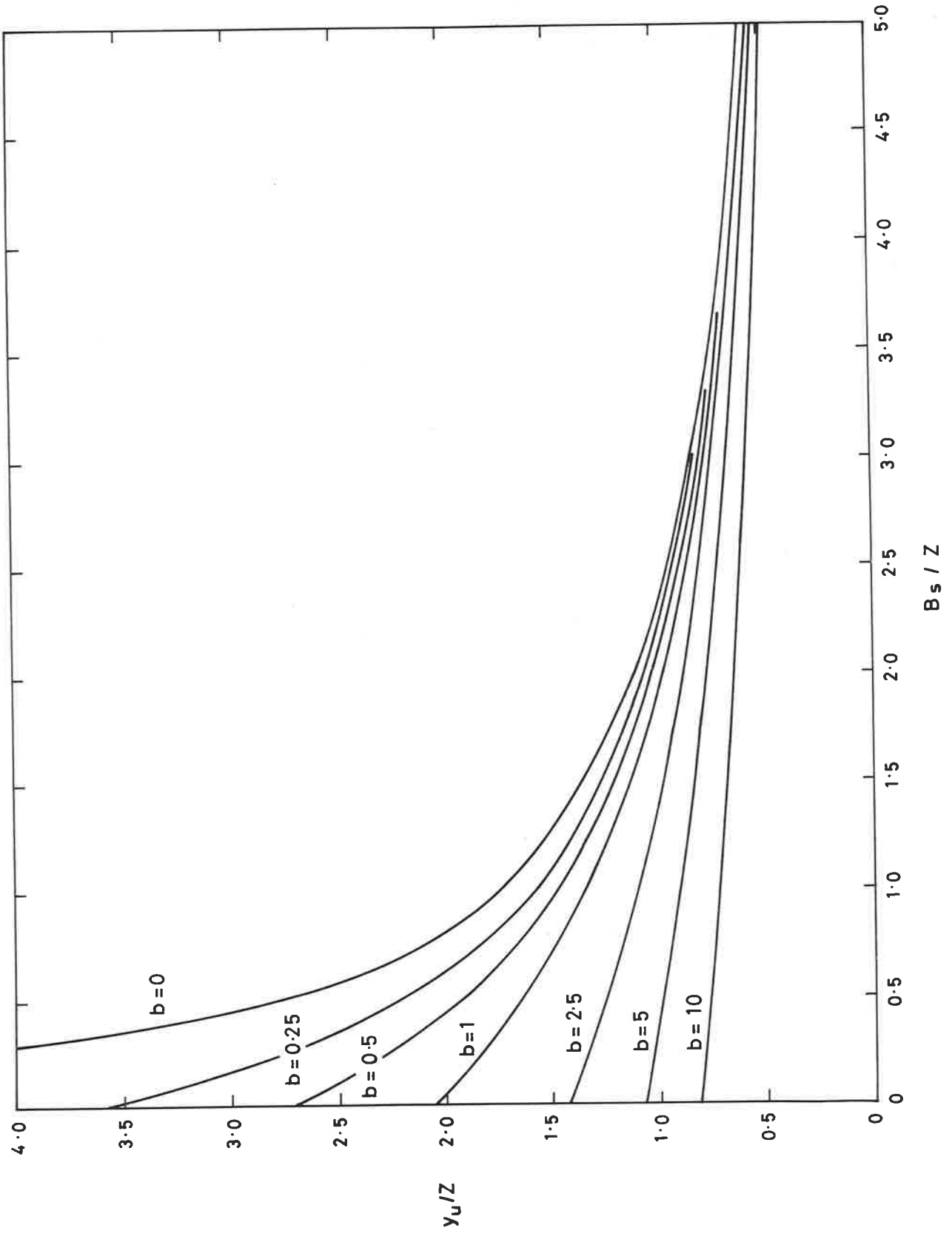

Fig 6a Theoretical curves for depth of flow at upstream end of freely-discharging trapezoidal gutter

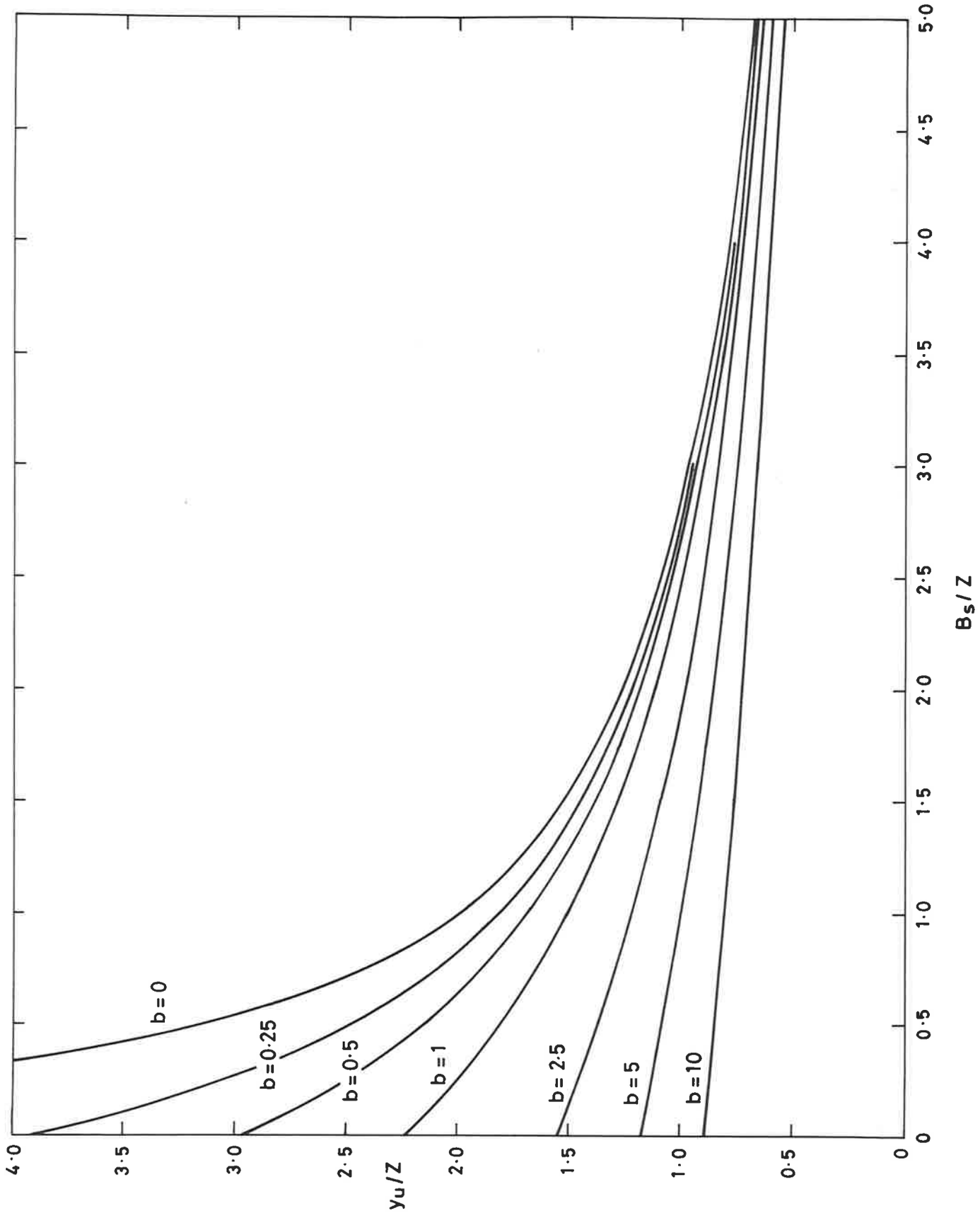

Fig 6b Design chart for depth of flow at upstream end of freely-discharging trapezoidal gutter

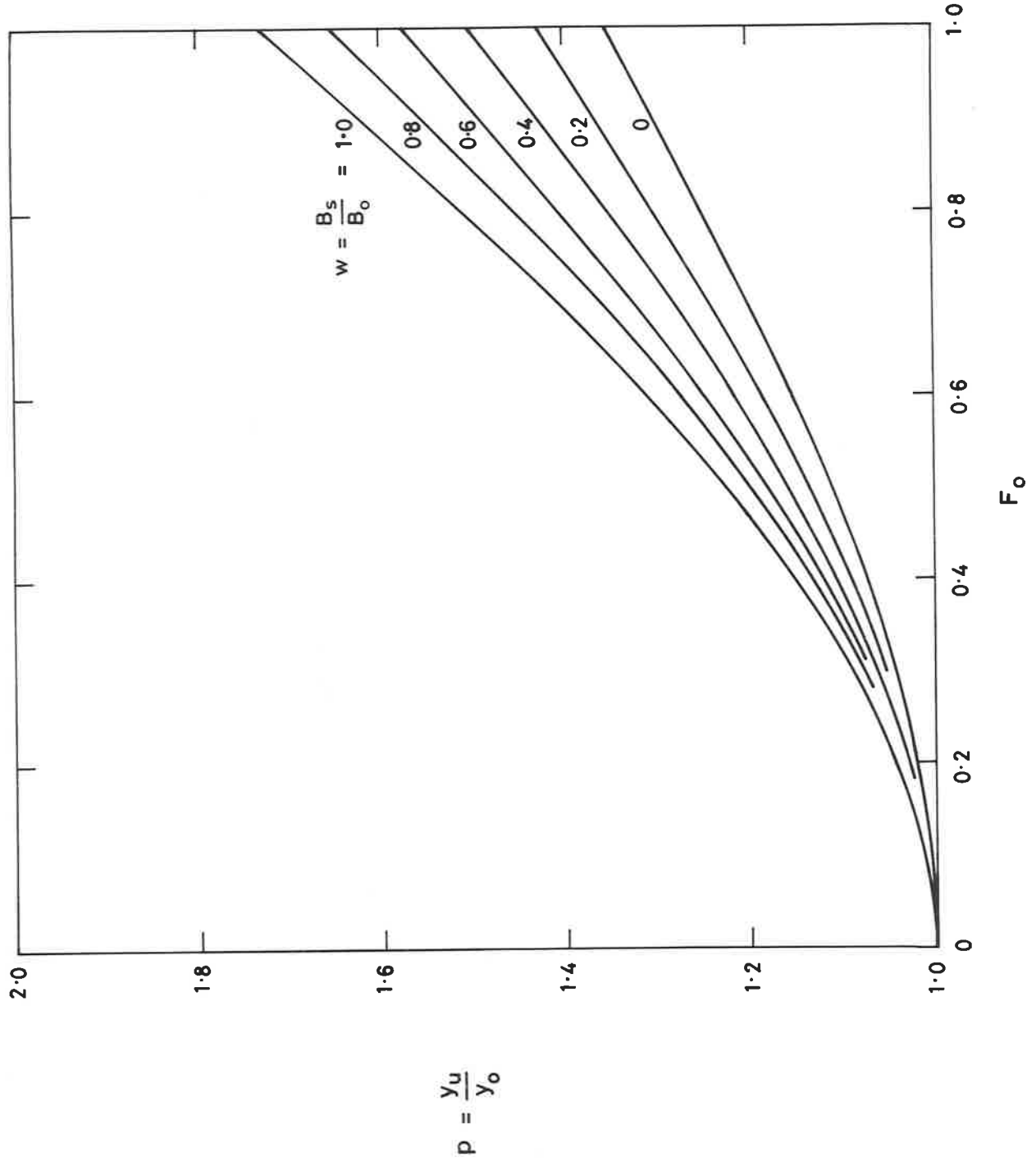

Fig 7a Variation of p with F_o and w for trapezoidal gutters : theoretical

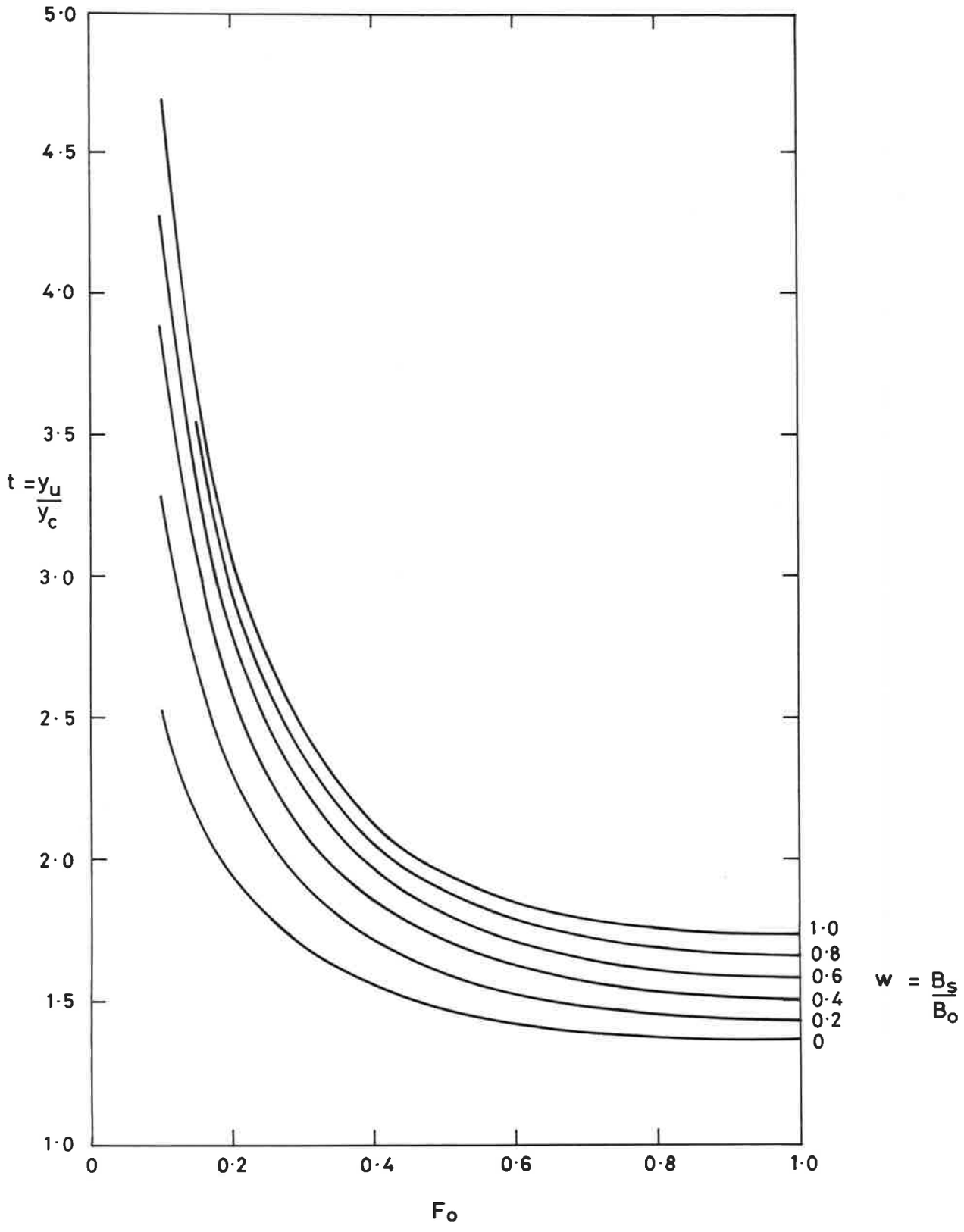

Fig 7b Variation of t with F_o and w for trapezoidal gutters : theoretical

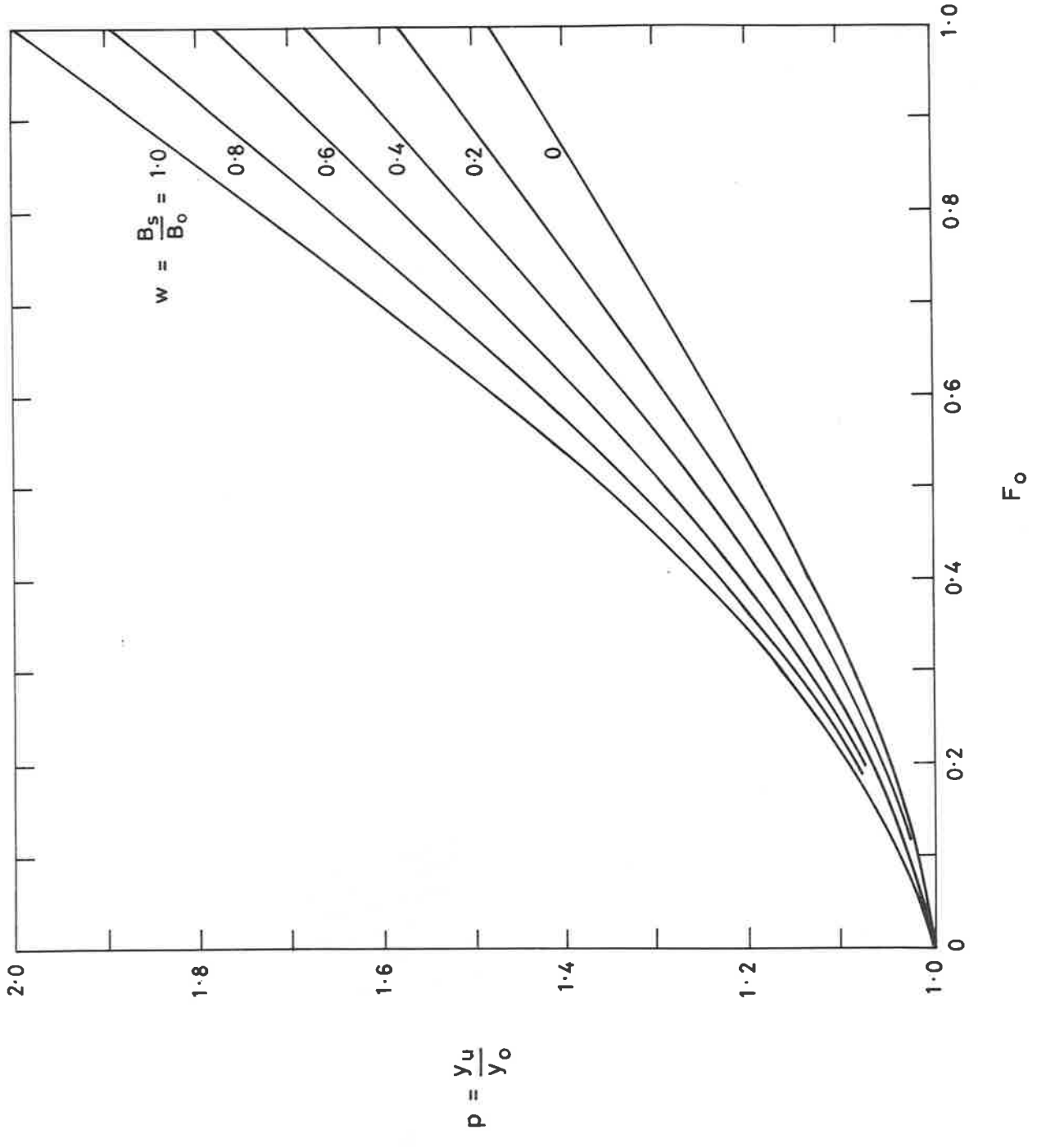

Fig 7c Variation of p with F_o and w for trapezoidal gutters : design

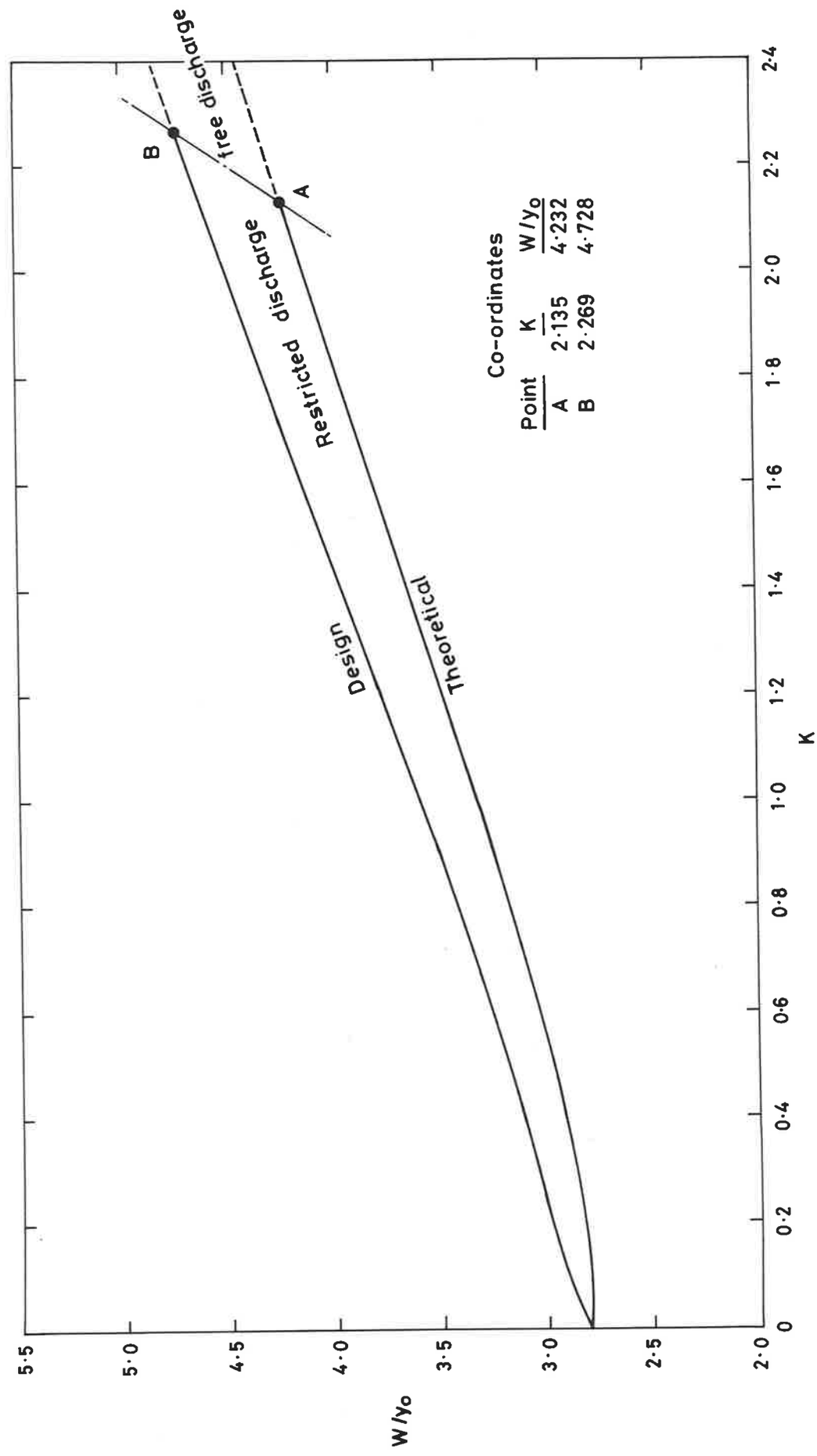

Fig 8a Size of true half-round gutters with restricted discharge

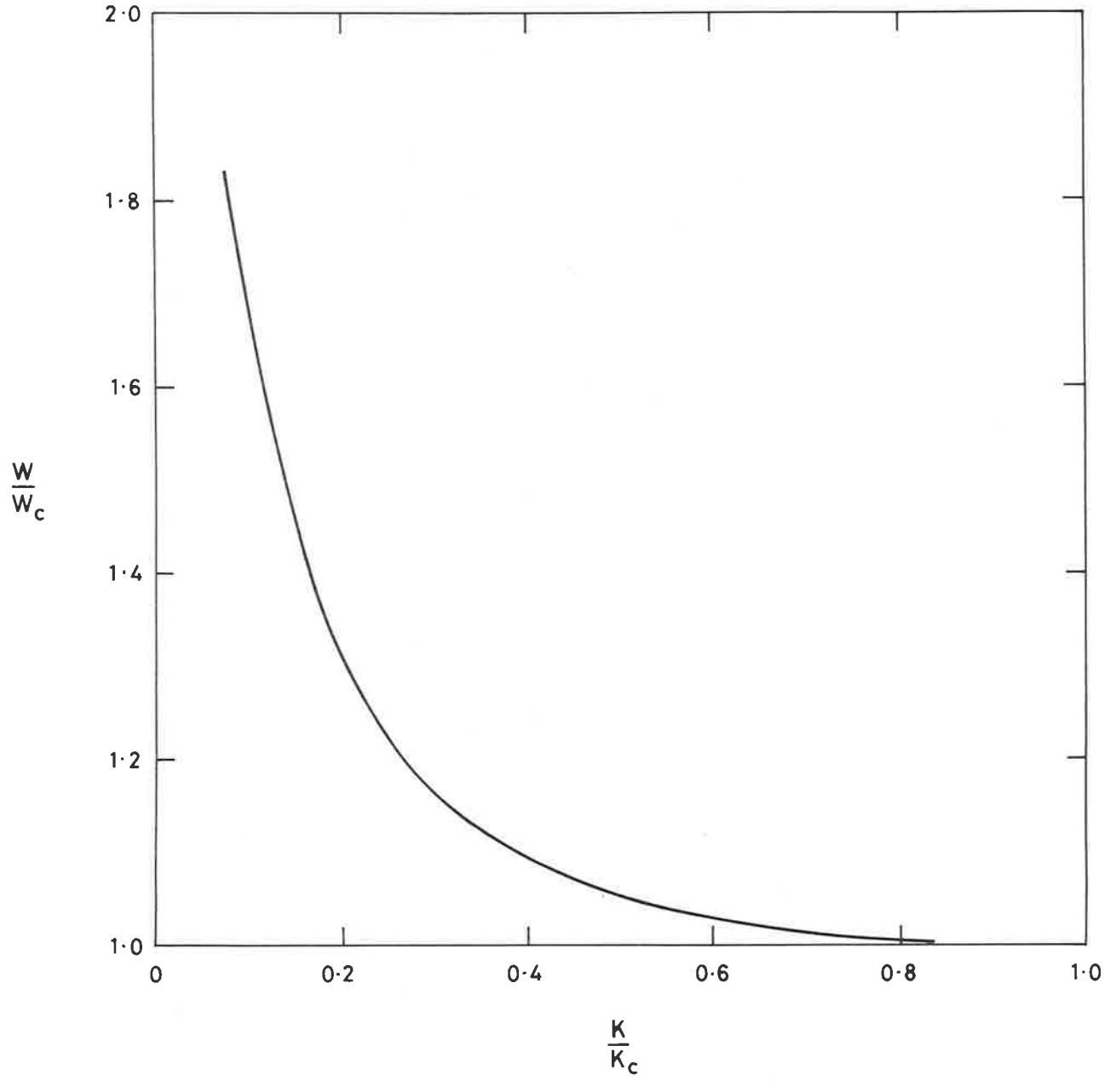

Fig 8b Effect of restricted discharge on size of true half-round gutter : theoretical

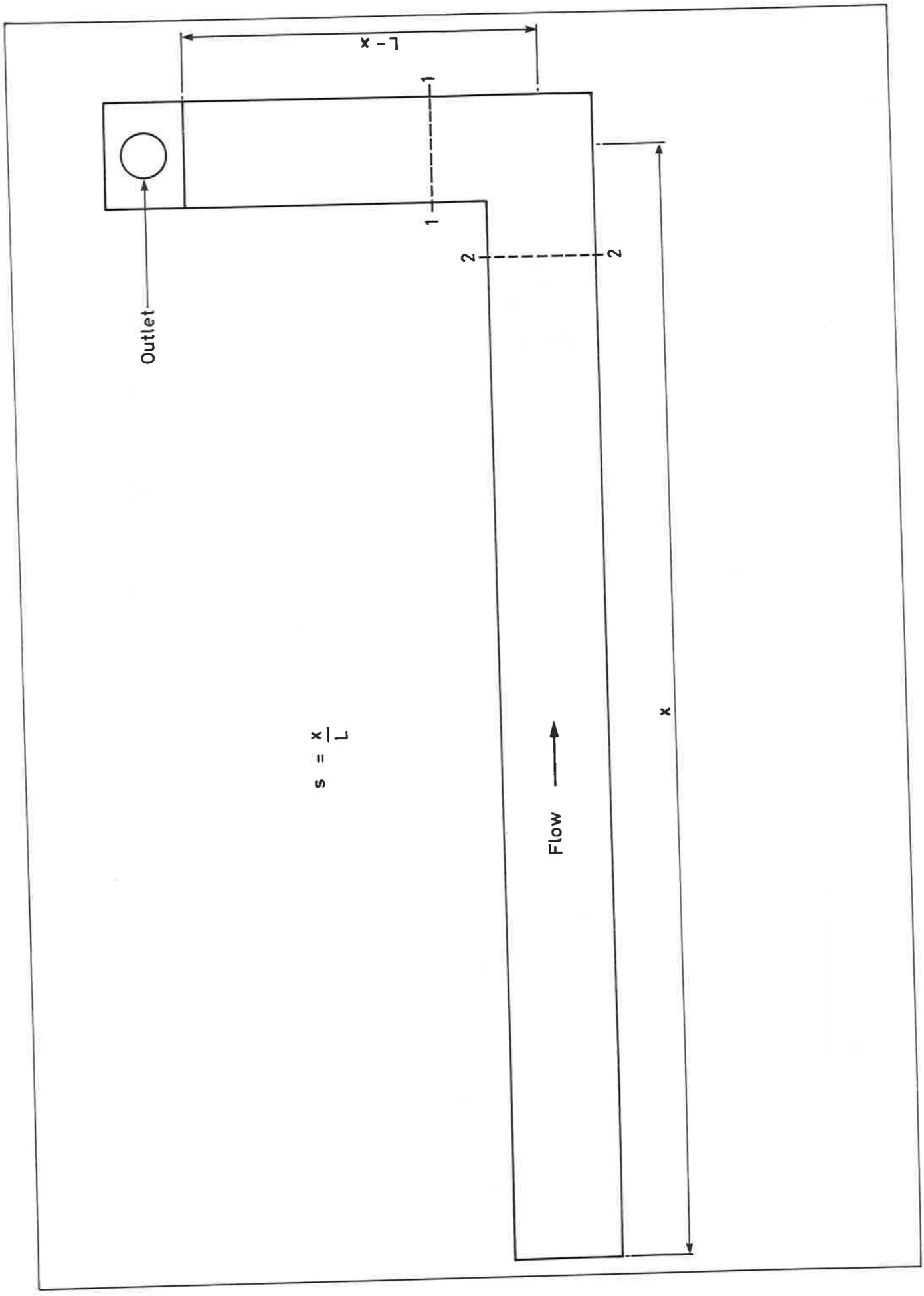

Fig 9 Plan view of bend in gutter

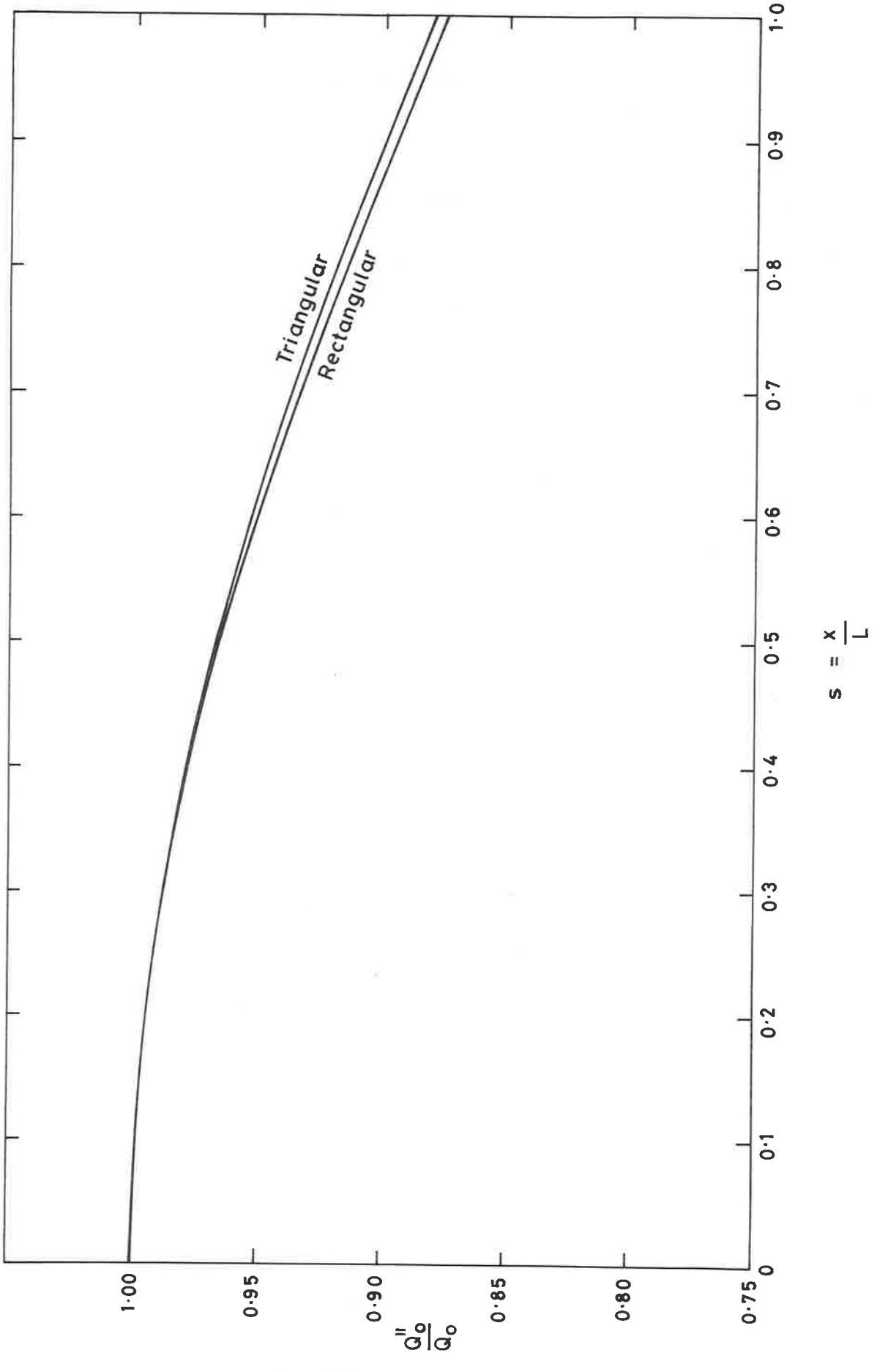

Fig 10 Variation of gutter capacity with position of 90° bend

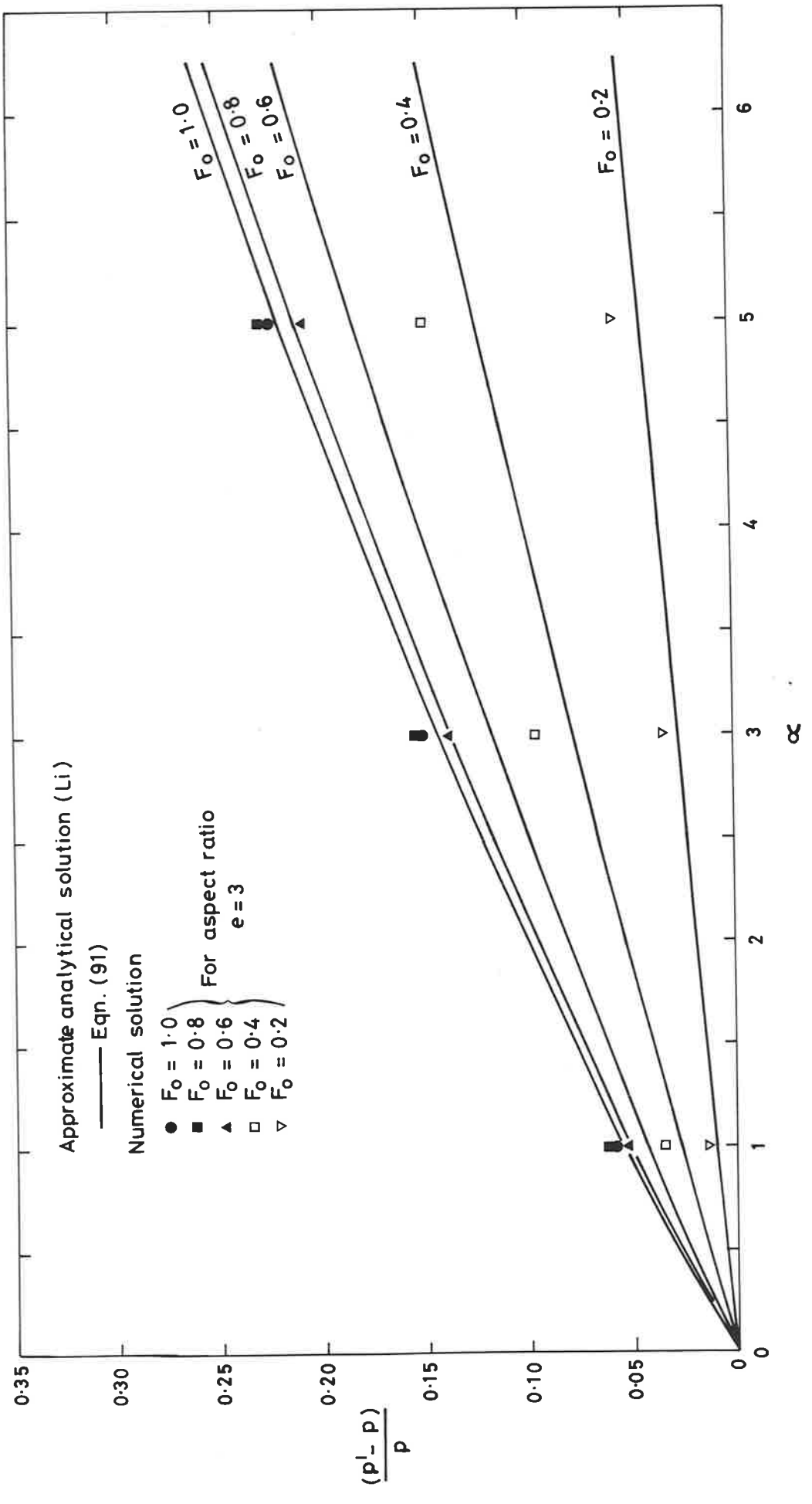

Fig 11a Effect of resistance on upstream depth in flow in level rectangular gutter

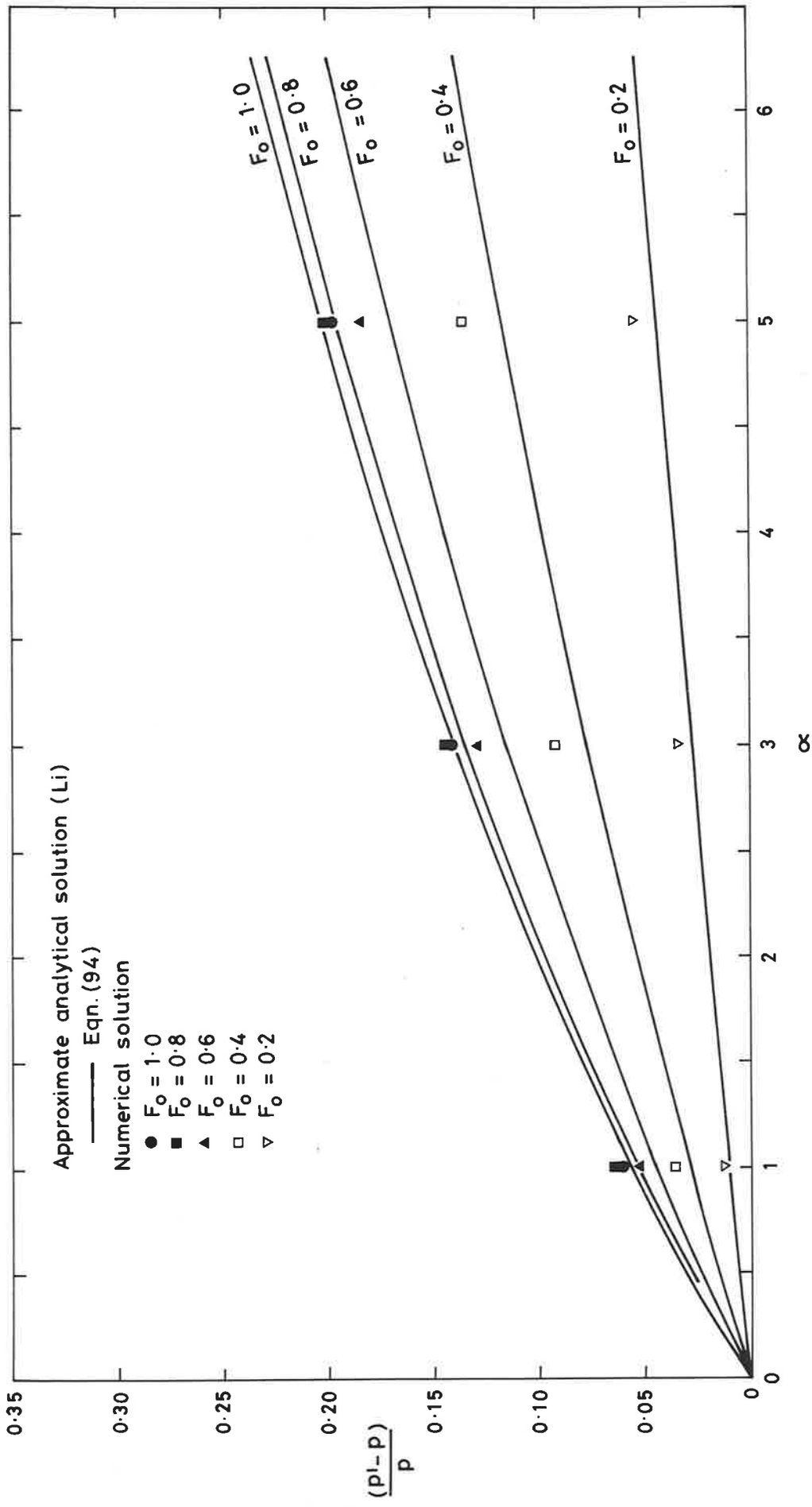

Fig 11b Effect of resistance on upstream depth of flow in level triangular gutter

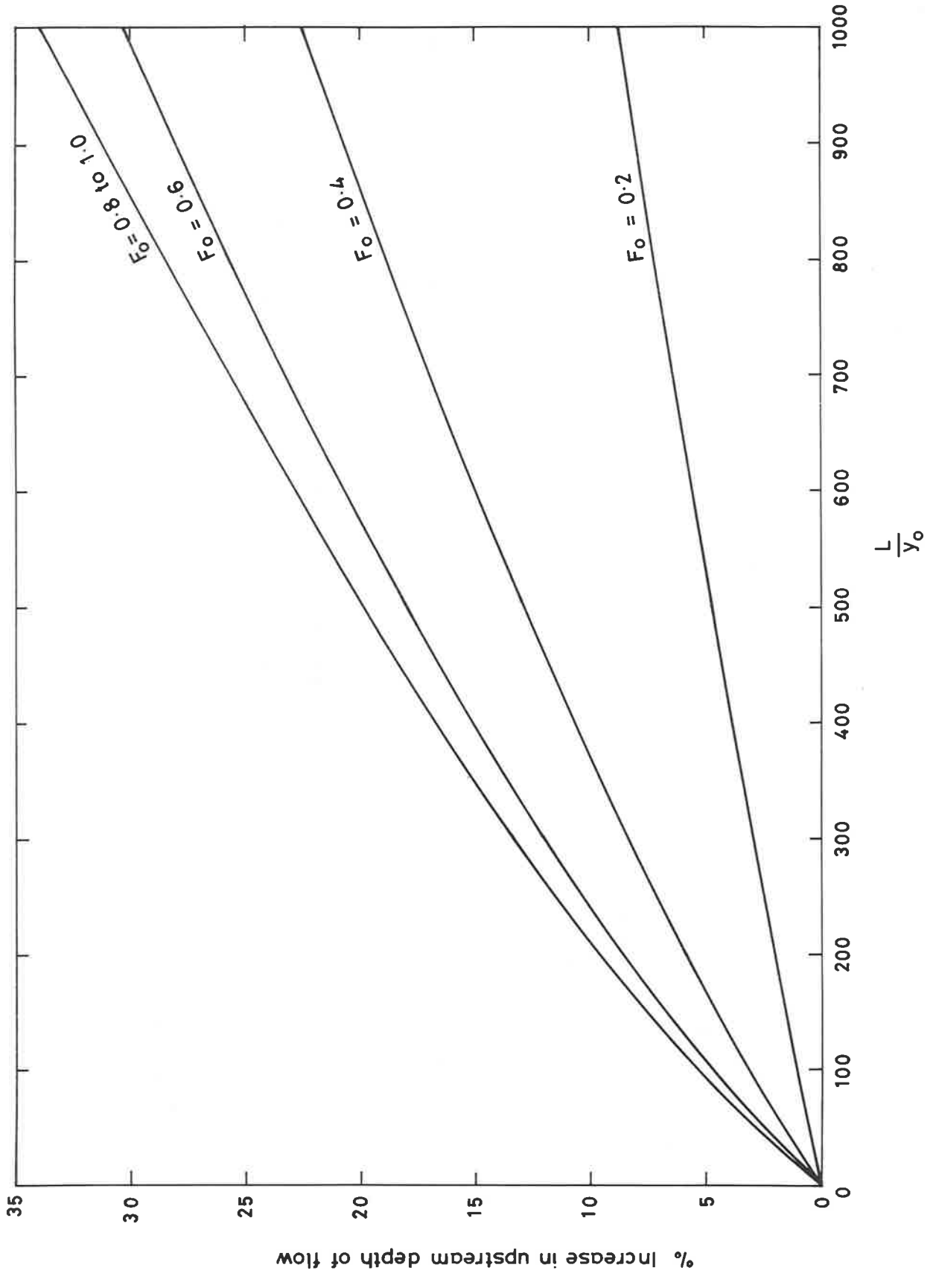

Fig 12a Design chart for effect of resistance in levels gutters

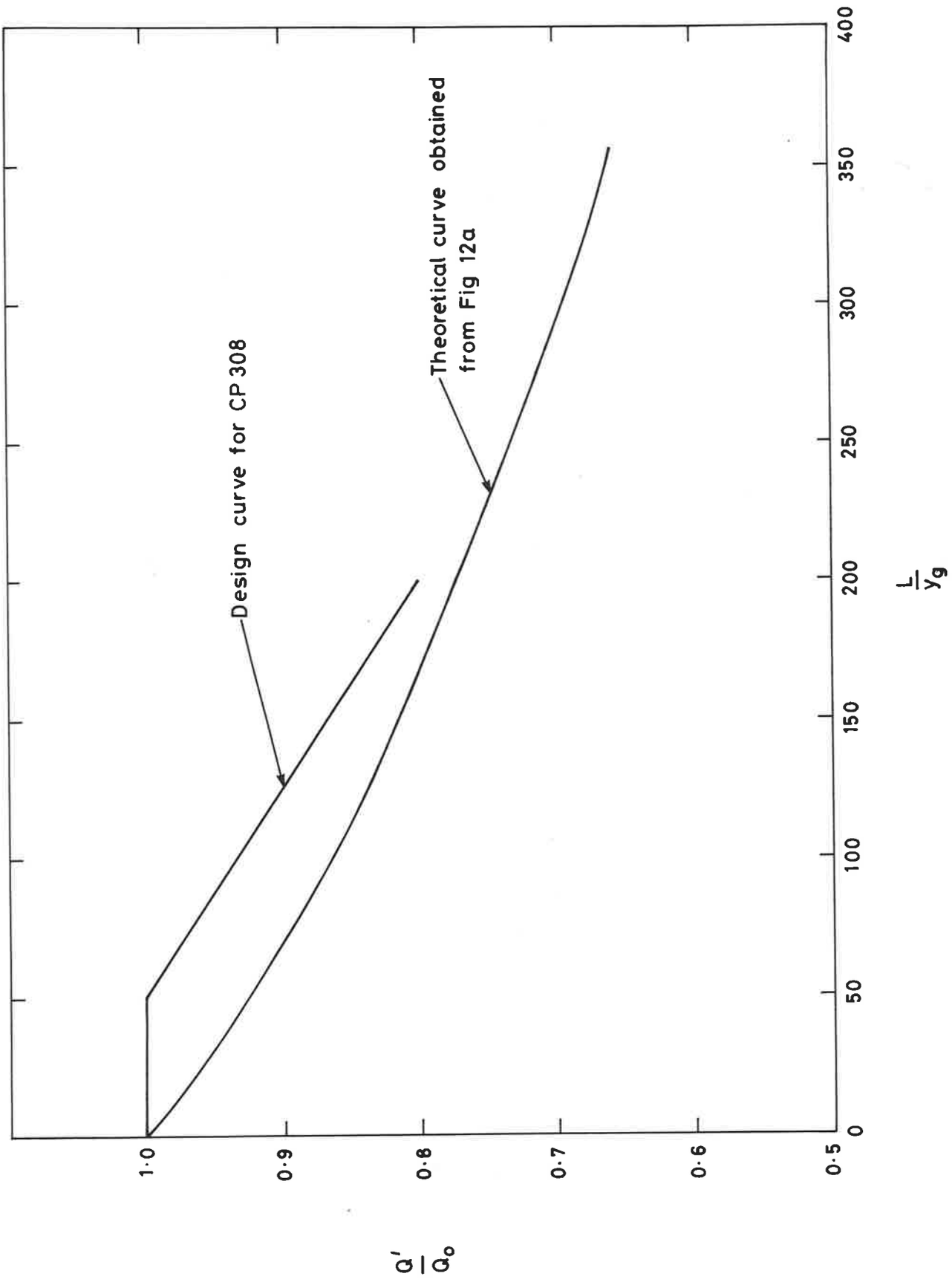

Fig 12b Effect of resistance on capacity of freely-discharging half-round eaves gutters

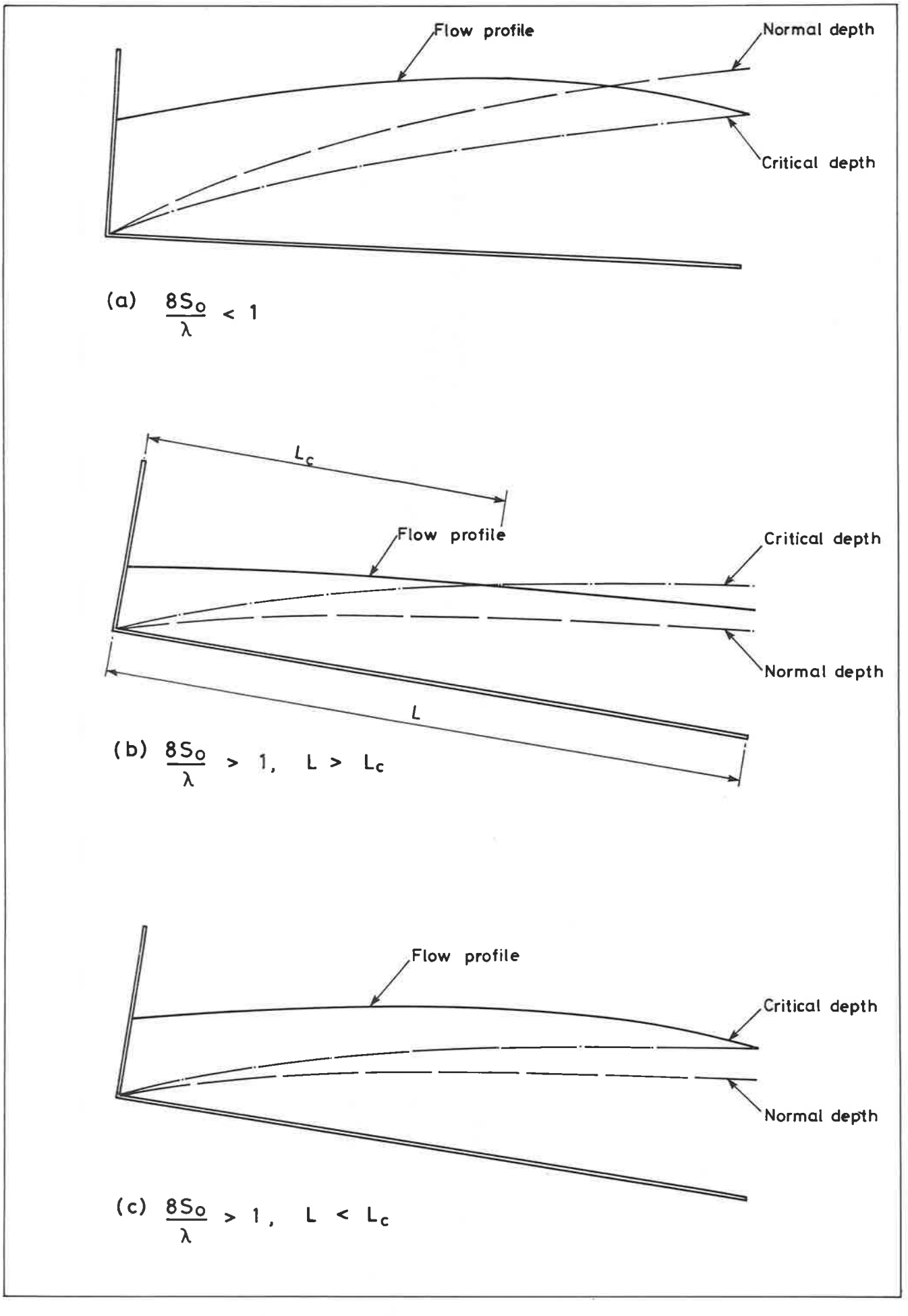

Fig 13 Types of flow profile in sloping gutters

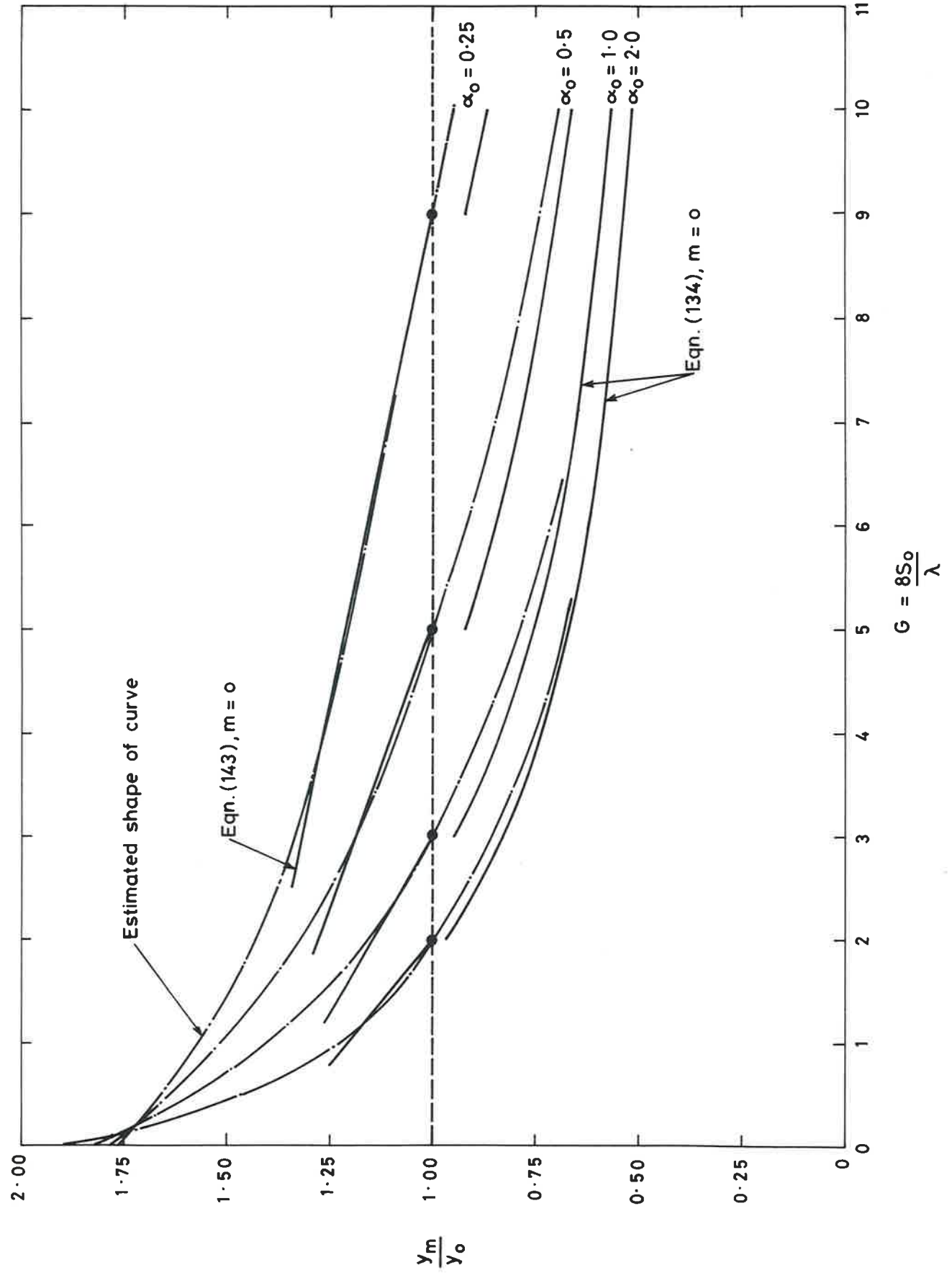

Fig 14a Effect of slope on maximum depth of flow in wide rectangular gutter

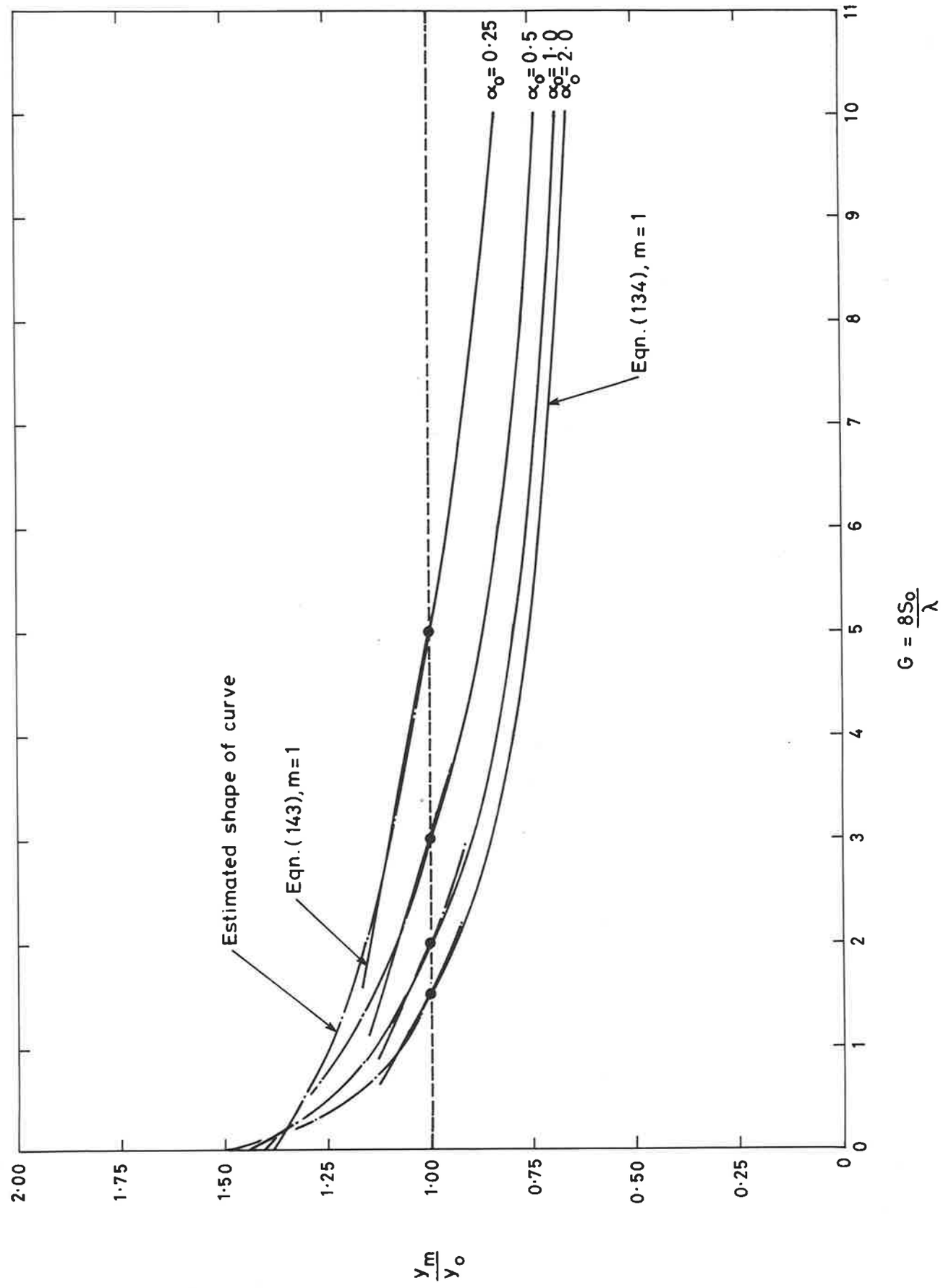

Fig 14b Effect of slope on maximum depth of flow in wide triangular gutter

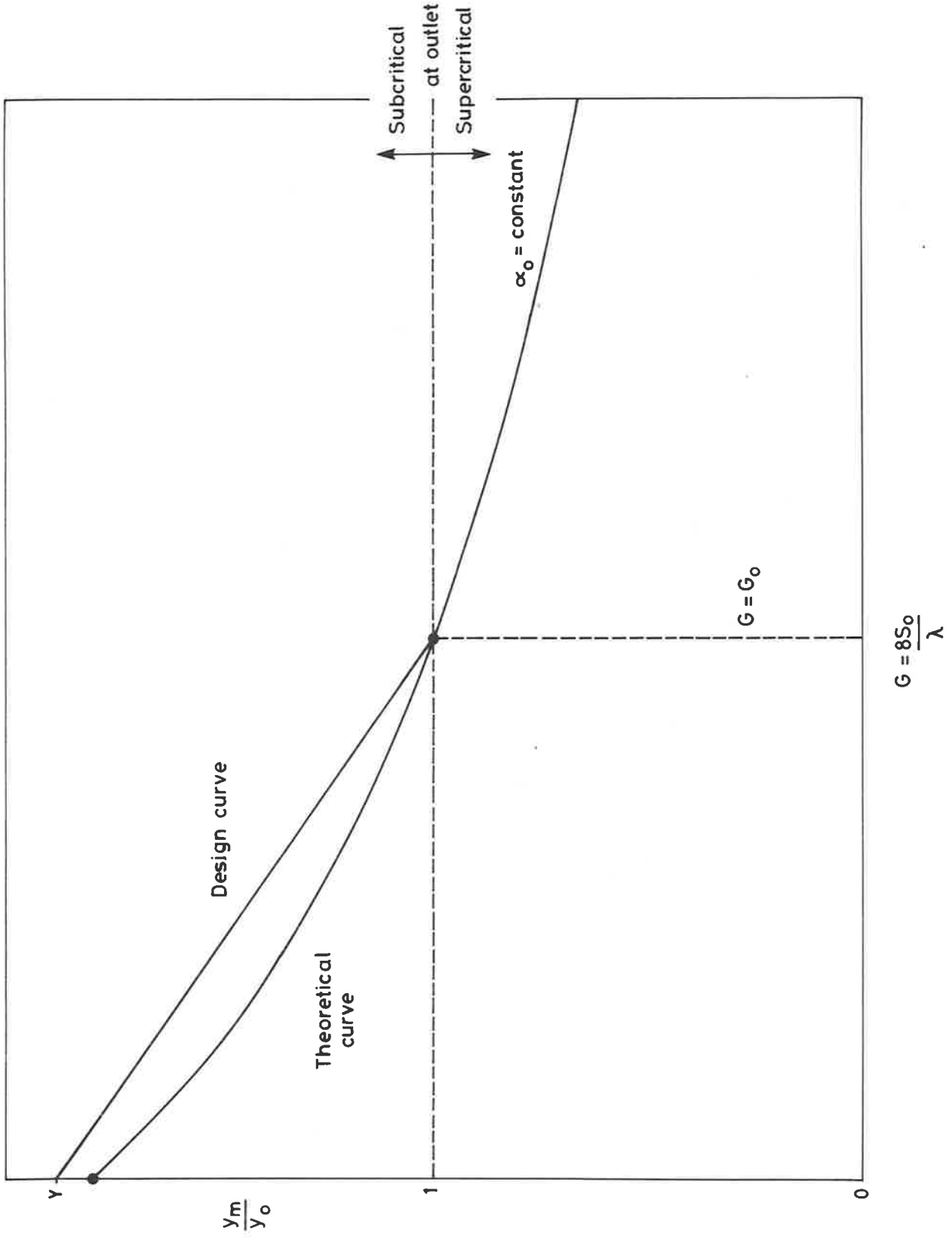

Fig 14c Definition sketch for design method for sloping gutters

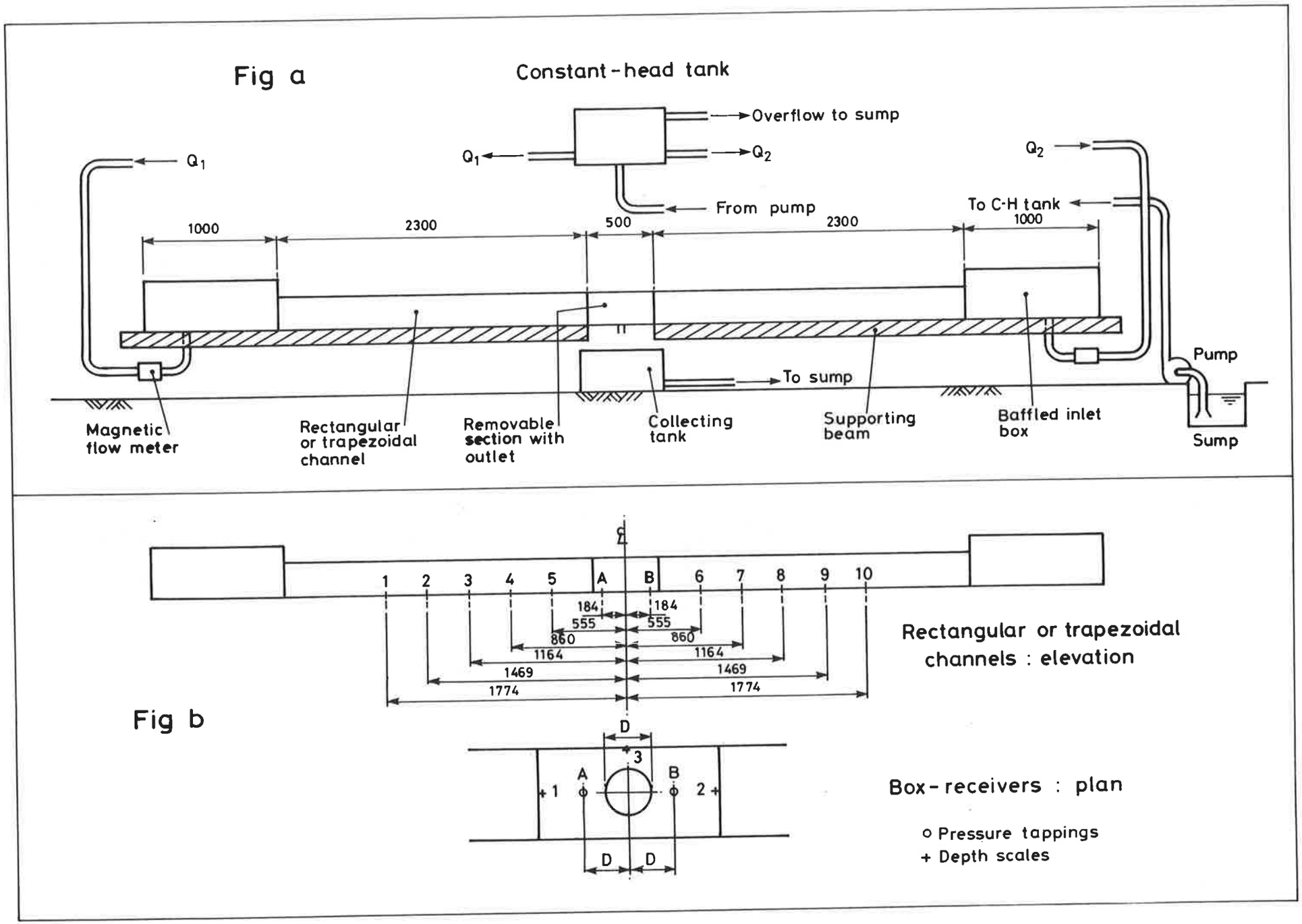

Fig 15a Layout of BHRA test rig for gutter outlets : elevation
15b Positions of pressure tappings

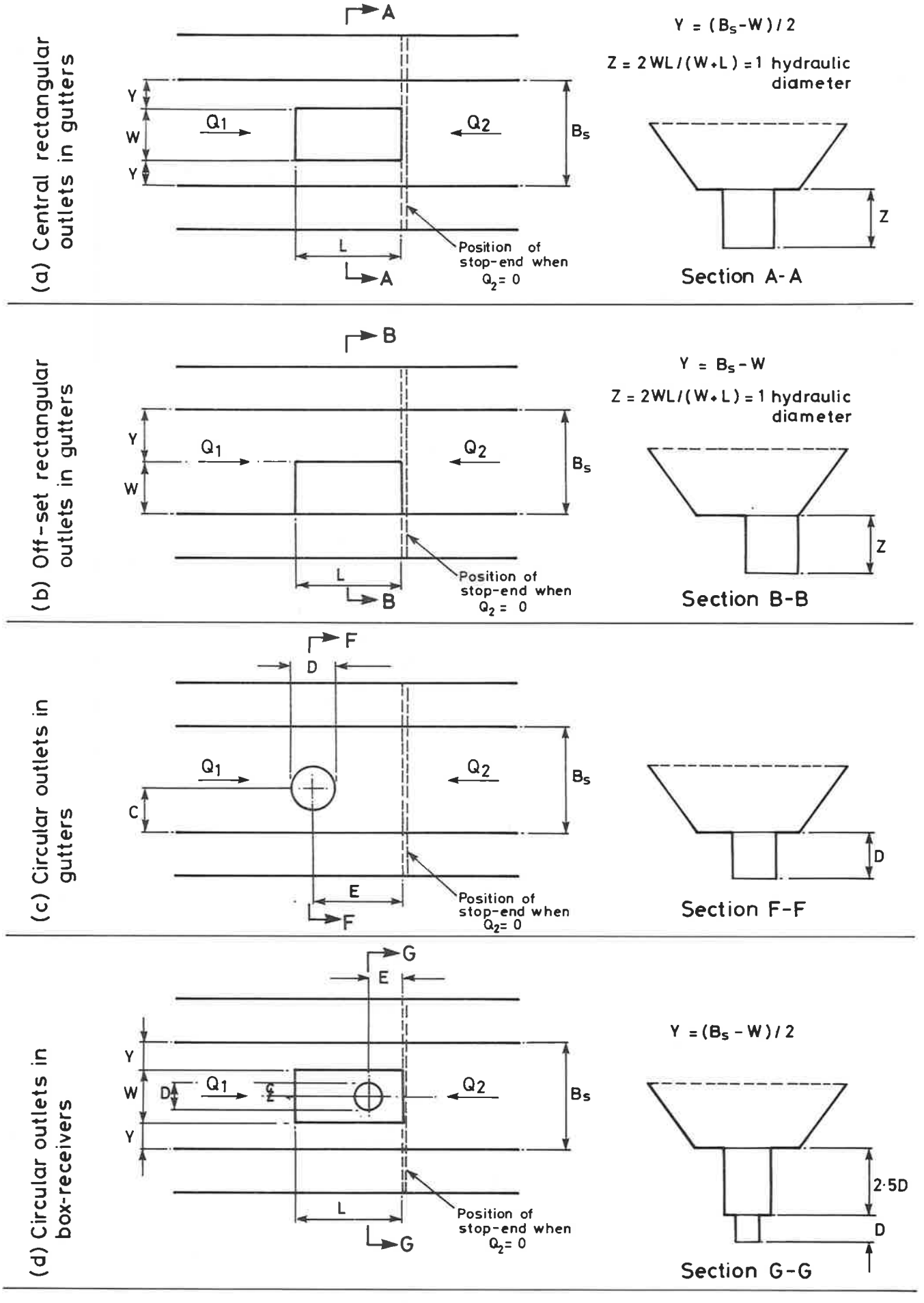

Fig 16 Position of outlets in gutters and box-receivers

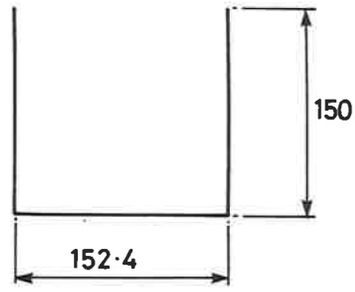

(a) Rectangular gutter

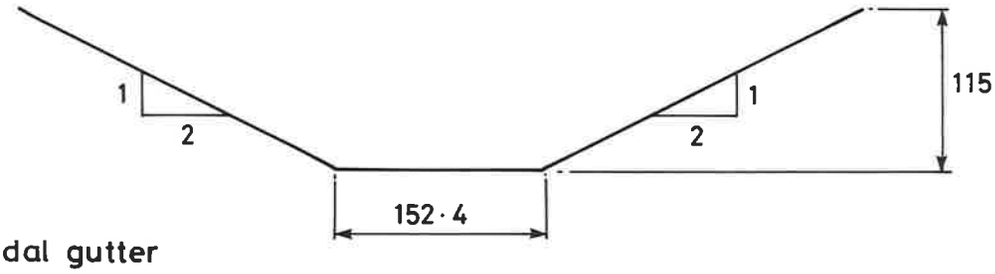

(b) Trapezoidal gutter

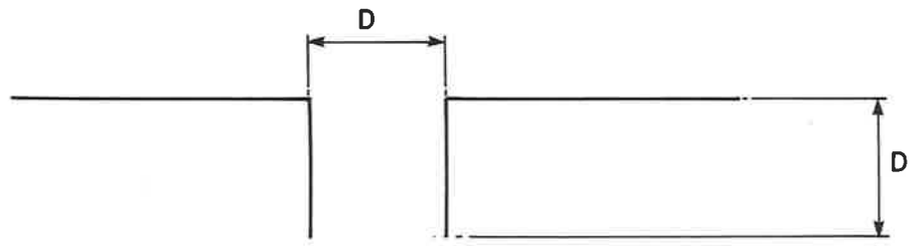

(c) Circular outlet : sharp-edged

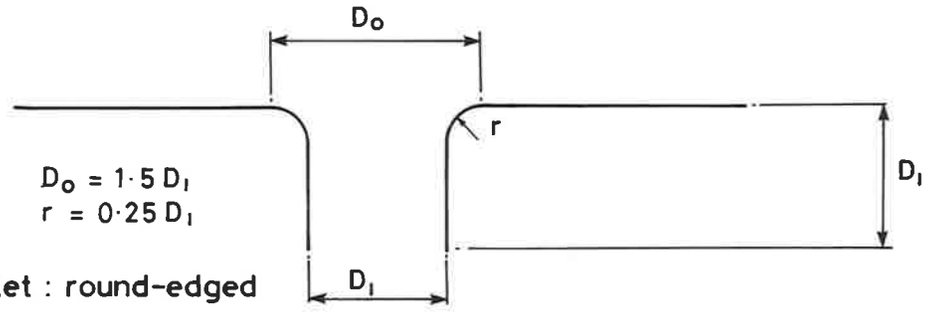

(d) Circular outlet : round-edged

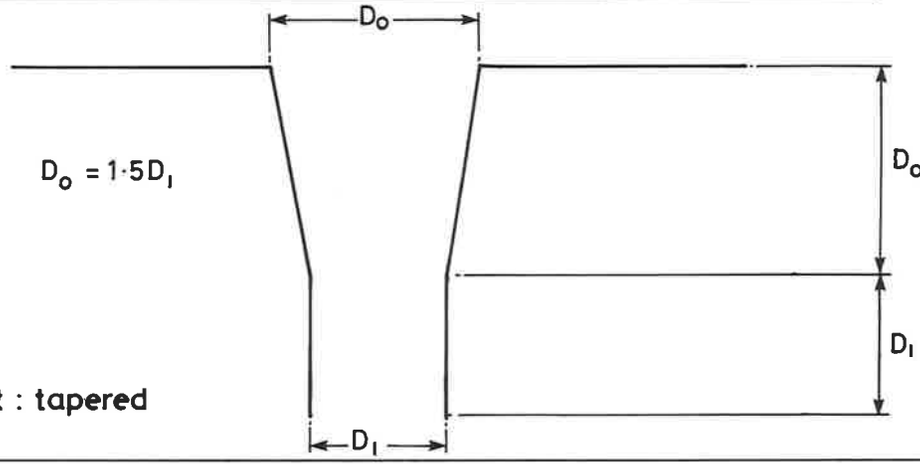

(e) Circular outlet : tapered

Fig 17 Cross-sectional shapes of gutters and outlets

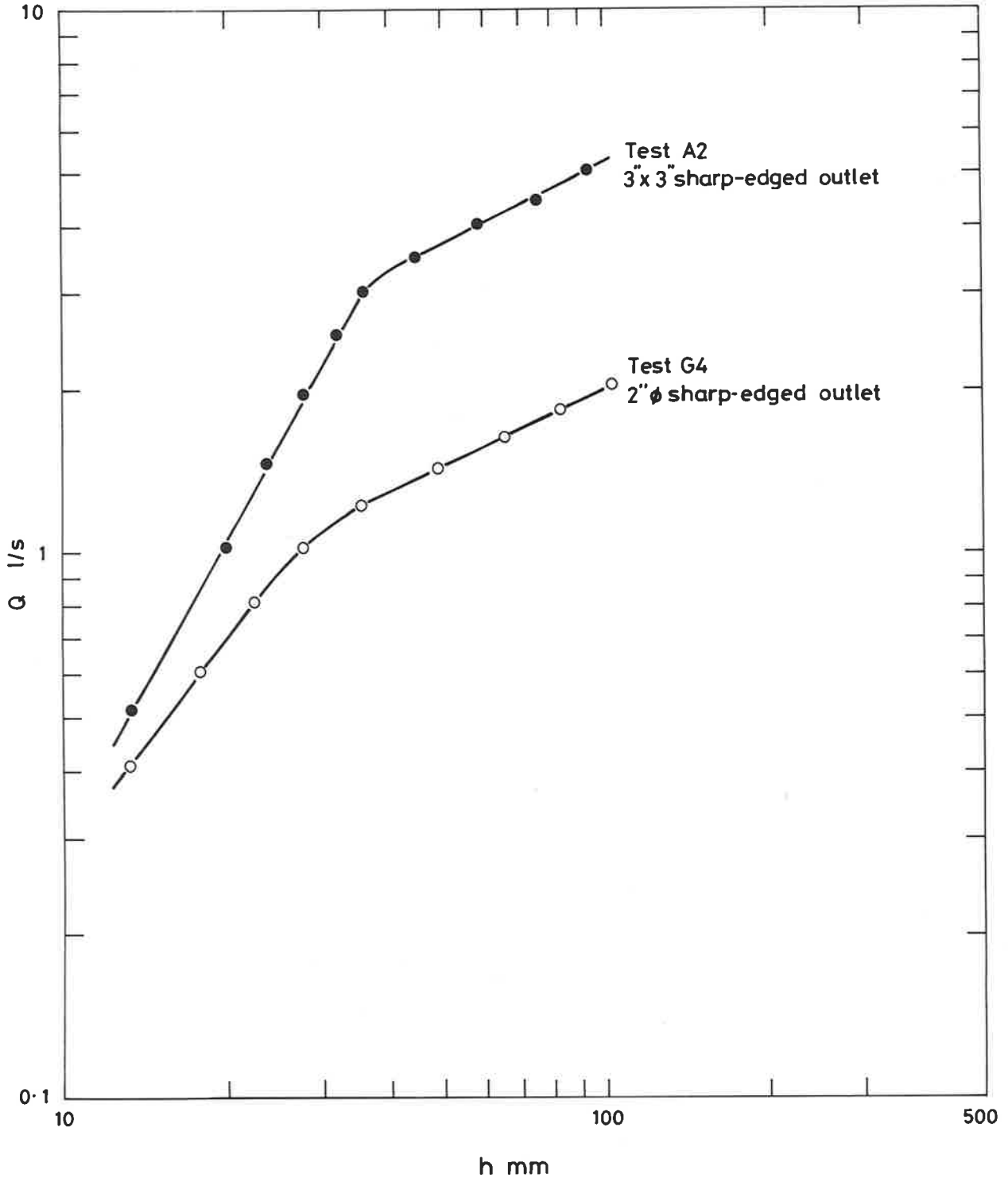

Fig 18a Typical results for sharp-edged outlets: discharge versus static head

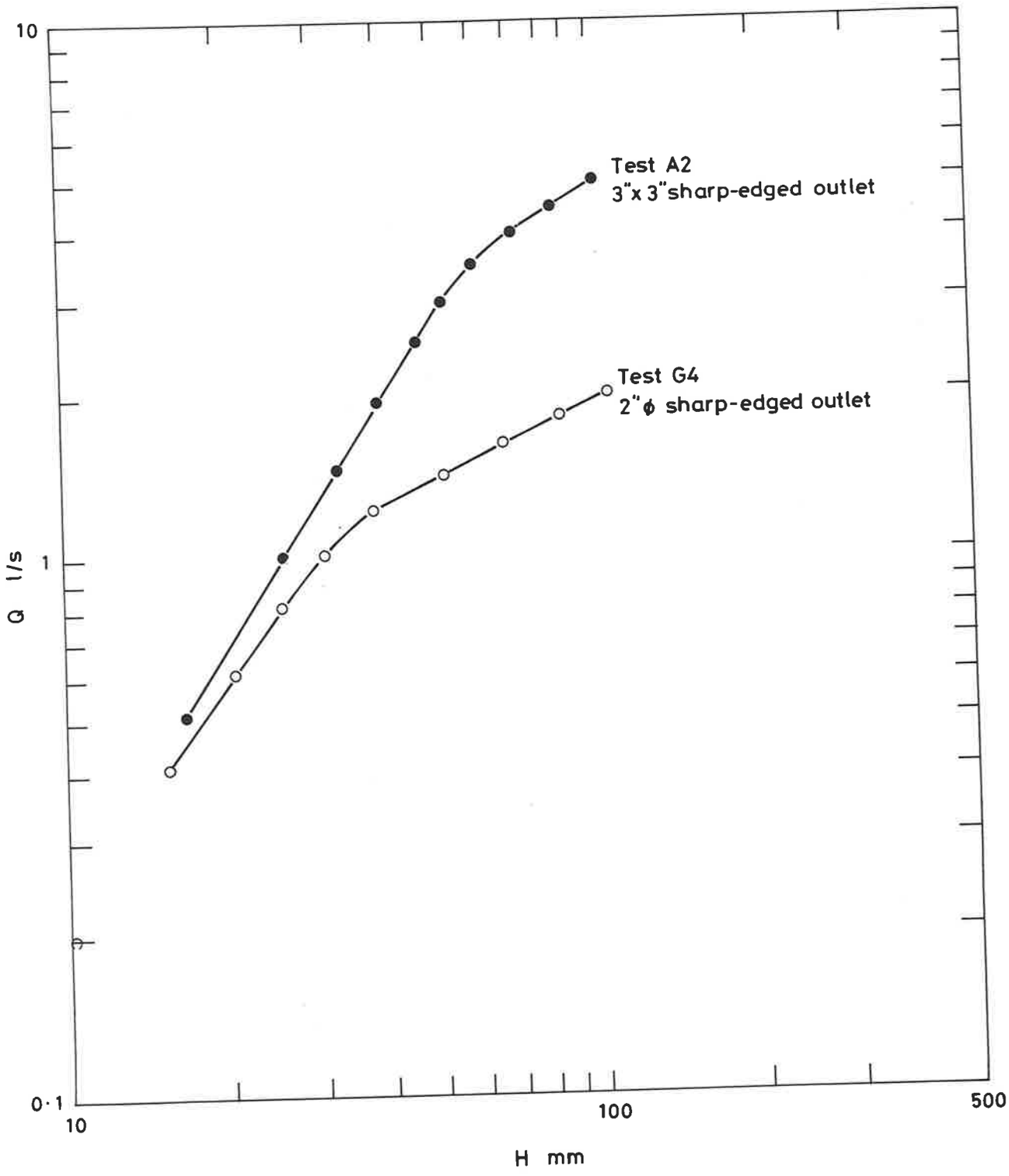

Fig 18b Typical results for sharp-edged outlets : discharge versus total head

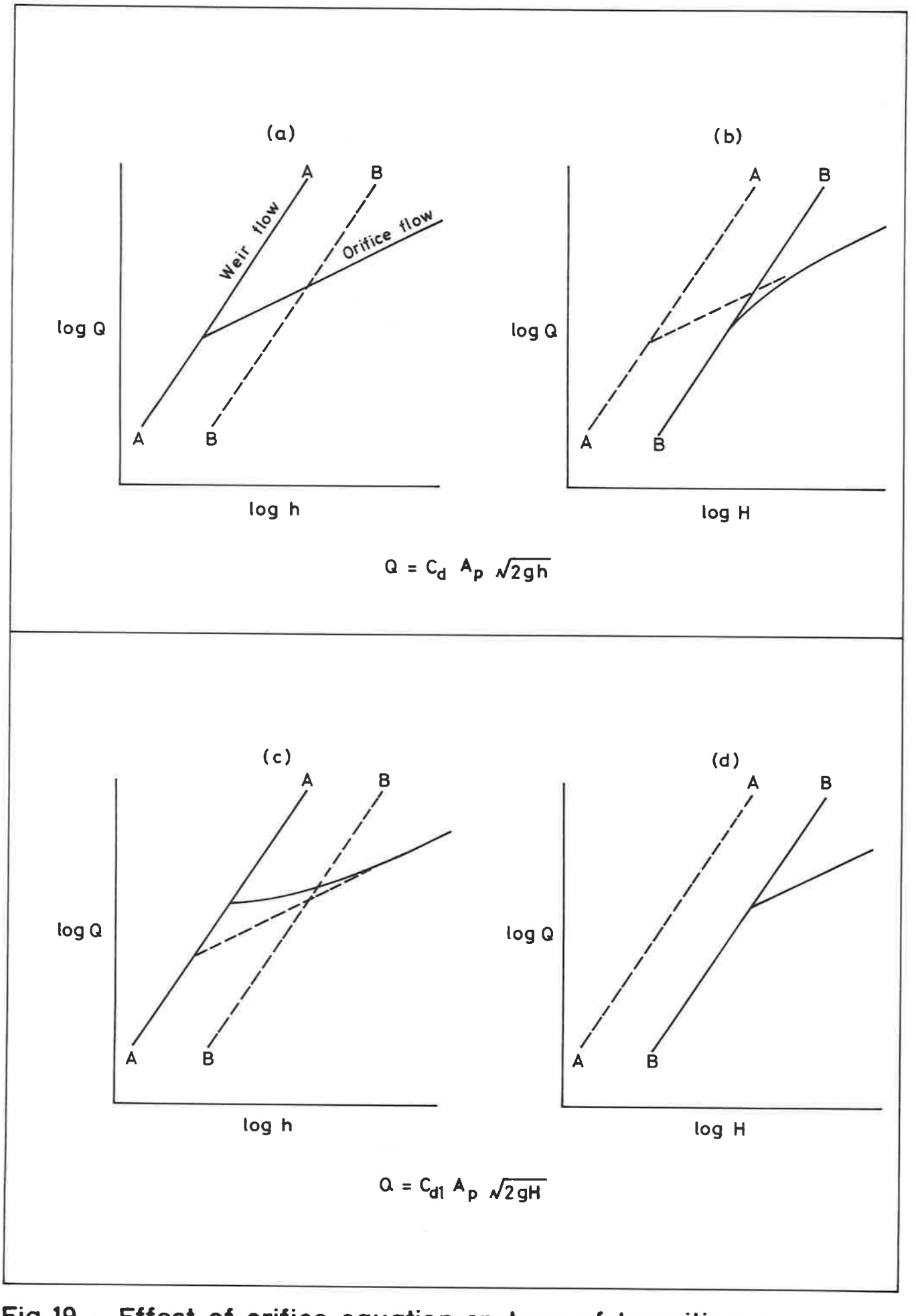

Fig 19 Effect of orifice equation on type of transition

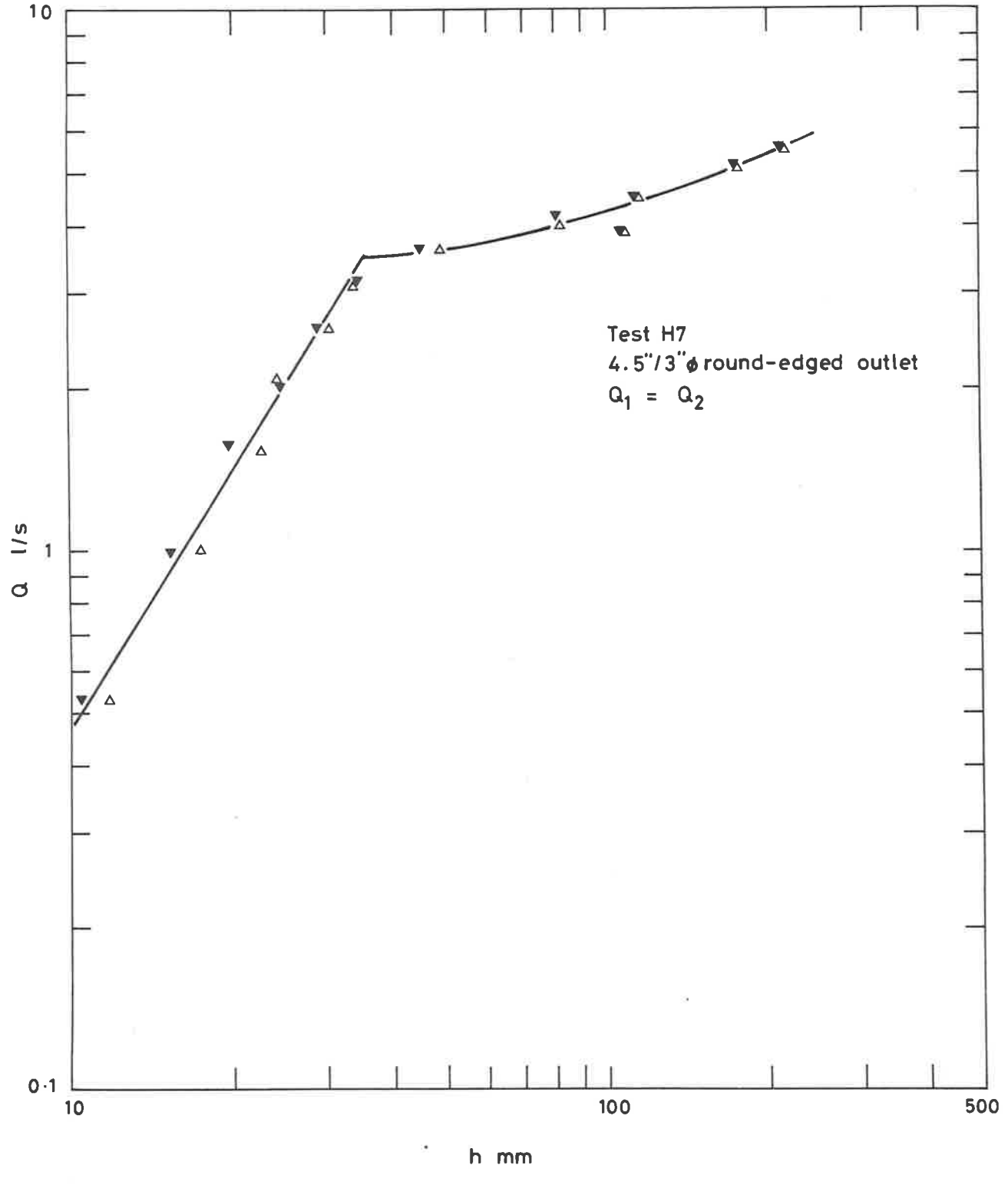

Fig 20a Typical results for round-edged outlets : discharge versus total head

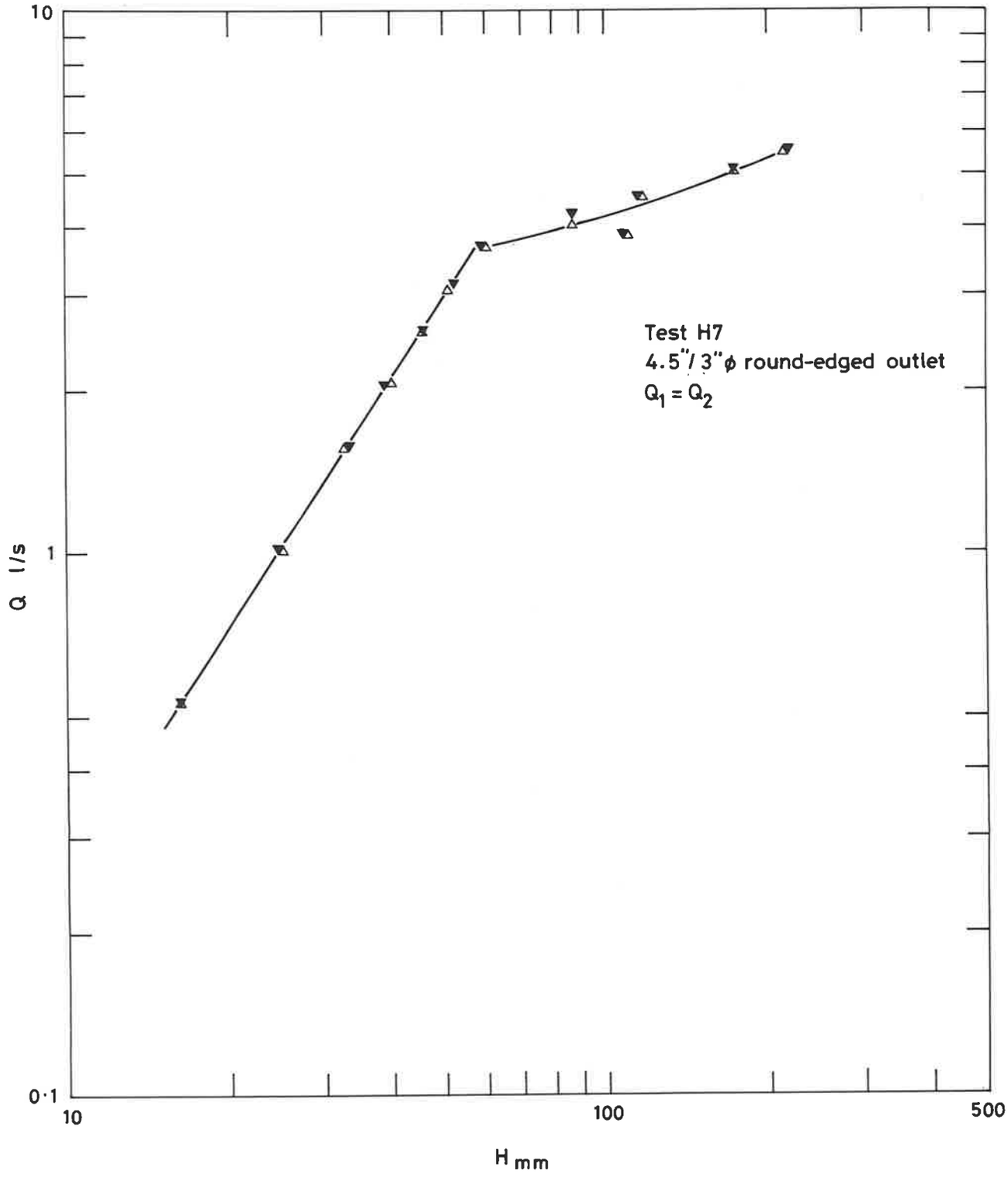

Fig 20b Typical results for round-edged outlets: discharge versus total head

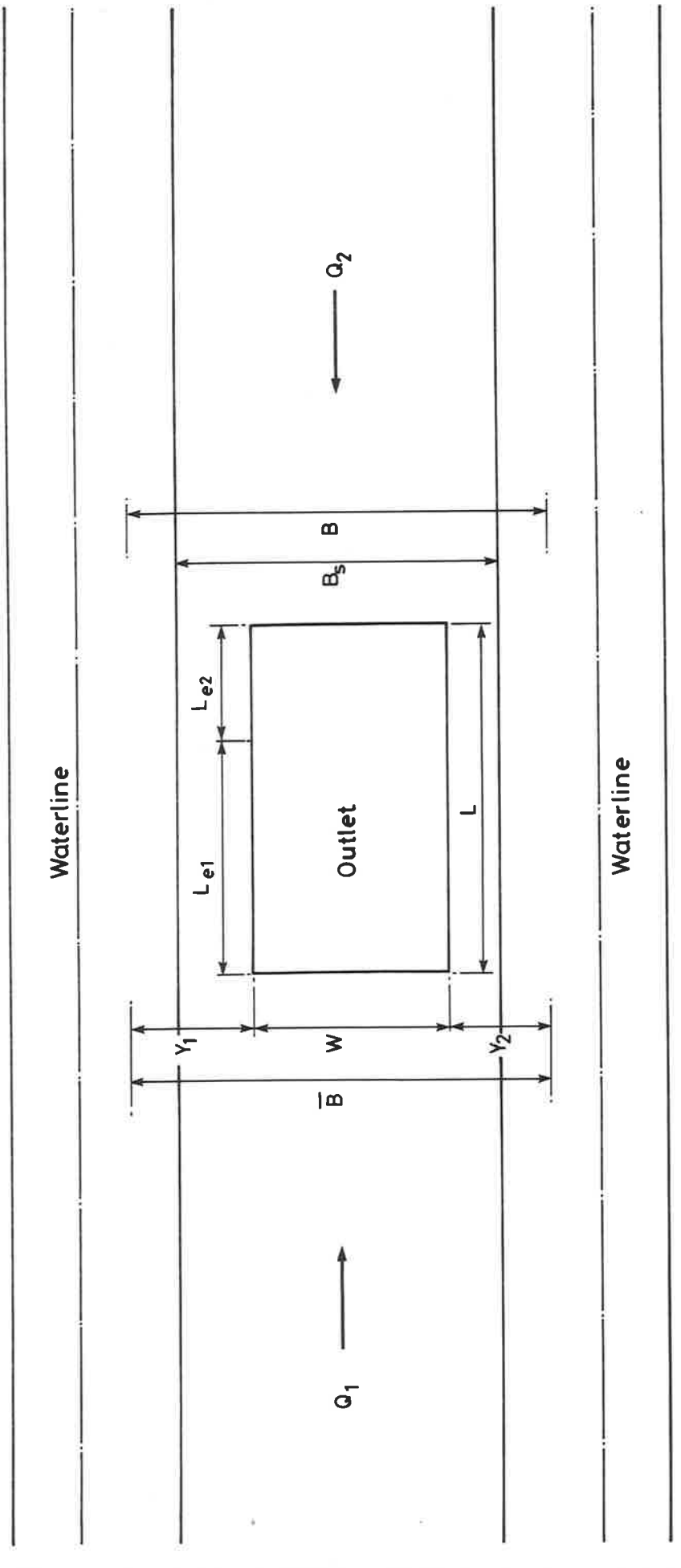

$\bar{B} = \frac{B + B_s}{2}$ = depth-averaged width of flow

B = width of flow $\quad B_s$ = sole width

$\frac{L_{e1}}{L} = \frac{Q_1}{Q_1 + Q_2} \qquad \frac{L_{e2}}{L} = \frac{Q_2}{Q_1 + Q_2}$

Fig 21 Plan of rectangular outlet in trapezoidal gutter

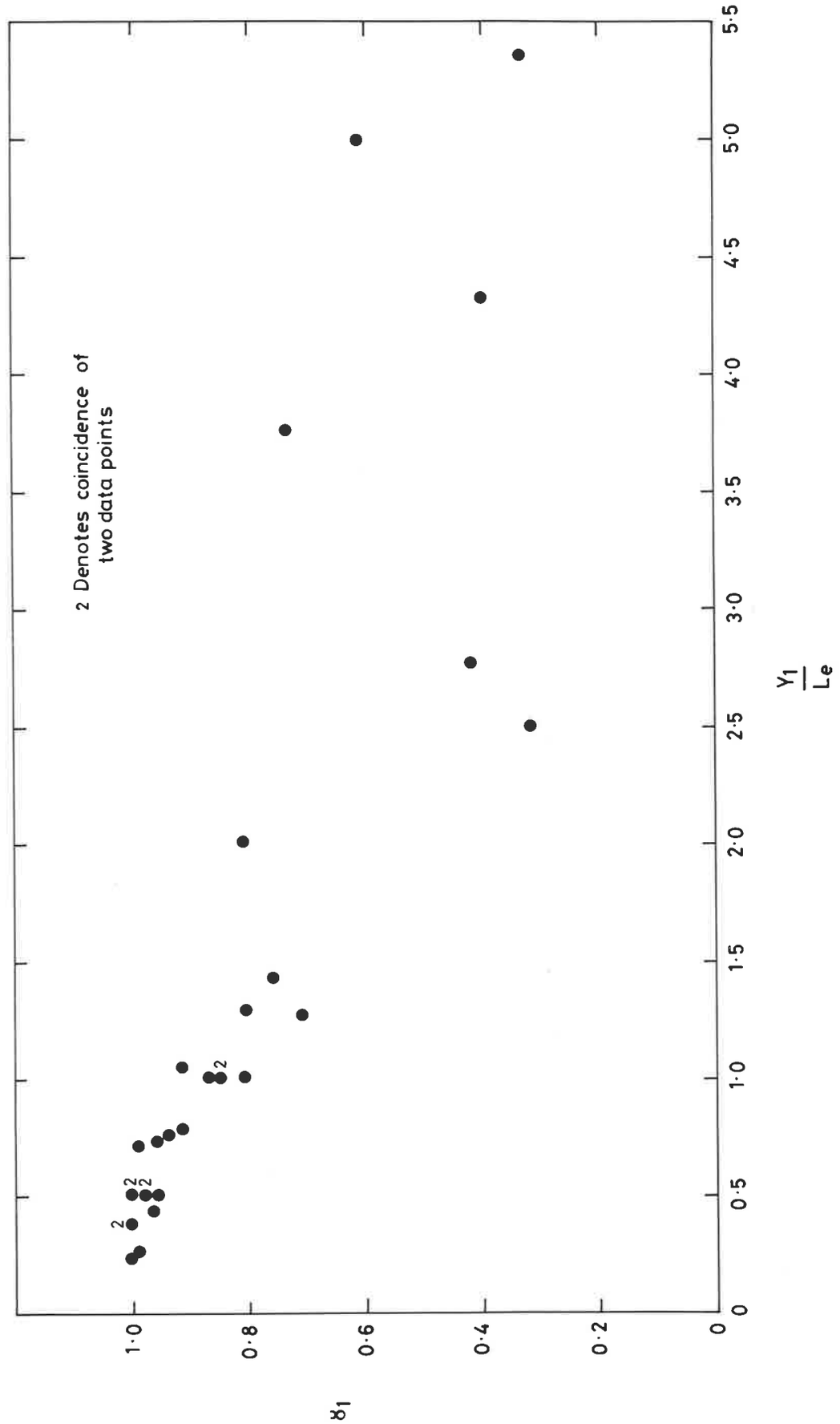

Fig 22 Variation of γ_1 with curvature of flow at rectangular outlet

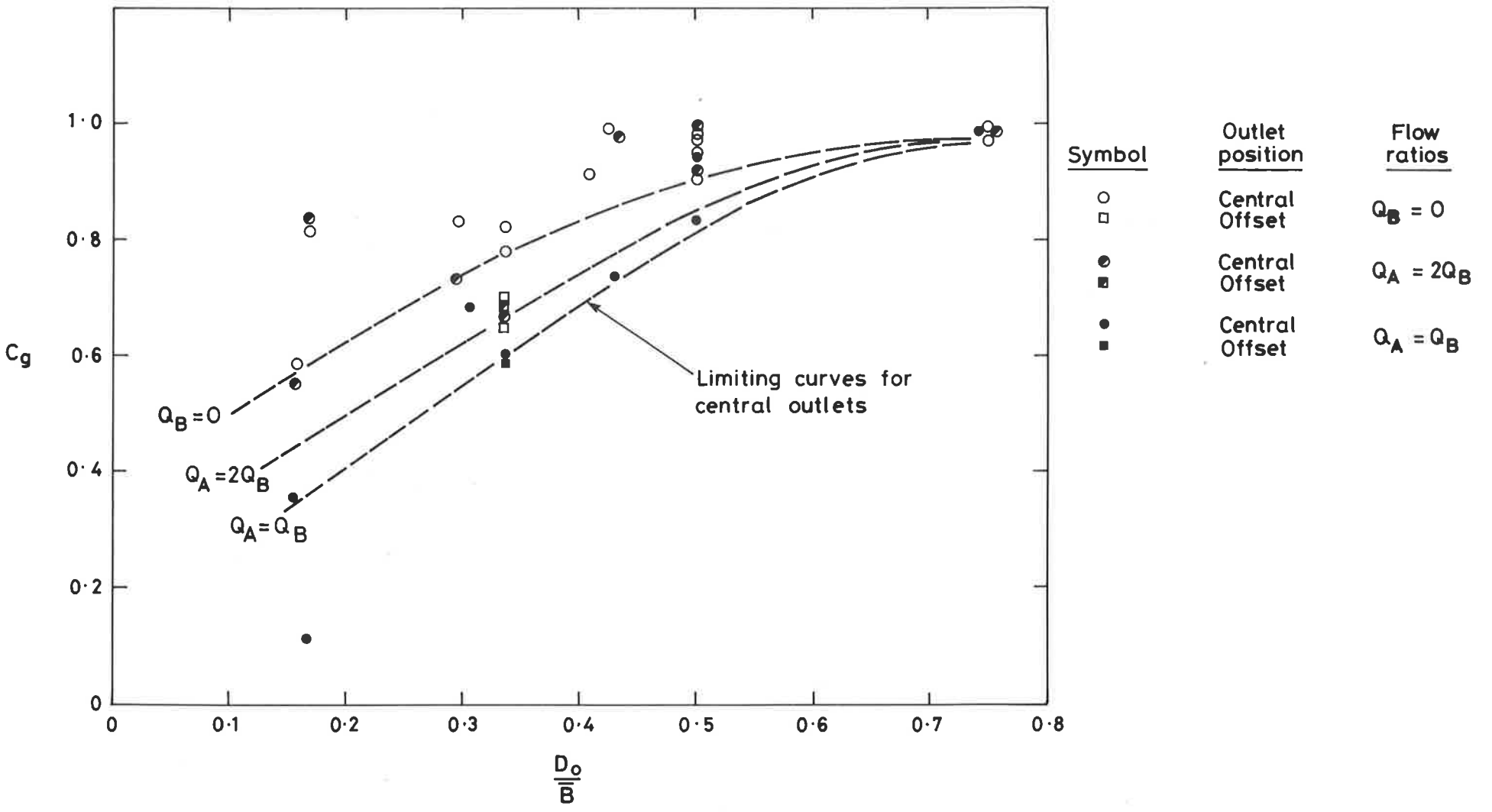

Fig 23 Variation of C_g with relative size of circular outlet

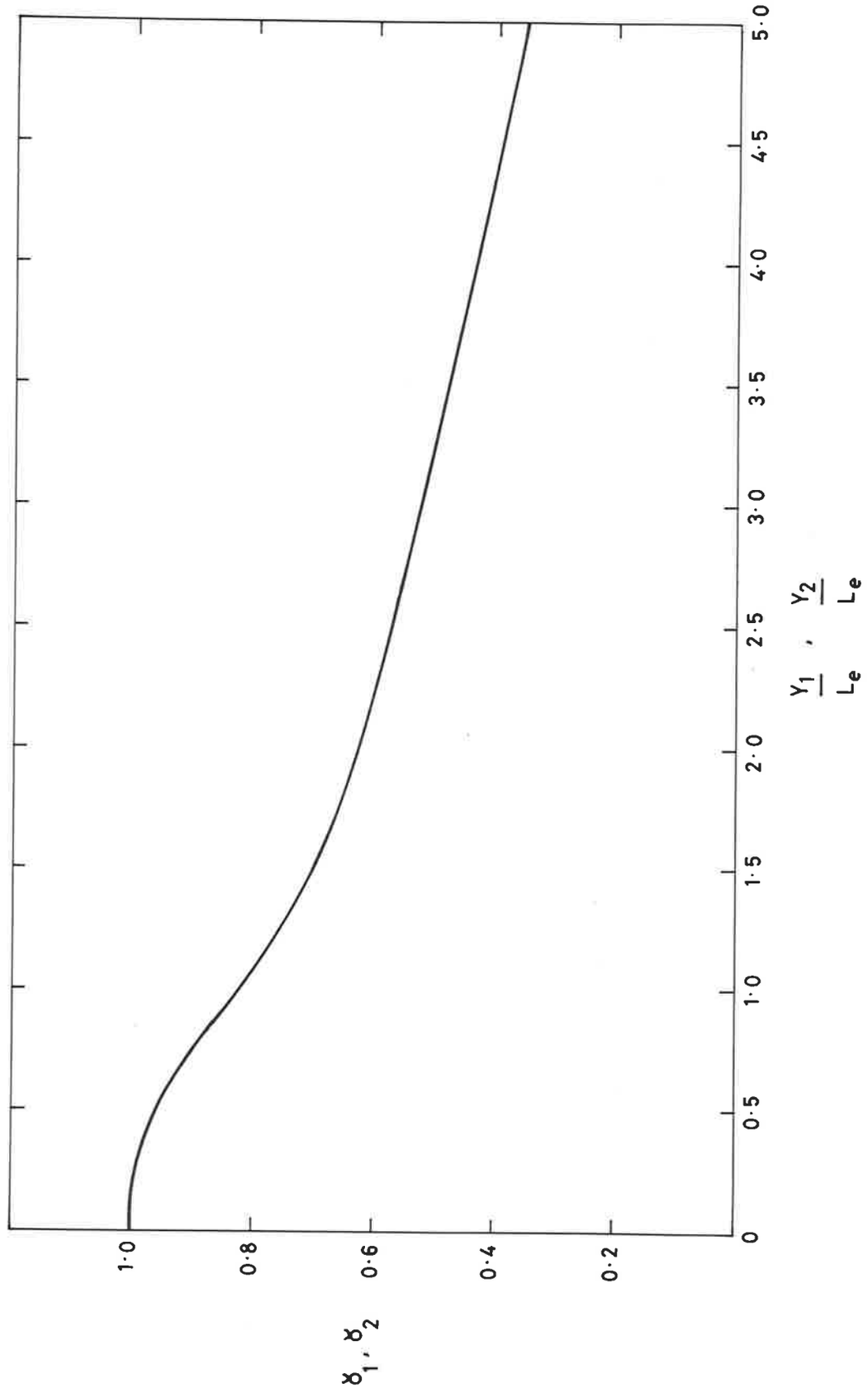

Fig 24 Design chart giving values of γ for rectangular outlets

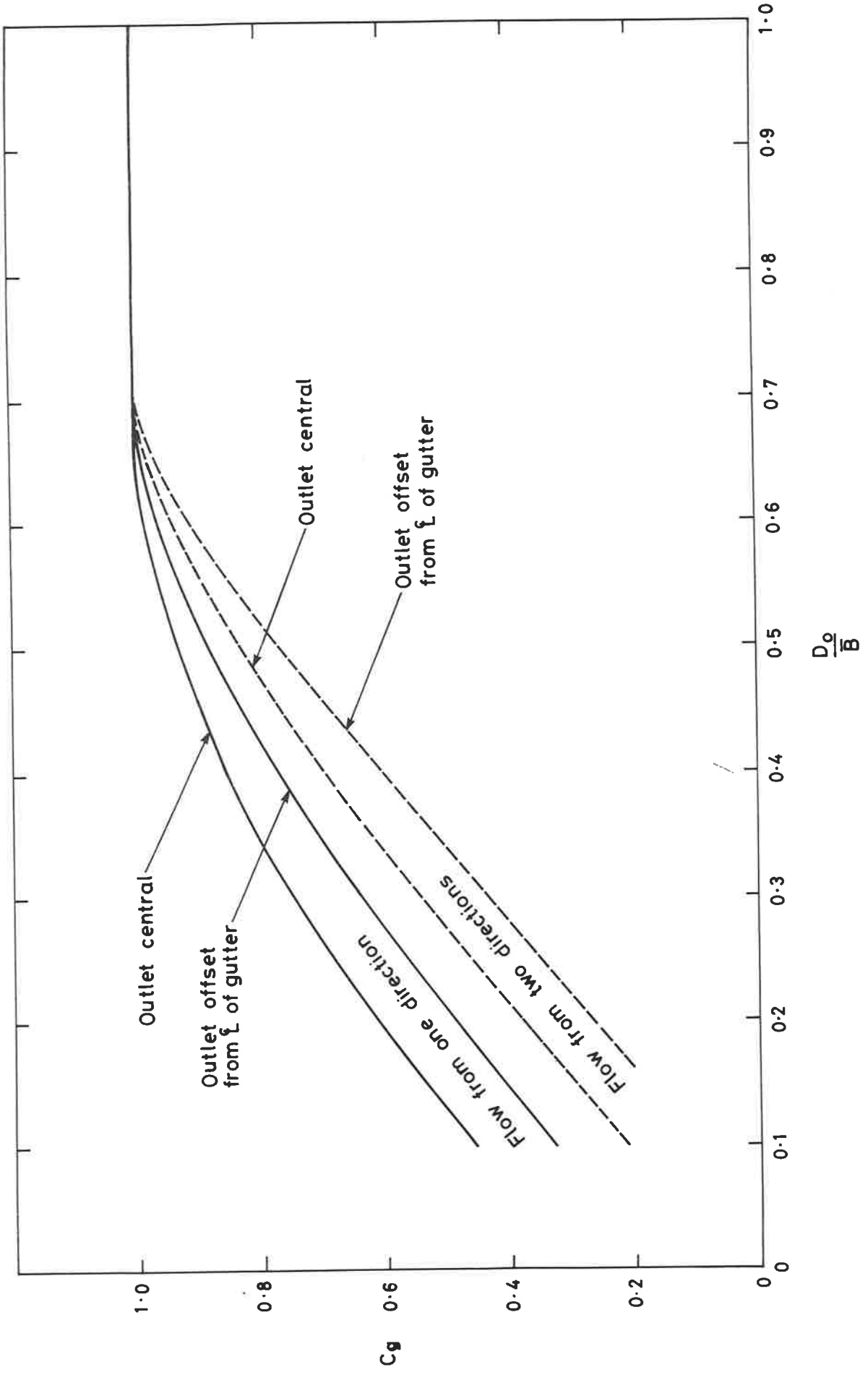

Fig 25 Design chart giving values of C_g for circular outlets

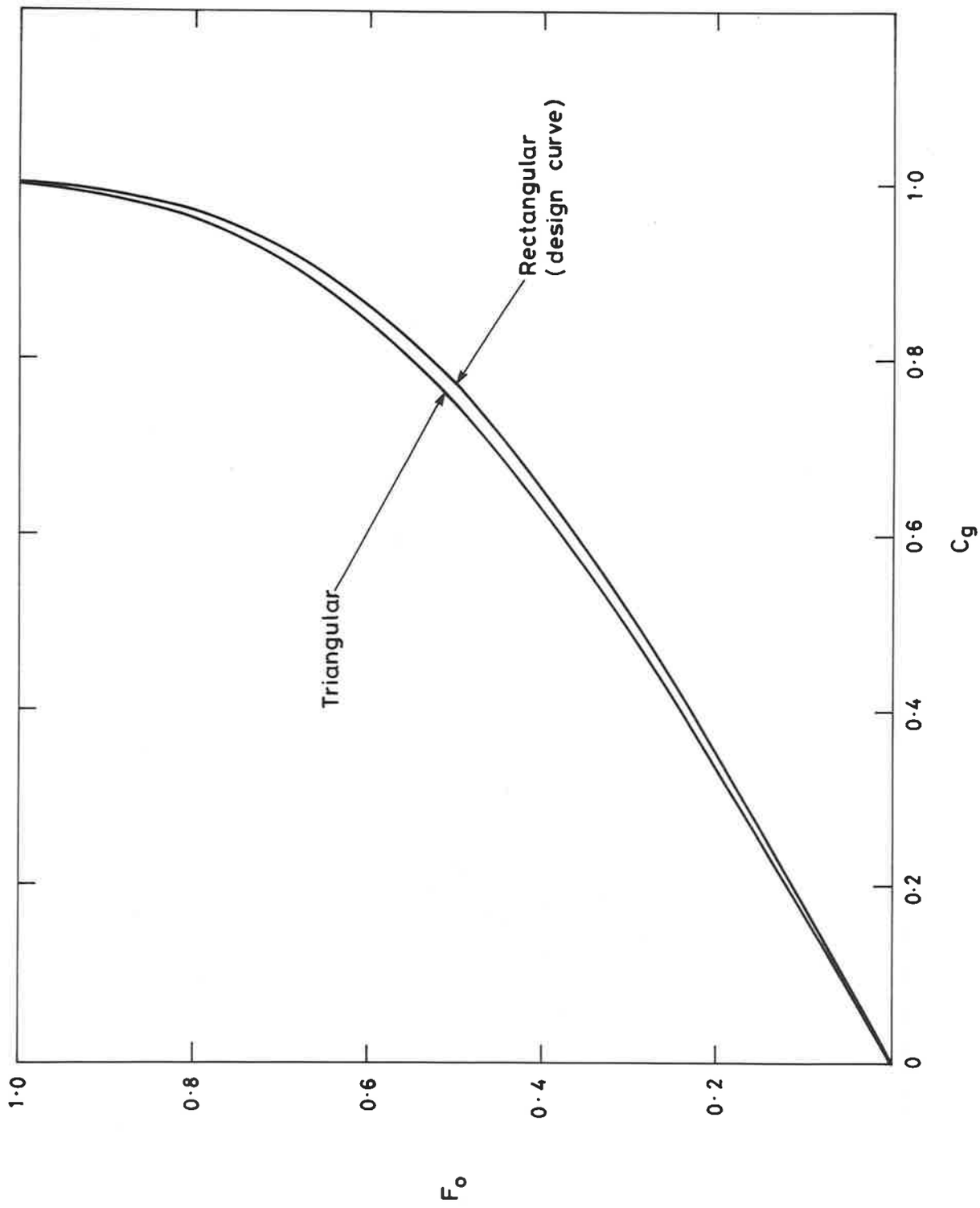

Fig 26 Relation between F_o and C_g for rectangular and triangular gutters

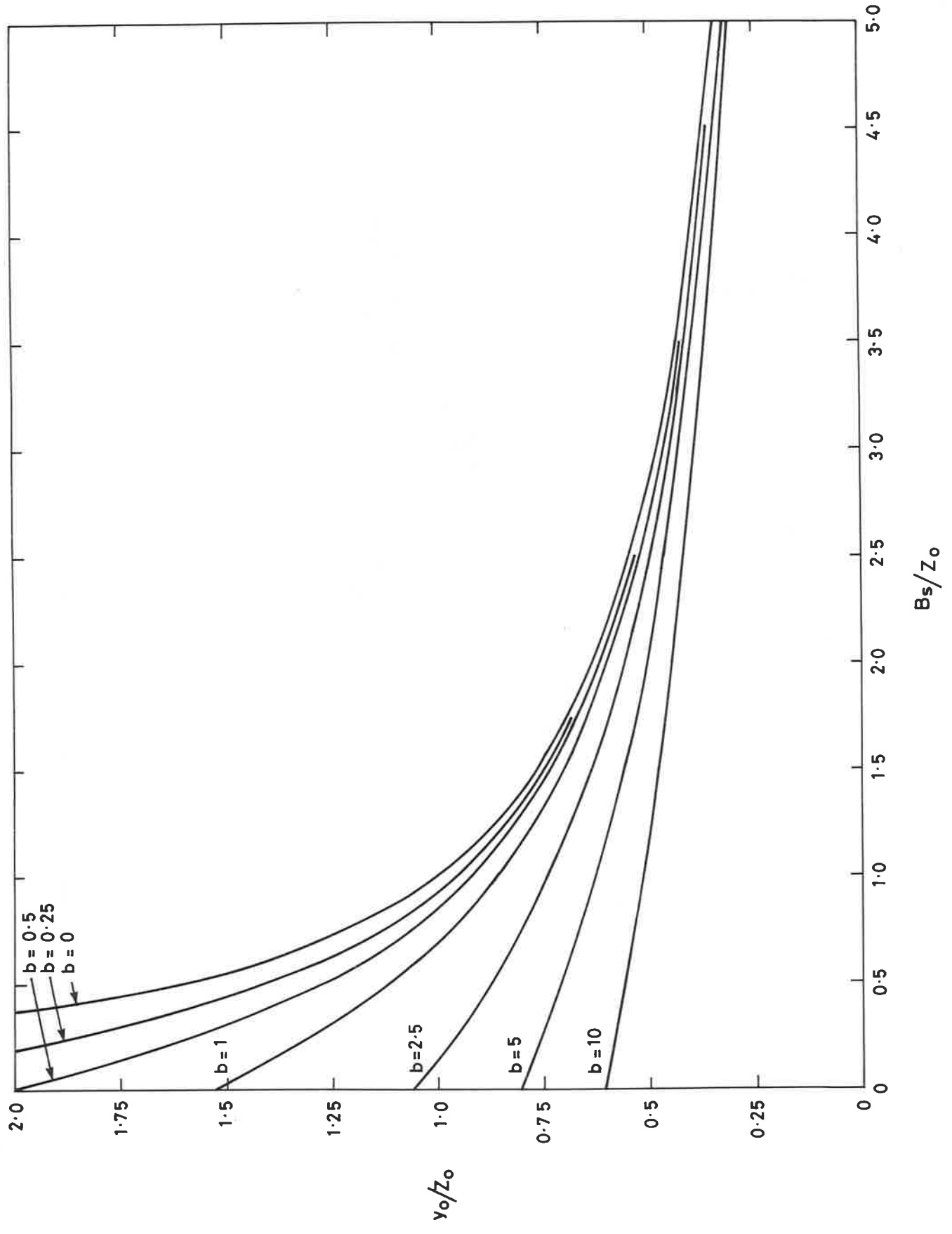

Fig 27 Chart for determining depth of flow at downstream end of trapezoidal gutter

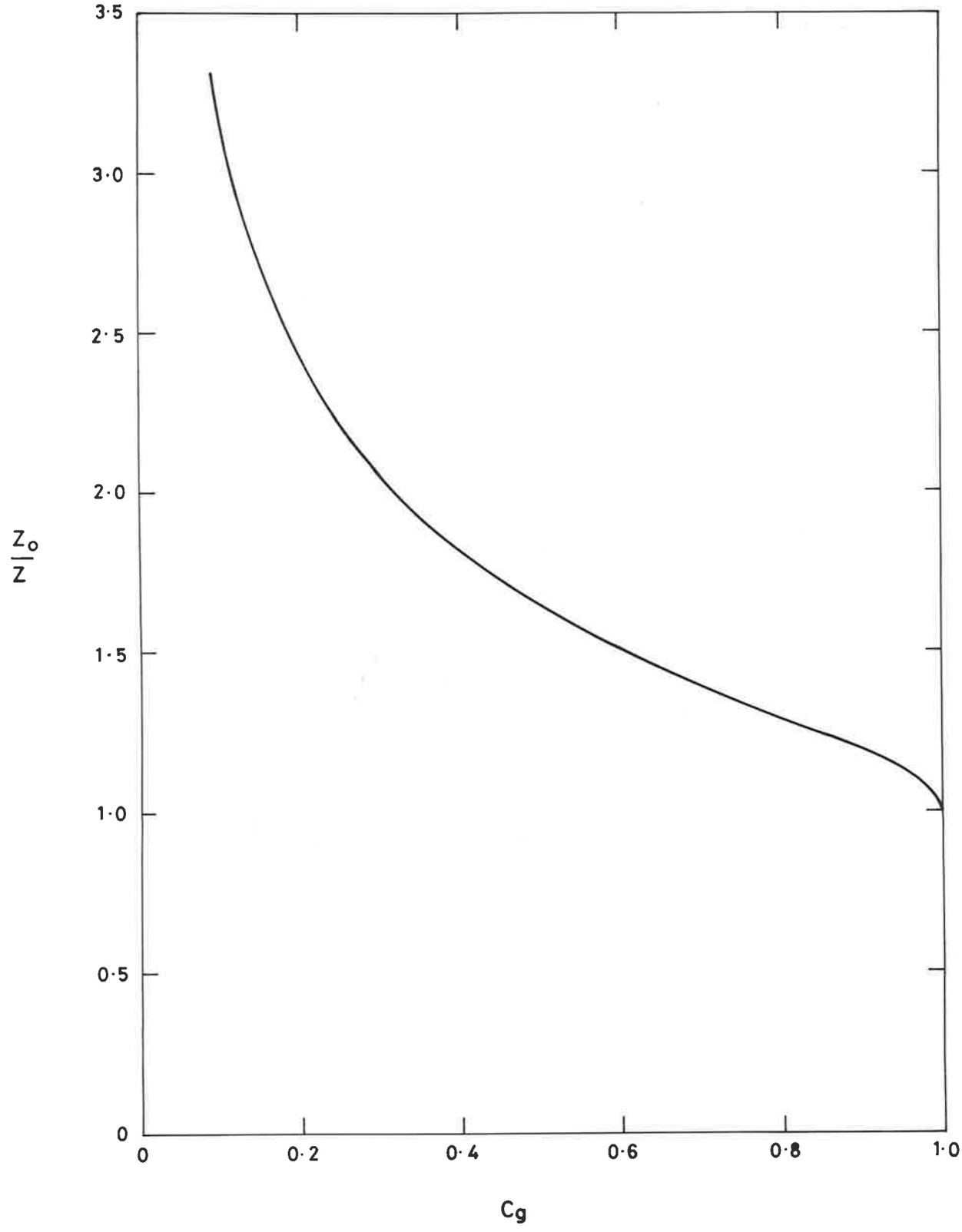

Fig 28 Variation of Z_o/Z with C_g

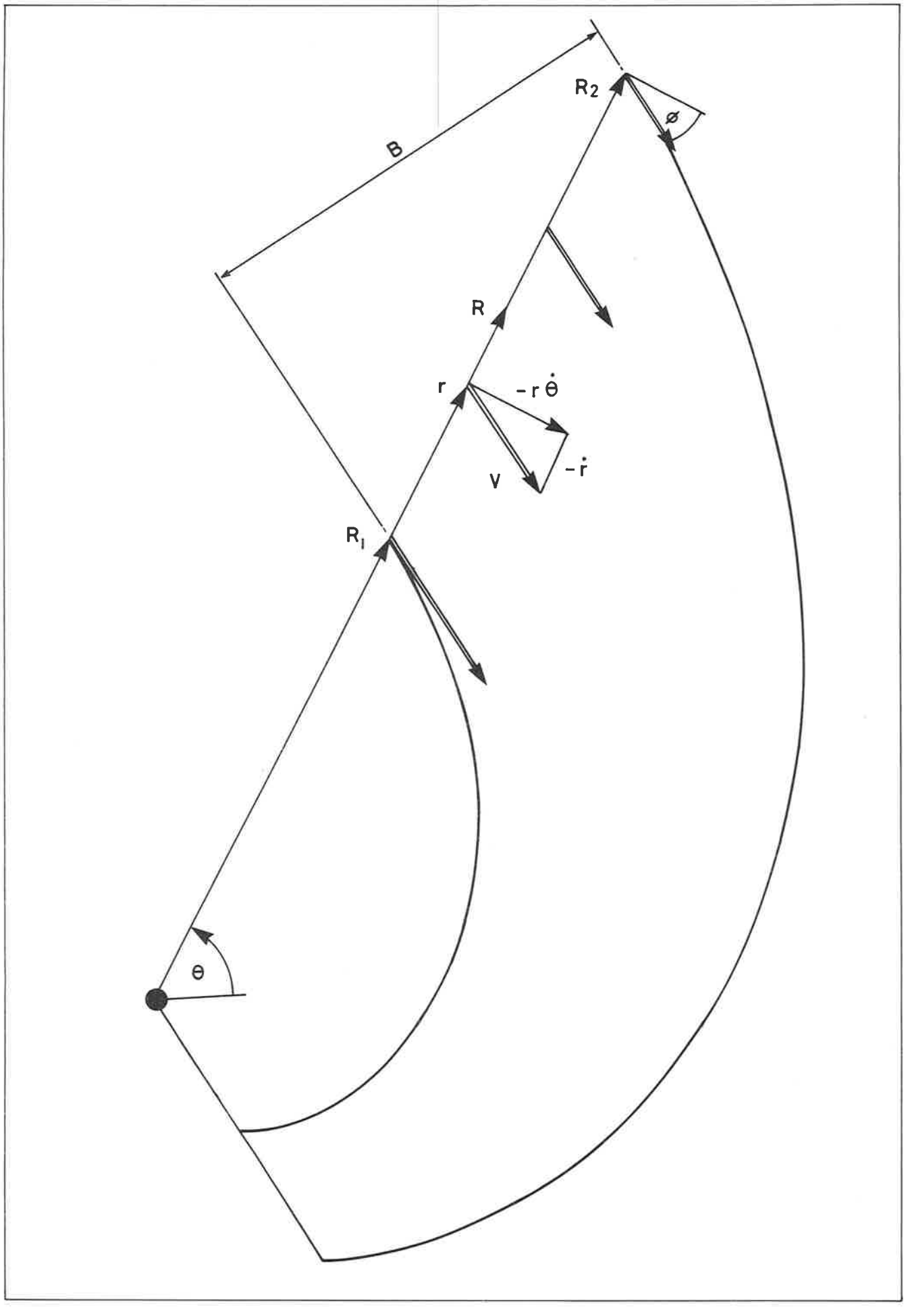

Fig 29 Spiral vortex : plan view

PLATES

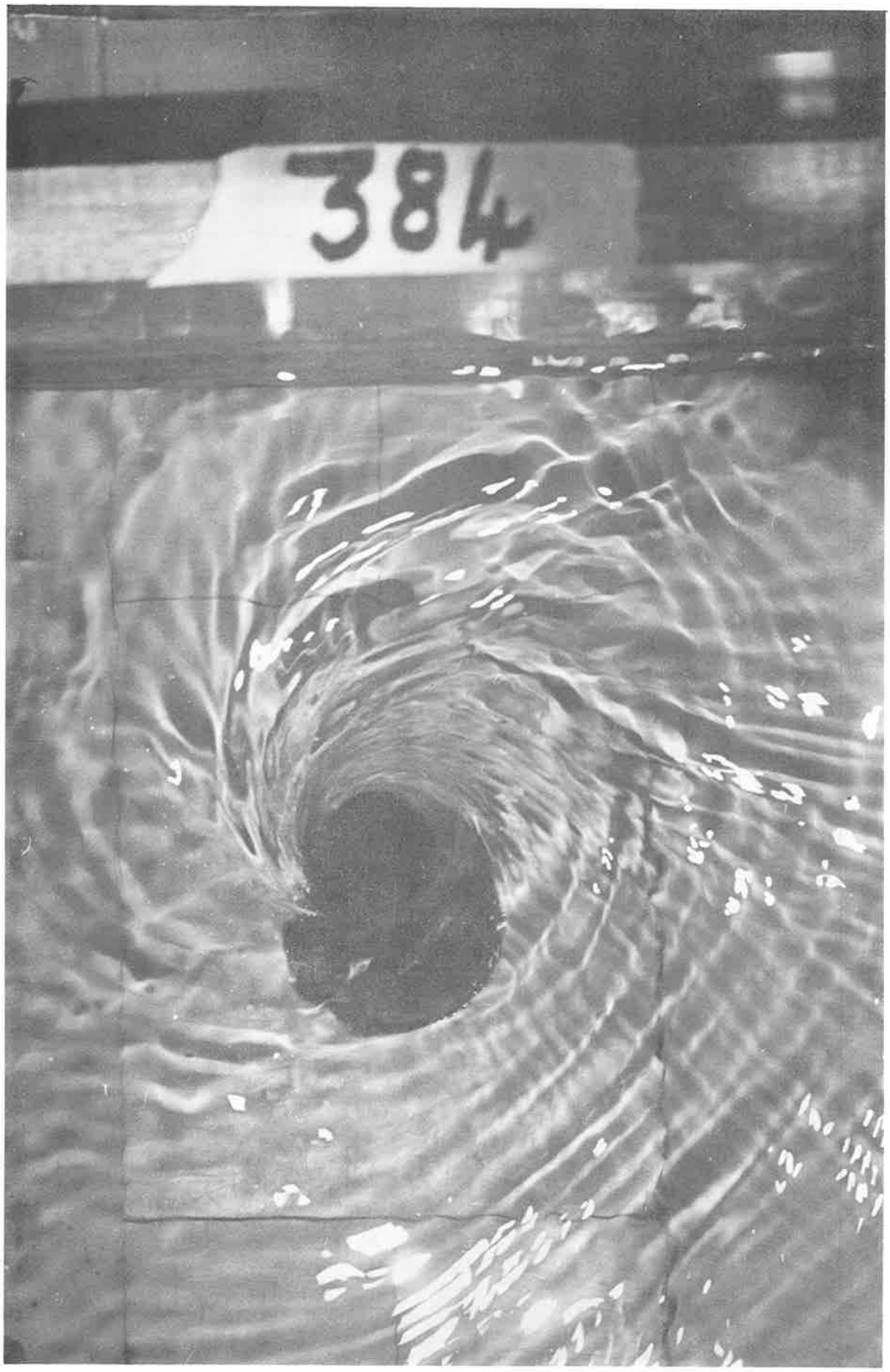

Plate I Orifice flow at circular outlet (Test 12)
by courtesy of BHRA

Plate II Orifice flow at rectangular outlet (Test C3)
by courtesy of BHRA

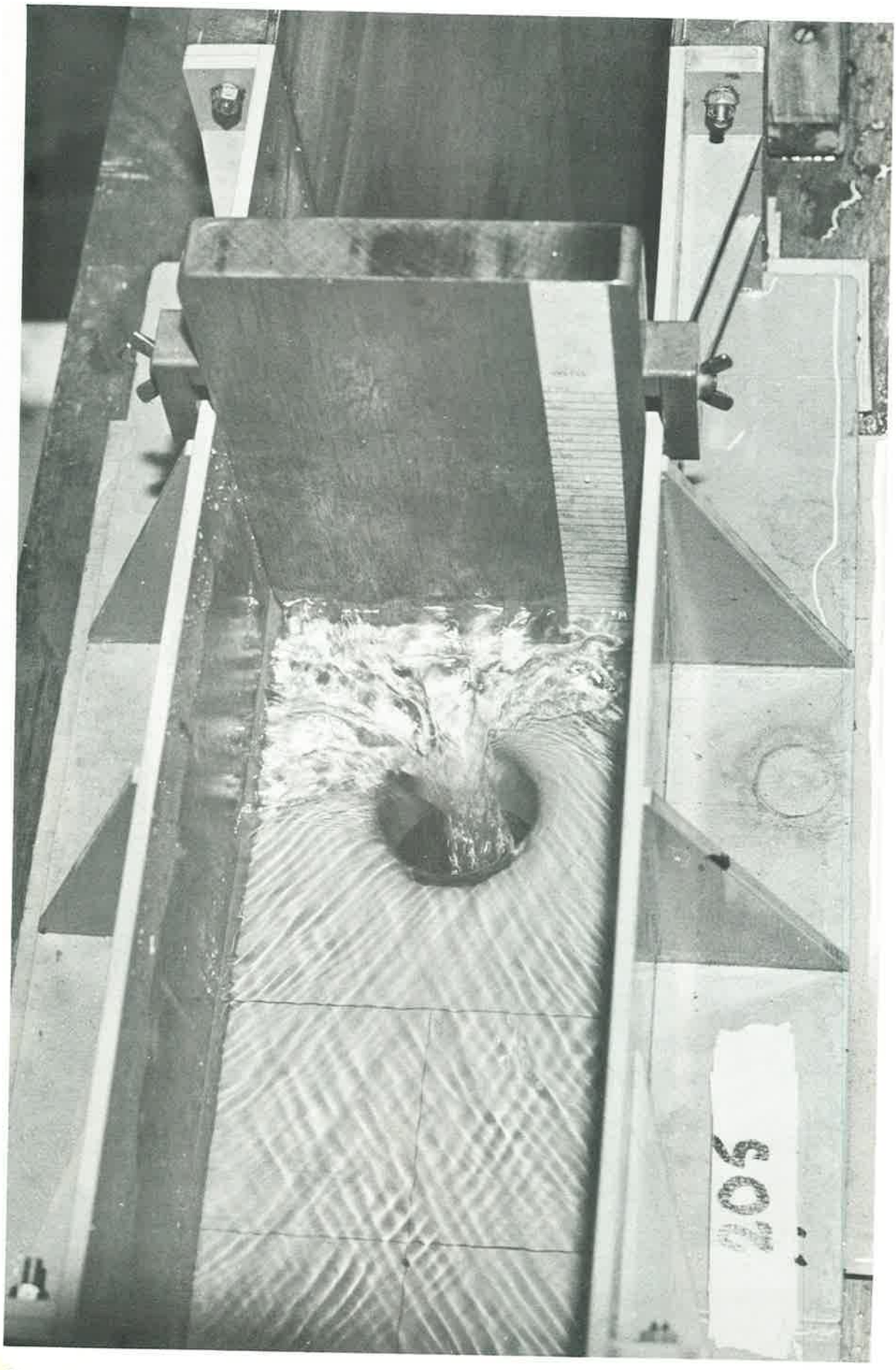

Plate III Weir flow at circular outlet (Test G2)
by courtesy of BHRA

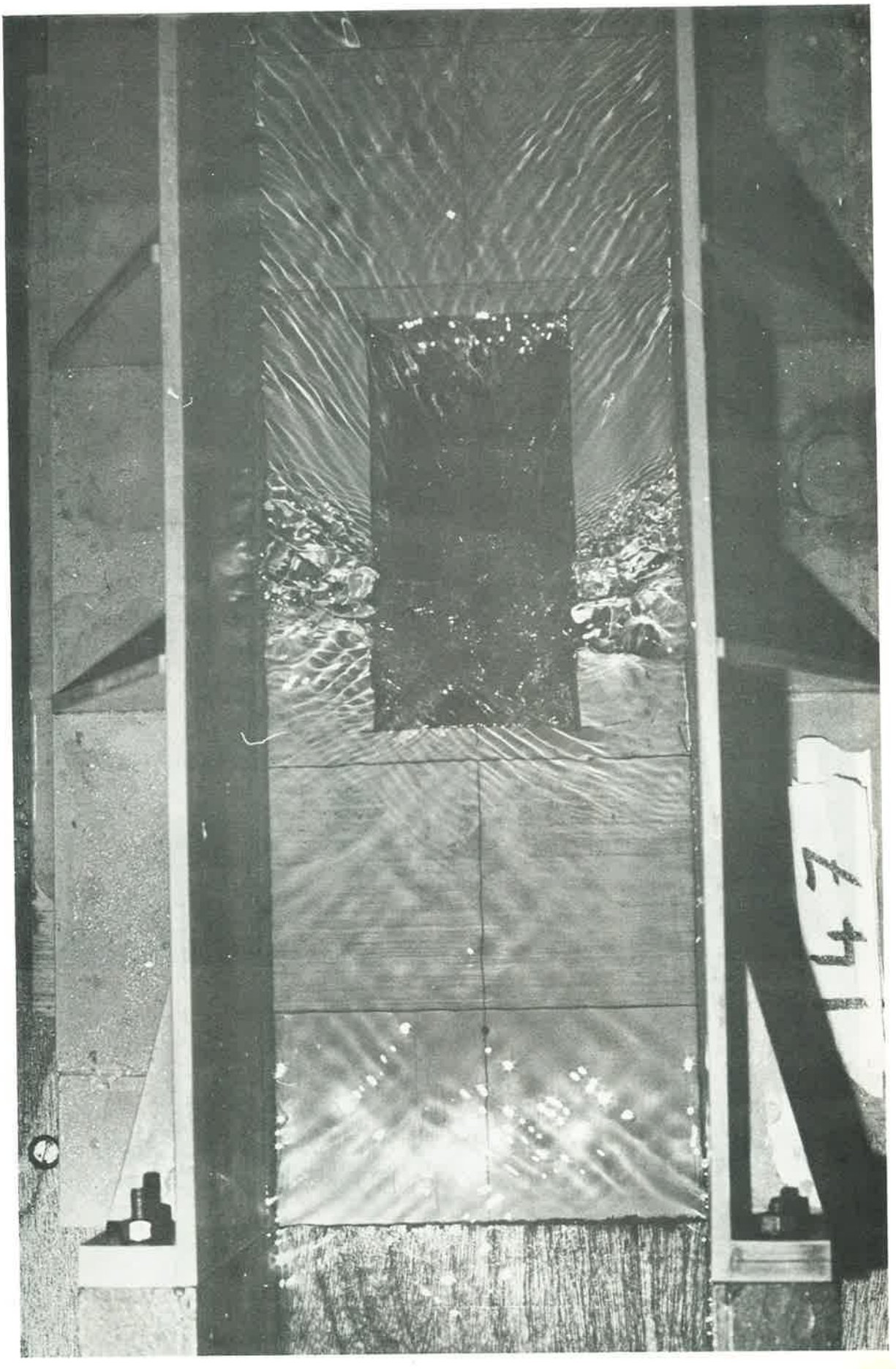

Plate IV Weir flow at rectangular outlet (Test C4)
by courtesy of BHRA

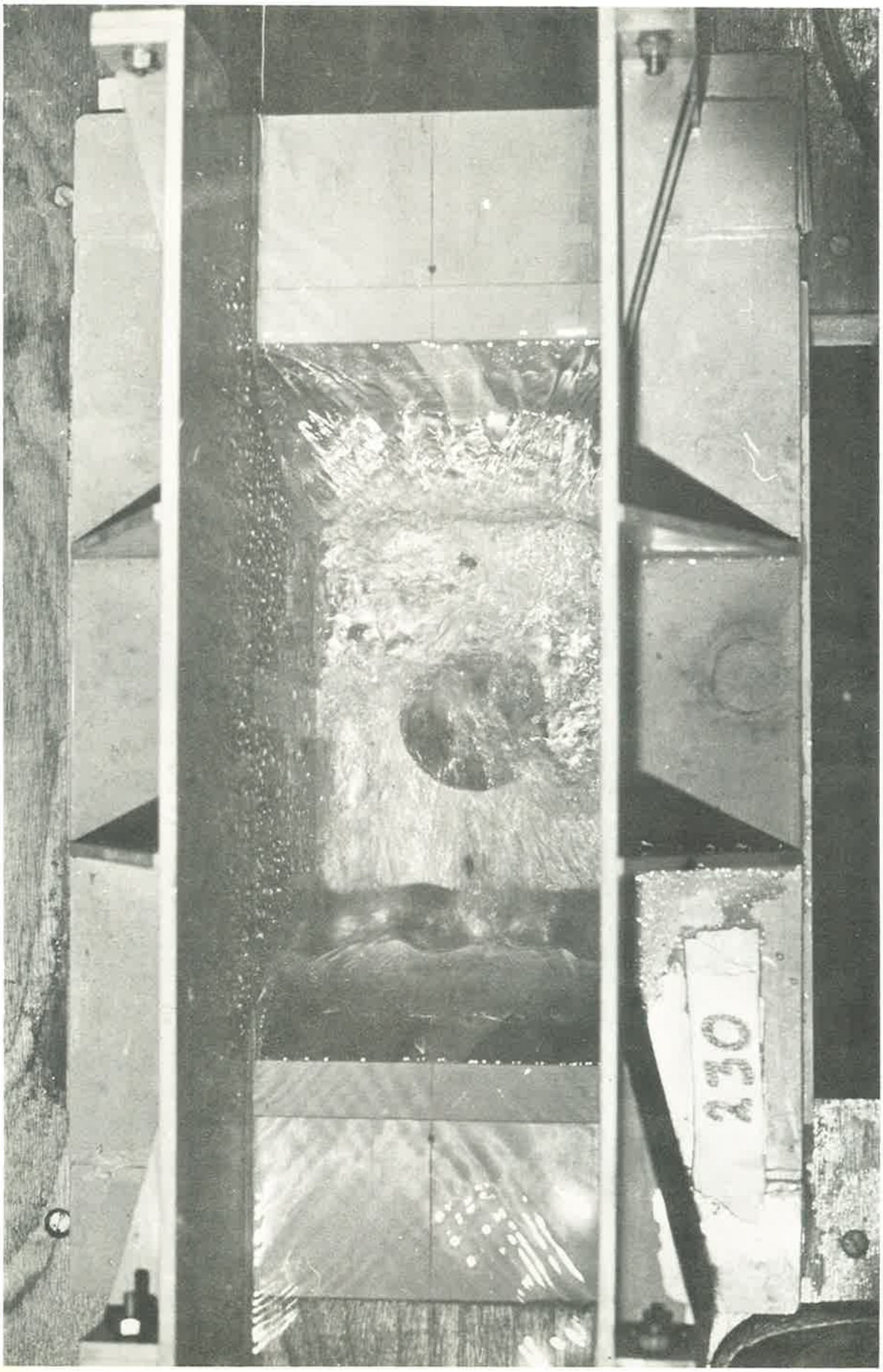

Plate V Weir flow at circular outlet in box-receiver (Test L3)
by courtesy of BHRA